UNIVERSIDADE ESTADUAL PAULISTA
"JÚLIO DE MESQUITA FILHO"
Campus de Botucatu

Instituto de Biociências de Botucatu - Unesp

Perfil de metilação do DNA em lesões tireoidianas

Mariana Bisarro dos Reis

BOTUCATU – SP

2015

UNIVERSIDADE ESTADUAL PAULISTA
"JÚLIO DE MESQUITA FILHO"
Campus de Botucatu

Instituto de Biociências de Botucatu - Unesp

UNIVERSIDADE ESTADUAL PAULISTA

"Julio de Mesquita Filho"

INSTITUTO DE BIOCIÊNCIAS DE BOTUCATU

Perfil de metilação do DNA em lesões tireoidianas

Mariana Bisarro dos Reis

Orientadora: Profa. Dra. Silvia Regina Rogatto

Tese apresentada aoInstituto de Biociências, Câmpus deBotucatu, UNESP, para obtenção do título de Doutor no Programa de PósGraduaçãoem Ciências Biológicas (Genética).

BOTUCATU – SP

2015

Dedico esse trabalho a minha família,
que sempre guiou meu caminho

AGRADECIMENTOS

À **Deus**, por me dar força para continuar, mesmo nos momentos mais difíceis.

À minha orientadora, **Profa. Dra. Silvia Regina Rogatto**, minha enorme gratidão pelo apoio e confiança depositada em mim em um momento tão decisivo na conclusão dessa etapa da minha vida. Obrigada pela orientação, pelo exemplo de profissionalismo, entusiasmo, motivação e por cada conversa, cada conselho que me ajudaram não só na vida profissional.

À minha família, meu porto seguro, principalmente aos **meus pais, Antonio e Silvana**, por não medirem esforços para que eu chegasse até aqui, pelos exemplos de força e luta. Aos meus irmãos, **Gabriela e Victor** e minha sobrinha **Maria Carolina**, por estarem ao meu lado e me trazerem tanta alegria cada vez que eu volto pra casa. Aos **meus avós, Victório, Mercedes e Alcina** (*in memorian*) e **Moacyr**, que sempre torceram pelo meu sucesso. Sem vocês nada seria possível. Obrigada por todo apoio incondicional, pelo amor e tudo que fizeram por mim.

À amiga **Hellen Kuasne**, por toda amizade ao longo desses anos, por me emprestar sua casa tantas vezes e apoio nos momentos mais difíceis dessa fase, dentro e fora do laboratório.

Aos amigos **Fabio Marchi** e **Mateus C. B. Filho**, por toda dedicação, ajuda essencial e inestimável em todas as etapas desse trabalho. À **Caroline Beltrami**, por compartilhar as descobertas desde o início desse projeto.

Aos **amigos do laboratório Neogene**, Priscila, Isabella, Marco, Juan, Luisa, Irina, Julia, André Guollo, André, Maisa, Sara, Tati, Graziela e agregados, Fernanda e Karina, por me acolherem tão bem e contribuírem, cada um a sua maneira, para a realização desse trabalho.

Aos **professores da pós graduação**, pela contribuição na minha formação acadêmica.

Aos **membros da banca examinadora**, pela colaboração e avaliação do trabalho.

Ao **Centro Internacional de Pesquisa e Ensino** (CIPE) do A.C Camargo Cancer Center, pela estrututa de trabalho.

À todos os funcionários do **Banco de Macromoléculas** do AC Camargo Cancer Center, pelo processamento de tecidos e extração de ácidos nucleicos utilizados nesse estudo

Ao **Conselho Nacional de Desenvolvimento Científico e Tecnológico** (CNPq) pela bolsa e **Fundação de Amparo à Pesquisa do Estado de São Paulo** (FAPESP) pelo auxílio financeiro concedidos.

Ao **Programa de Pós Graduação em Ciências Biológicas– Genética** do Instituto de Biociências de Botucatu, UNESP.

À **Jennice**, sempre atenciosa e prestativa, disposta a ajudar em qualquer momento.

Aos **pacientes**, que mesmo em um momento difícil se dispuseram a ajudar, permitindo que este trabalho fosse realizado.

À **Profa Dra. Adriane Pinto Wasko**, pela paciência, conversas e ajuda para que tudo desse certo durante meu doutorado.

Ao **Dr. Luiz Paulo Kowalski**, pela parceria no projeto.

Aos pesquisadores **Dr. Herceg Zdenko** e **Dr. Srikant Ambatipudi**, do grupo de Epigenética do IARC, Lyon, França, pela colobaração e suporte com as análises de bioinformática.

Às amigas **Mariana Ribeiro**, **Ana Paula Paschoal** e **Danielle Broto**, pela amizade, incontáveis conversas e conselhos que me ajudaram muito em etapas decisivas, na vida acadêmica e pessoal. À amiga **Luana**, pela amizade e hospedagem em sua casa em SP.

Muito obrigada!

RESUMO

O câncer de tireoide (CT) é a neoplasia mais comum do sistema endócrino. O carcinoma papilífero da tireoide (CPT) compreende 80-85% dos casos, seguido dos carcinomas foliculares (CFT), pouco diferenciados (CPDT) e anáplasicos (CAT). O diagnóstico dos CT, principalmente nos casos bem diferenciados, ainda é um desafio devido a semelhanças morfológicas compartilhadas por esses tumores e lesões benignas (LBT). O objetivo desse estudo foi avaliar o perfil de metilação do DNA para identificar marcadores epigenéticos envolvidos no desenvolvimento das lesões benignas e dos diferentes subtipos histológicos de carcinomas. Além disso, buscou-se identificar marcadores prognósticos nos CT. Foram incluídos nesse estudo 17 lesões benignas da tireoide (8 adenomas, 6 bócios tireoideanos e 3 tireoidites), 60 CPT, 8 CFT, 2 carcinomas de células de Hurthle (CCH), 1 CPDT e 3 CAT, além de 50 tecidos não neoplásicos (TN) obtidos dos pacientes que tiveram CPT. As análises de metilação diferencial foram realizadas utilizando a plataforma *microarray* Infinium® Human Methylation450 BeadChip (Illumina). Na primeira etapa do estudo, os resultados obtidos de sondas diferencialmente metiladas foram utilizados na construção de um algoritmo útil como classificador diagnóstico. Na segunda etapa, o perfil de metilação do DNA das lesões benignas e dos diferentes subtipos tumorais foi comparado aos dados de tecidos não neoplásicos. Somente sondas significativamente alteradas no presente estudo e aquelas confirmadas no GEO (*Gene Expression Omnibus*) foram selecionadas para a construção de algoritmos. Foram delineados três algoritmos diagnósticos baseados na metilação diferencial de nove sondas selecionadas a partir de área abaixo da curva de 0,75 para o classificador de LBT e 0,90 para os classificadores CFT e CPT além de análise multivariada. Foram também aplicados métodos lineares de classificação. A aplicação do algoritmo diagnóstico utilizando os dados do presente estudo permitiu a correta classificação dos tecidos não neoplásicos, lesões benignas e malignas (sensibilidade: 91,9% e especificidade: 76,5%). A mesma estratégia foi realizada utilizando o banco de dados GEO (sensibilidade: 92,1% e especificidade: 81,3%) e, portanto, confirmando o potencial diagnóstico dessa ferramenta. A aplicação de um dos algoritmos utilizando os dados de 479 CPT (TCGA) foi capaz de associar os menores escores obtidos com acometimento linfonodal. A análise de metilação diferencial entre as LBT e CFT/CCH comparadas aos TN revelou 1531 e 4100 sondas hipermetiladas e 222 e 1475 sondas hipometiladas, respectivamente. A análise dos outros subtipos tumorais revelou um maior número de sondas hipometiladas (2773 em CPT e 28252

em CPDT/CAT) quando comparados às sondas hipermetiladas (242 em CPT e 6195 CPDT/CAT). A análise *in silico* revelou um grande número de vias preditas alteradas em cada grupo de estudo. A comparação do perfil de metilação dos pacientes com carcinomas bem diferenciados que apresentaram bom prognóstico em relação aos pacientes com prognóstico desfavorável permitiu a identificação de cinco sondas, as quais foram capazes de predizer a evolução clínica dos pacientes. Os achados desse estudo mostram a existência de perfis alterados de metilação do DNA que ajudam na compreensão da biologia das lesões originadas de células foliculares de tireoide, além de permitirem a identificação de marcadores diagnósticos e prognósticos que poderão ser úteis na prática clínica.

ABSTRACT

Thyroid cancer (TC) is the most prevalent type of endocrine cancer. Papillary thyroid carcinoma (PTC) comprises 80-85% of the diagnosed thyroid cancers, followed by follicular (FTC), poorly differentiated (PDTC) and anaplastic carcinomas (ATC). Diagnosis of thyroid carcinomas, especially of well-differentiated carcinomas is a challenge due to morphological similarities between these tumors and benign lesions. The aim of this study was to evaluate the methylation profile to identify diagnostic markers involved in benign lesions and in different histological subtypes of carcinomas. Moreover, a search for reliable molecular prognostic markers was also performed in TC. The study included 17 benign lesions (8 adenomas, 6 goiters and 3 thyroiditis), 60 PTCs, 8 FTCs, 2 Hürthle cell carcinomas (HCC), 1 PDTC and 3 ATC, as well as 50 non-neoplastic tissues (NT) obtained from patients who had PTC. Differential methylation analyzes were performed using the Infinium® Human Methylation450 BeadChip microarray (Illumina). In the first stage of the study, the results of differentially methylated probes were used in the development of diagnostic classifier algorithm. In second step, the methylation profile of benign lesions and tumor subtypes was compared to data from non-neoplastic tissues. Only probes significantly altered in the current study and those confirmed by GEO data (Gene Expression Omnibus) were selected for the development of the algorithms. Three diagnostic algorithms were developed based on differential methylation of nine probes selected from area under the curve of 0.75 for BTL classifier and 0.90 for FTC and PTC classifiers and multivariate analysis. It was also applied linear classification methods. Application of the algorithm diagnosis allowed the correct classification of non-neoplastic tissues, benign and malignant lesions (sensitivity: 91.9% and specificity: 76.5%). The same strategy was performed using the GEO database (sensitivity: 92.1% and specificity: 81.3%) confirming the diagnostic potential of this tool. Application of our algorithm using data from 479 PTC (TCGA) was able to associate the lower scores obtained with lymph nodes involvement. The differential methylation analysis between BTL and FTC/HCC compared to NT revealed 1531 and 4100 hypermethylated probes and 222 and 1475 hypomethylated probes, respectively. The analysis of other tumor subtypes showed an increased number of hypomethylated probes (2773 in PTC and 28252 in PDTC/ATC) when compared to the number of hypermethylated probes (242 in PTC and 6195 PDTC/ATC). *In silico* analysis revealed several predicted altered pathways for each studied group. The comparison of the methylation profile of patients with well-differentiated carcinomas

presenting good prognosis and patients with poor prognosis allowed the identification of five probes that were able to predict the clinical outcome of the patients. The findings show the existence of altered DNA methylation profiles that improve the understanding of biology of lesions originated from thyroid follicular cells, and allowed the identification of diagnostic and prognostic markers that may be useful in the clinical practice.

LISTA DE FIGURAS

LISTA DE TABELAS

LISTA DE SIGLAS E ABREVIATURAS

AFT	Adenoma Folicular de Tireoide
ASI/LFSI	Atipia de Significado Indeterminado/ Lesão Folicular de Significado Indeterminado
AUC*	*Area Under Curve*
BEC	Boa evolução clínica
BMIQ*	*Beta-Mixture Quantile Normalization*
BRAF*	*Human v-raf Murine Sarcoma Viral Oncogene Homolog B1*
CAT	Carcinoma Anaplásico de Tireoide
CCH	Carcinoma de Células de Hürthle
CCP*	*Compound Covariate Predictor*
CEP	Comitê de Ética em Pesquisa
CFT	Carcinoma Folicular de Tireoide
CH_3	Grupos metil
CMT	Carcinoma Medular de Tireoide
COBRA	*Combined Bisulfite Restriction Analysis.*
CPDT	Carcinoma Pouco Diferenciado de Tireoide
CpG	Citosina - ligação fosfodiéster - Guanina
CPT	Carcinoma Papilífero de Tireoide
CT	Câncer de tireoide
DLDA*	*Diagonal Linear Discriminant Analysis*
DNA*	*Deoxyribonucleic Acid*
DNMTs	DNA metiltransferases
dNTPs	Deoxinucleotídeos trifosfatados
EDTA*	*Ethylenediaminetetraacetic Acid*
ECR	Evolução clínica ruim
CTF	Carcinoma folicular de tireoide
g	Grama
GEO*	*Gene Expression Omnibus*
HDACs*	*Histone deacetylases*
HRAS*	*Human v-Ha-ras Harvey Rat Sarcoma Viral Oncogene Homolog*

HTT	Tumor trabecular hialinizante
INCA	Instituto Nacional do Câncer
IPA*	*Ingenuity Pathway Analysis*
KRAS*	*Human v-Ki-ras2 Kirsten Rat Sarcoma Viral Oncogene Homolog*
L	Litro
LBT	Lesões Benignas de Tireoide
M	Molar
MAPK*	*Mitogen Activated Protein Kinase*
MBP*	*Methyl-CpG-binding domain protein*
mCPT	Microcarcinoma Papilífero de Tireoide
mg	Miligrama
MI	Índice de metilação
miRNA	microRNA
mL	Mililitro
mM	Milimolar
MSP *	*Methylation Specific PCR*
MS-MLPA*	*Methylation Specific Multiplex Ligation-dependent Probe Amplification*
N1	Linfonodos comprometidos ao diagnóstico
N0	Linfonodos livre de comprometimento ao diagnóstico
Nx	Metástases linfonodais não identificadas
NCI*	*Nacional Cancer Institute*
NF/SNF	Neoplasia folicular/Suspeito de neoplasia folicular
ng	Nanograma
Ni	Não Informado
nM	Nanomolar
NRAS*	*Human Neuroblastoma Rat Sarcoma Viral Oncogene Homolog*
P	valor-p de significância estatística
PAAF	Punção Aspirativa por Agulha Fina
Pb	Par de bases
PCR*	*Polymerase Chain Reaction*
PI3K*	*Phosphatidylinositol 3-Kinase*
qMSP*	*Real Time Quantitative Methylation Specific PCR*
RET*	Ret proto-oncogene

RI	Radioiodo
ROC*	*Receiver Operating Characteristic*
rpm	Rotações por minuto
SAM*	*Adenosylmethionine*
SEER*	*Surveillance Epidemiology and End Results*
SM	Suspeito de malignidade
SNPs*	*Single Nucleotide Polymorphisms*
SPSS*	*Statistics Packet for Social Sciences*
SVM*	*Support Vector Machine*
T3	Triiodotironina
T4	Tiroxina
TCGA*	*The Cancer Genome Atlas*
Tg	Tireoglobulina
TN	Tireoide Não Neoplásica
TP	Tireoidectomia Parcial
Tris	Tris (hidroximetil) aminometano
TSH*	*Thyroid-Stimulating Hormone*
TT	Tireoidectomia Total
VDE-PTC	Variante difusa esclerosante de CPT
VPN	Valor Preditivo Negativo
VPP	Valor Preditivo Positivo
µg	Micrograma
µL	Microlitro
µM	Micromolar

*siglas ou abreviaturas derivadas do inglês

ÍNDICE

1. INTRODUÇÃO

A glândula tireoide é um dos mais importantes órgãos do sistema endócrino, sendo responsável pela produção dos hormônios tiroxina (T4) e triiodotironina (T3), com um importante papel no crescimento, desenvolvimento e no metabolismo celular, especialmente durante o desenvolvimento fetal e infantil (MOELLER; FÜHRER, 2013). A tiroide é também responsável pela secreção da calcitonina, um hormônio envolvido no metabolismo do cálcio (MUKHERJEE et al., 2011).

A produção de hormônios tiroidianos é controlada por um sistema de *feedback* negativo envolvendo o hipotálamo, a hipófise e a própria glândula tireoide (CHIASERA, 2013). O hipotálamo é responsável pela secreção do hormônio TRH (*Thyrotropin-releasing Hormone*) que é então transportado para a hipófise, onde este se liga a receptores celulares levando a produção e secreção do hormônio TSH (*Thyroid-stimulating Hormone*). Na glândula tireoide, este hormônio se liga a receptores nas células foliculares e estimula a produção e a secreção dos hormônios T3 e T4. A produção desses hormônios inibe a síntese de TRH e TSH estabelecendo um equilíbrio que mantém o organismo com quantidades adequadas de T3 e T4 (CHIASERA, 2013; GUYTON; HALL, 2006)

Os nódulos na glândula tireoide são frequentes, sendo os palpáveis encontrados em aproximadamente 3-7% da população adulta (SYRENICZ et al., 2014). Aproximadamente 60% dos indivíduos submetidos à ultrassonografia e outras técnicas sensíveis de imagem apresentam nódulos tireoidianos (EZZAT et al., 1994; GUTH et al., 2009). A maioria desses nódulos é benigna (em torno de 95%) incluindo os adenomas foliculares, bócios, cistos e tireoidite (NIEDZIELA, 2014; WANG et al., 2011).

O câncer de tireoide (CT) é a neoplasia mais comum do sistema endócrino (XING, 2013), sendo também o tipo de câncer mais comum localizado na cabeça e pescoço (REN et al., 2007). Em 2008, a ocorrência do CT foi aproximadamente de 213.000 casos (The GLOBOCAN Project, 2008), correspondendo a 1% dos tumores diagnosticados nos países ocidentais. No Brasil, entre os anos de 1994 a 1998, o câncer de tireoide correspondeu a 1,3% de todos os casos de câncer (INCA, 2014). Em 2014, a estimativa foi de 9.200 novos casos de câncer da tireoide, com um risco estimado de 7,91 casos a cada 100 mil mulheres, o que torna esse tumor o quinto mais incidente na

população feminina no Brasil (excluindo o câncer de pele não melanoma) (INCA, 2014).

A incidência do câncer de tireoide varia entre diferentes populações, possivelmente decorrente de uma combinação de fatores étnicos e ambientais. Segundo o banco de dados do SEER (*Surveillance, Epidemiology and End Results*) do NCI (*National Cancer Institute*) a incidência desse tipo de câncer triplicou nos últimos 36 anos (NCI, 2014), embora o mesmo não tenha sido observado para a taxa de mortalidade.

A etiologia do câncer de tireoide está associada com fatores hormonais, histór co familiar, inflamação e principalmente deficiência de iodo e exposição à radiação (VIGLIETTO; DE MARCO, 2011). Dentre estes fatores de risco, a radiação é o mais estudado, principalmente ao que se refere ao seu amplo uso na terapia médica e exposição como resultado de acidentes nucleares (NIKIFOROV; NIKIFOROVA, 2011).

A maioria dos tumores de tireoide é originada de células epiteliais foliculares, enquanto uma pequena porcentagem (5 a 10%) é originada de células parafoliculares ou células C (ELISEI; PINCHERA, 2012). Histologicamente os tumores de células foliculares são classificados em bem diferenciados (papilífero e folicular), pouco diferenciados (insular) e não diferenciados (anaplásico) (Tabela 1).

Tabela 1. Principais características dos subtipos histopatológicos dos tumores de tireoide.

Tipo de Tumor	Célula de origem	Prevalência	Características	Variante
Carcinoma papilífero de tireoide (CPT)	Células Foliculares	80-85%	Bem diferenciado com arquitetura papilifera, núcleos grandes com formato oval, cromatina hipodensa; fendas nucleares.	Clássica, folicular, células altas e raras
Carcinoma folicular de tireoide (CFT)	Células Foliculares	10-15%	Bem diferenciado, hipercelular com padrões microfoliculares, falta das caracteristicas do CPT, invasão capsular ou vascular.	Carcinoma de células de Hürthle (CCH)
Carcinoma pouco diferenciado de tireoide (CPDT)	Células Foliculares	5-10%	Pouco diferenciado, com sobreposição com os CPT e CFT. Agressividade intermediária entre carcinomas bem e indiferenciados	-
Carcinoma anaplásico de tireoide (CAT)	Células Foliculares	2-3%	Indiferenciado, células pleomórficas gigantes, epitelióides ou fusiformes. Agressivo. Surgimento a partir de CPT, CFT e PDT ou *de novo*.	-
Carcinoma medular de tireoide (CMT)	Células C/Parafoliculares	2-3%	Agressividade moderada, mutações em *RET*. Forma familial.	-

Fonte: Dados adaptados de Xing (2013).

Os carcinomas bem diferenciados são de 2 a 4 vezes mais frequentes (Sherman, 2003) e aparecem em idade média mais precoce no gênero feminino (feminino: 40-50 anos e homens: 50- 60 anos) (JIN et al., 2013).

Entre os carcinomas bem diferenciados, o carcinoma papilífero é o subtipo mais frequentee representa cerca de 80-85% dos casos diagnosticados (XING, 2013). Este subtipo é responsável pelo aumento da incidência de câncer de tireoide no mundo (NIKIFOROV; NIKIFOROVA, 2011). A forma clássica do carcinoma papilífero apresenta diferenciação das células foliculares e é caracterizada pela formação de papilas e um conjunto distinto de alterações nucleares (RIESCO-EIZAGUIRRE; SANTISTEBAN, 2007).

O carcinoma folicular da tireoide (CFT) é o segundo tipo mais comum entre os CT, sendo responsável por 10-15% dos casos (XING, 2013). Entretanto, em regiões que apresentam deficiência de iodo a prevalência do CFT é maior quando comparada a áreas com uma dieta rica desse elemento (WHO, 2004). Histologicamente, a morfologia desse câncer varia de pequenos a médios folículos contendo colóide a padrões de crescimento trabecular ou sólido, além da presença de invasão de cápsula, vaso ou extensão extratireoidiana (BALOCH; LIVOLSI, 2014; SOBRINHO-SIMÕES et al., 2011).

Os carcinomas pouco diferenciados são classificados como intermediários entre os carcinomas bem diferenciados e indiferenciados, no que diz respeito a morfologia, aparência e comportamento biológico (PATEL; SHAHA, 2014). Esses carcinomas apresentam um padrão de crescimento sólido, trabecular ou insular, ausência de alterações nucleares como aquelas encontradas no carcinoma papílifero (TALLINI, 2011). A prevalência desse tipo tumoral é variável dependendo de fatores ambientes ou a diferenças na interpretação histopatológica (ASIOLI et al., 2010; VOLANTE; RAPA; PAPOTTI, 2008).

O carcinoma anaplásico apresenta a menor prevalência entre os derivados de células foliculares, sendo responsável por 2 a 3% dos casos diagnosticados. Acredita-se que esse tipo tumoral possa se desenvolver a partir de carcinomas papilíferos ou foliculares já existentes e, uma vez estabelecido, apresente uma alta taxa de proliferação celular (SMITH; NUCERA, 2014). São caracterizados por apresentarem células atípicas e multinucleadas, núcleos grandes e ausência de características de tecidos diferenciados (O´NEILL et al., 2010).

1.1 Diagnóstico de carcinoma de tireoide

A presença do nódulo tireoidiano é a principal manifestação clínica das doenças que podem acometer a glândula tireoide. A ultrassonografia é muito utilizada ao diagnóstico, sendo muitas vezes o nódulo descoberto em exames de rotina, entretanto os achados não são específicos quanto à sua natureza benigna ou maligna (FRATES et al., 2005). Como resultado da análise histopatológica verifica-se que maioria dos nódulos é benigno, entretando o maior desafio é a identificação dos nódulos malignos com rapidez e acurácia (NIKIFOROV; NIKIFOROVA, 2011).

O padrão ouro para o diagnóstico dos nódulos de tireoide é a punção aspirativa por agulha fina (PAAF) seguida de análise histológica da amostra. Este procedimento apresenta, até o presente, o melhor custo-benefício sendo capaz de identificar os casos em que são necessários os tratamentos cirúrgicos (BOSE; WALTS, 2012; SCHNEIDER; CHEN, 2013). O resultado desse procedimento é definido em seis categorias diagnósticas, de acordo com o critério de Bethesda: I- Não diagnóstico/Insatisfatório; II- Benigno; III- Atipia de significado indeterminado/Lesão folicular de significado indeterminado (ASI/LFSI); IV- Neoplasia folicular/Suspeito de neoplasia folicular (NF/SNF); V- Suspeito de malignidade (SM); VI- Maligno (CIBAS; ALI, 2009).

Como pode ser verificado pela categorização dos nódulos e acurácia desse procedimento, há limitações devido a certos fatores que englobam a qualidade do material e/ou características dos nódulos. Uma meta análise publicada por Wang et al. (2011), revelou que a grande maioria das PAAFs realizadas é diagnosticada como benigna (72%), 5% são malignas, 6% são não diagnosticadas e 17% das lesões apresentam um diagnóstico indeterminado. Essas lesões de significado incerto (categorias III, IV e/ou V do critério de Bethesda), nas quais não é possível definir a existência ou ausência de lesões malignas, são devido principalmente às características citológicas de lesões com padrão de crescimento folicular (NIKIFOROV et al., 2009; FERRAZ; ESZLINGER; PASCHKE, 2011). A distinção entre carcinomas foliculares e adenomas é uma das maiores dificuldades diagnósticas devido a suas características citológicas semelhantes, sendo a presença de invasão vascular ou capsular, avaliados histologicamente, que define a lesão como maligna. Entretanto carcinomas papilíferos, em especial aqueles considerados variante folicular, também são diagnosticados após

resultados indeterminados na PAAF (SCLABAS et al., 2003; YANG et al., 2007).

Entre os casos de significado indeterminado que foram submetidos a cirurgia, 66% (WANG et al., 2011) e 73,6% (PIANA et al., 2010) foram confirmados histopatologicamente na peça cirúrgica como benignos. Em um outro estudo, 24% dos 45 casos considerados discordantes na cirurgia e diagnosticados como benignos na citologia foram considerados no seguimento do paciente como malignos (falso negativos na PAAF) (YLAGAN; FARKAS; DEHNER, 2004). Esses resultados revelam que um grande número de pacientes são submetidos a cirurgias desnecessárias ou sofrem um atraso no ínicio de seus tratamentos.

Testes moleculares têm potencial para aumentar a confiabilidade dos exames citológicos e muitas das alterações genéticas descritas no câncer de tireoide, nas últimas décadas, são consideradas promissoras para serem aplicadas na prática clínica (BHAIJEE; NIKIFOROV, 2011). Em um estudo publicado por Nikiforov et al. (2011), um painel de mutações incluindo *BRAF*, *NRAS*, *KRAS*, *HRAS* e rearranjos em *RET/PTC1*, *RET/PTC3* e *PAX8/PPARγ* foram analisados em um conjuto de 1056 de PAAF com citologia indeterminada. Os autores detectaram que a presença de mutações nas amostras foi associada com um diagnóstico final de câncer em 88% dos casos com citologia de atipia, 87% dos casos de neoplasia folicular/suspeito para neoplasia folicular e 95% dos casos suspeitos para neoplasia. Quando os resultados das citologias foram correlacionados com os achados nas amostras cirúrgicas, todas as mutações foram confirmadas, entretanto, foram encontradas amostras com mutações e que durante a citologia foram consideradas negativas para as mesmas.

Apesar dos recentes estudos mostrarem a eficiência na detecção de amostras malignas utilizando painéis de mutações, os quais aumentam a acúracia das citologias, muitos tumores não apresentam essas alterações. Nesse sentido alguns estudos têm buscado marcadores diagnósticos para os carcinomas de tireoide baseados em análises de expressão de transcritos (ROSEN et al., 2005; ALEXANDER et al., 2012; KARGER et al., 2012), microRNAs (CANTARA et al., 2014; WEI et al., 2014) e metilação do DNA (HU et al., 2006a; KELLER et al., 2013; ZHANG et al., 2014). Recentemente, nosso grupo identificou a expressão de três genes (*CLDN10*, *HMGA2* e *LAMB3*) a qual foi capaz de classificar tumores e amostras não tumorais com uma alta sensibilidade e especificidade (CAMARGO BARROS-FILHO et al., 2015).

Atualmente, existem dois testes para o diagnóstico diferencial em câncer de tireoide. O primeiro teste molecular clinicamente validado descrito é conhecido como

Veracyte Afirma Gene Expression Classifier (GEC; Veracyte, San Francisco, CA) o qual é baseado no perfil de expressão gênica (142 genes identificados na plataforma *Affymetrix Human Exon Array*). Este ensaio foi testado inicialmente em 265 nódulos com diagnóstico indeterminado e apresentou alta sensibilidade (92%) e baixa especificidade (52%) na identificação de nódulos benignos (ALEXANDER et al., 2012). O segundo teste é baseado em um painel customizado (ThyroSeq) que foi desenvolvido para a análise de 284 mutações em 12 genes, utilizando uma pequena quantidade de DNA (5-10ng). Este teste apresenta uma acurácia de 100% (NIKIFOROVA et al., 2013).

A utilização de alterações no padrão de metilação do DNA como biomarcadores diagnósticos para o câncer tem sido avaliada e considerada uma grande promessa não somente para a detecção da doença, mas também na sua classificação e monitoramento da recorrência tumoral (LAIRD, 2003; LAIRD, 2005).

1.2 Fatores prognósticos no carcinoma de tireoide

Uma avaliação prognó tica precisa e a estratificação do risco na abordagem inicial do paciente com câncer de tireoide são importantes na determinação da terapia e na caracterização do risco de recorrência e avaliação da morbidade e mortalidade (COOPER et al., 2009; XING, 2007a).

O comportamento bioló ico do carcinoma papílifero de tireoide é indolente e com um excelente prognó tico (VIGLIETTO; DE MARCO, 2011). As características associadas com prognóstico desfavorável incluem a presença da doença em idade jovem, tumor primário de grande dimensão (> 4 cm), comprometimento de linfonodos, extensão extracapsular, extensão extratireoidiana e metástases (GONZALEZ-GONZALEZ et al., 2011; ITO; MIYAUCHI, 2009). Raramente são relatadas metástases localizadas fora da região do pescoço (5 a 7% dos casos) (LIVOLSI, 2011), sendo consideradas um fator de pior prognóstico (GARDNER et al., 2000).

As variantes do carcinoma papilífero são fatores importantes na determinação do prognó tico do paciente. Os microcarcinomas de uma maneira geral, apresentam um excelente prognóstico, com raros casos de metástases, sendo estas mais comuns em pacientes jovens (KHANAFSHAR; LLOYD, 2011). A Organização Mundial de Saúd caracteriza as variantes esclerosante difusa, de célula colunar e a de células altas como

as mais agressivas; esta última tende a ser maior e mais invasiva com a presença de metástases locais e à distância, além de apresentar um maior risco de recorrência (KHANAFSHAR; LLOYD, 2011; VIGLIETTO; DE MARCO, 2011).

Embora os carcinomas diferenciados estejam associados com baixa taxa de mortalidade, as taxas de recorrência são altas (20 a 30%) (MAZZAFERRI; JHIANG, 1994), sendo mais frequentes em pacientes mais idosos (GONZALEZ-GONZALEZ et al., 2011).

A associação entre a idade e o gênero de pacientes com carcinoma papilífero e a agressividade tumoral é um fator bem descrito em literatura. As mulheres têm uma média de idade mais baixa ao diagnóstico, entretanto, em homens a doença tende a ser mais agressiva (RAHBARI et al., 2010). Em relação a idade, pacientes diagnosticados entre 21 e 45 anos de idade tem menor risco de desenvolver metástases, ao contrário do que se observa em pacientes mais jovens (JARZAB; HANDKIEWICZ-JUNAK, 2007) e com mais de 45 anos, onde se observa uma maior taxa de metástases à distância, invasão extratireoidiana e, principalmente, metástases linfonodais (IYER; SHAHA, 2010).

O papel das mutações no desenvolvimento do câncer de tireoide foi muito estudado, tendo sido também relatada uma associação com características prognósticas. Vários estudos têm sido publicados a respeito do potencial diagnóstico (KABAKER et al., 2012; ROSSI et al., 2012) e prognóstico (XING et al., 2009) da mutação V600E em *BRAF* no carcinoma papilífero de tireoide, sendo esta mutação associada com invasão extratireoidiana, metástase linfonodal, avançado estádio TNM (T: tamanho do tumor, N: comprometimento de linfonodos, M: ocorrência de metástase) e recorrência (GUERRA et al., 2012; KIM et al., 2012; LUPI et al., 2007). Relatos em literaturam indicam uma associação entre a mutação T1799A em *BRAF* com vários fatores prognósticos, sendo essa mutação considerada um potencial marcador molecular de agressividade do carcinoma papilífero de tireoide (NIKIFOROVA et al., 2003a; Daliri et al., 2014; XING, 2014). Em uma revisão descrita por Xing (2007a), o status de *BRAF* foi associado significativamente com metástase linfonodal, extensão extratireoidiana e estádios III e IV do câncer papilífero de tireoide.

Assim como para os carcinomas papilíferos, o prognóstico dos pacientes com carcinoma folicular depende da idade, tamanho e estágio do tumor, presença de metástase e também a resposta ao tratamento com radioiodo (RI) (KIM et al., 2014; MAZZAFERRI; JHIANG, 1994; SOBRINHO-SIMÕES et al., 2011). O significado do

subtipo histoló ico ainda é controverso, entretanto, é aceito que pacientes com carcinoma de células de Hür hle apresentam um prognóstico desfavorável (*American Thyroid Association*, 2009). Em um estudo publicado por Ríos et al. (2013), a sobrevida livre da doença de pacientes com carcinoma folicularem 5 anos foi de 81%,71%, 50% e 0% para os estádios I, II, III e IV, respectivamente.

Os carcinomas pouco diferenciados apresentam um comportamento biológico de agressividade intermediária. Hiltzik et al. (2006) analisaram a atividade mitótica presente nas células e/ou a presença de necrose e demonstraram que os pacientes com carcinomas pouco diferenciados apresentam um prognóstico intermediário entre carcinomas bem diferenciados e anáplasicos. A classificação TNM, idade, tamanho do tumor, extensão extratireoidiana, presença de invasão linfonodal e metástase também são considerados fatores prognósticos para pacientes com carcinomas pouco diferenciados de tireoide (JUNG et al., 2007; LIN; CHAO; HSUEH, 2007).

O prognóstico dos pacientes com carcinoma anaplásico de tireoide é quase sempre fatal (O'NEILL et al., 2010). Kim et al. (2007) relataram que a média de sobrevida desses pacientes foi de 5,1 meses. Os autores relataram que a taxa de sobrevida doença-específica foi de 42%, 16% e 9% em 6, 12 e 24 meses, respectivamente. Foi também relatada que a idade inferior a 60 anos e a presença detumores menores que 7 cm eram preditores de baixa mortalidade.

Vários relatos em literatura foram focados na busca de potenciais marcadores em câncer de tireoide com o objetivo de aplicação na prática clínica baseados. De uma maneira geral, a maioria dos estudos tem como objetivo encontrar alterações moleculares que possam ser utilizadas no diagnóstico desses carcinomas e são poucos os que buscam marcadores prognósticos. Em adição, a maioria deles são baseados em análises de expressão global de transcritos (MONTERO-CONDE et al., 2007; WREESMANN et al., 2004) e poucos são os relatos de estudos de análises globais de metilação do DNA (ELLIS et al., 2014; MANCIKOVA et al., 2014).

1.3 Alterações genéticas em carcinomas de tireoide

O conhecimento das alterações genéticas no câncer de tireoide tem se expandido consideravelmente. A maioria das alteraçõesdescritas compreende mutações em ponto em *BRAF* e *RAS* e rearranjos em *RET/PTC* e *PAX8/PPARG* (NIKIFOROV, 2011), além

de mutações que afetam a via *PI3K–AKT* (XING, 2013). A Tabela 2 apresenta as alterações genéticas identificadas no câncer de tireoide derivadas de células foliculares.

A mutação mais comum encontrada no gene *BRAF* é a substituição T1799A que leva a troca do aminoácido valina pelo ácido glutâmico (V600E) (DAVIES et al., 2002). Esta alteração é responsável por 99% das mutações em *BRAF* encontradas no câncer de tireoide (WITT et al., 2013). No carcinoma papilífero, esta mutação é encontrada em aproximadamente 40-45% dos casos em adultos (GÓMEZ SÁEZ, 2011; NIKIFOROV; NIKIFOROVA, 2011), com maior prevalência no carcinoma com histologia clássica e variante de células altas e menos comum na variante folicular (GÓMEZ SÁEZ, 2011; NIKIFOROVA et al., 2003a). Outros mecanismos menos frequentes podem estar envolvidos na ativação do gene *BRAF*, como por exemplo, a mutação em ponto K601E, pequenas inserções/deleções *in frame* próx ma ao códon 600 (GÓMEZ SÁEZ, 2011) e rearranjo em *AKAP9/BRAF* (CIAMPI et al., 2005).

A proteína BRAF é um membro da família RAF as quaisatuam como quinases citoplasmáticas serina/treonina na via de sinalização MAPK (CANTWELL-DORRIS et al., 2011). A via de transdução de sinal MAPK é requerida para a manutenção das atividades celulares como crescimento celular, proliferação, diferenciação e apoptose (MACCORKLE; TAN, 2005). A ativação fisiolóica dessa via acontece por meio da ativação de RAS por uma gama dereceptores de membrana celular (receptores acoplados a proteínas G); a proteína RAS ativada recruta RAF que uma vez ativada, fosforila e ativa a quinase MAP-ERK (MEK). Uma vez fosforilada MEK ativa ERK, que no núcleo leva a ativação de múltiplos fatores de transcrição (CARONIA et al., 2011) (Figura 1). A mutação V600E é capaz de levar a uma ativação constitutiva de *BRAF* e consequentemente a uma ativação ininterrupta da via MAPK (GÓMEZ SÁEZ, 2011) que tem papel central no desenvolvimento e progressão do câncer de tireoide (LI; ABDEL-MAGEEd; KANDIL, 2012).

Tabela 2. Principais mutações descritasnos diferentes tipos histopatológicos dos tumores de tireoide derivados de células foliculares.

Alteração Genética	Carcinoma papilífero de tireoide (CPT)	Carcinoma folicular de tireoide (CFT)	Carcinoma pouco diferenciado de tireoide (CPDT)	Carcinoma anaplásico de tireoide (CAT)
Rearranjos em *RET/PTC*	10-20%	-	-	-
Mutação em *BRAF*	40-45%	-	10-20%	20-40%
Mutação em *RAS*	10-20%	40-50%	20-40%	20-40%
Mutação em *TRK*	<5%	-	-	-
Rearranjos *PAX8/PPARG*	-	30-35%	-	-
Mutação em *PI3KCA*	-	<10%	5-10%	10-20%
Mutação em *PTEN*	-	<10%	-	5-15%
Mutação em *CTNB*1	-	-	10-20%	5-60%
Mutação em *AKT1*	-	-	5-10%	5-10%
Mutação em *TP53*	-	-	20-30%	50-80%

Fonte: Dados adaptados de Nikiforov e Nikiforova (2011).

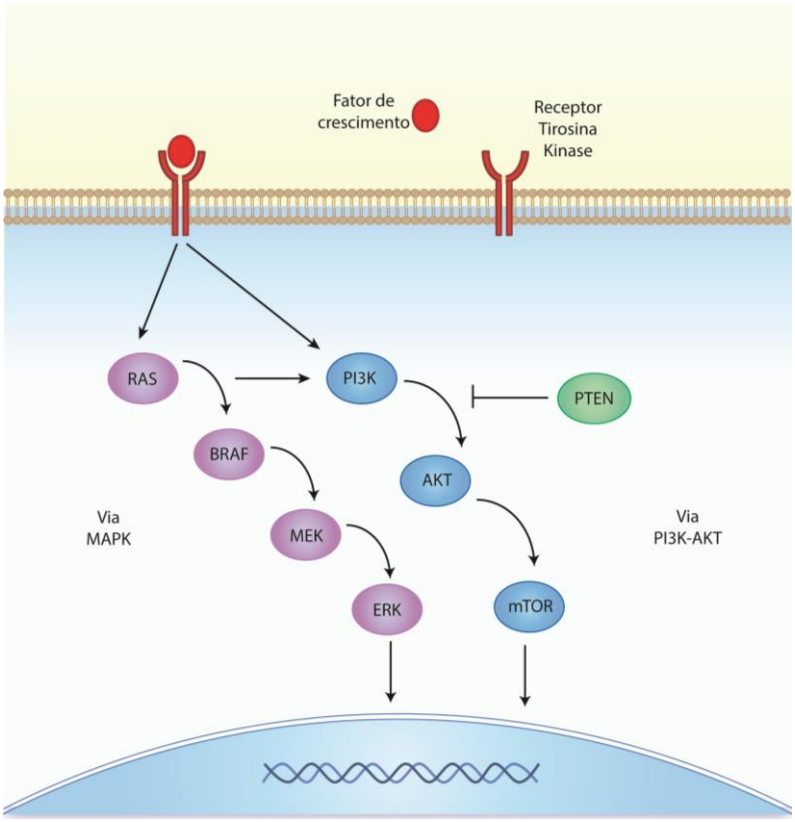

Figura 1. Via de sinalização MAPK e PI3K-AKT-MTOR e seu papel na tumorigênese da tireoide. As vias estão associadas comreceptores tirosina quinases na membrana celular e são responsáveis pela transdução de sinais extracelulares de crescimento para o meio intracelular. Mutações em ponto podem ocorrer em *RAS* e em *BRAF*, assim como rearranjos em *RET/PTC*, mantendo a via MAPK constitutivamente ativa. Mutações em genes da via PI3K são menos comuns. As alterações incluem mutação nos genes *RAS, PIK3CA* e amplificação em *AKT1* além de mutação ou deleção no gene *PTEN*, regulador negativo da via PI3K.
Fonte: modificado Nikiforov e Nikiforova (2011).

A idade de início de apresentação dos CPTs parece estar associada com a prevalência das mutações em *BRAF* e *RET/PTC*. As alterações em *BRAF* tendem a ser mais frequentes em adultos, enquanto os rearranjos em *RET/PTC* são mais prevalentes em crianças e também nos grupos onde o câncer é consequência da exposição à radiação (CARONIA et al., 2011; MACIEL et al., 2005).

Em muitos carcinomas pouco diferenciados e anaplásicos, existe a presença concomitante de carcinoma bem diferenciado com a mutação *BRAF V600E,* a qual está presente nestes dois componentes histológicos. Isto sugere que a mutação em *BRAF* está

presente nos estágios iniciais do desenvolvimento do carcinoma de tireoide (O´NEILL et al., 2010; NIKIFOROV; NIKIFOROVA, 2011).

As mutações em *RET* encontradas nos carcinomas papilíferos de tireoide são exclusivamente rearranjos resultando em proteínas quiméricas (VU-PHAN; KOENIG, 2014). São relatados mais de 11 tipos de rearranjos envolvendo o gene *RET* (TANG; LEE, 2010). Esses rearranjos compreendem a porção 3' do gene *RET* e a 5' de vários genes, sendo mais comuns o RET/PTC1 (gene *H4/D10S170*) e RET/PTC3 (gene *ELE1*) (SANTORO; MELILLO; FUSCO, 2006; NIKIFOROV, 2011). O protoncogene *RET* é um receptor tirosina quinase altamente expresso em células parafoliculares C e com baixa expressão em células foliculares da tireoide (TANG; LEE, 2010). Quando ativado por rearranjos, o domínio tirosina quinase é inalterado e é capaz de ativar a cascata RAS-RAF-MAPK iniciando assim o processo de tumorigênese na tireoide (NIKIFOROV, 2011).

Os três membros da família de genes *RAS* (*H-RAS*, *K-RAS* e *N-RAS*) codificam proteínas localizadas na superfície interna da membrana celular que desempenham um papel central na transdução de sinais que derivam de receptores acoplados a proteíns G, ativando vias importantes de diferenciação e proliferação celular, como a MAPK (DOWNWARD, 1998; NIKIFOROVA et al., 2003b). Mutações envolvendo o códon 61 dos genes *NRAS* e *HRAS* e o códon 12 e 13 de *KRAS* são as mais comumente relatadas nos carcinomas de tireoide originados de epitélio folicular (NIKIFOROV, 2011). As mutações resultam em alelos do gene *RAS* que apresentam maior afinidade com GTP (códons 12 e 13) ou com capacidade de inativar domínios autocatalíticos com função GTPase (códon 61) (HOWELL; HODAK; YIP, 2013). Como resultado, ocorre uma ativação permanente de RAS e uma estimulação crônica de seus alvos nas vias de sinalização MAPK e PI3K/AKT (Figura 1) (NIKIFOROV, 2011). A prevalência das mutações em *RAS* varia de acordo com o subtipo histológico do carcinoma de tireoide. Além disso, a presença destas mutações foi associada com progressão do carcinoma bem diferenciado para pouco diferenciado da tireoide (MOTOI et al., 2000). Evidências em literatura indicam que em CPT as mutações em *RAS* não são eventos comuns mas quando detectadas ocorrem preferencialmente na variante folicular desse carcinoma (MICCOLI, 2014).

Mutações no gene supressor tumoral *TP53* são frequentemente encontradas no carcinoma anaplásico e no pouco diferenciado de tireoide. A presença desta mutação é considerada um evento mais tardio no desenvolvimento do câncer de tireoide (FAGIN;

MITSIADES, 2008; NIKIFOROV; NIKIFOROVA, 2011). A proteína p53 desempenha um papel fundamental no controle do ciclo celular, reparo a danos no DNA e apoptose (revisado por HANEL; MOLL, 2012). Mutações em ponto no *TP53* promovem um aumento da intabilidade genômica, proliferação celular, angiogênese e desdiferenciação (O'NEILL; SHAHA, 2013).

Adicionalmente às alterações genéticas já descritas, as alterações epigenéticas podem desempenhar um papel crítico no desenvolvimento do carcinoma de tireoide.

1.4 Alterações epigenéticas no carcinoma de tireoide

O câncer tem sido descrito como um conjunto de doenças que surge devido a alterações genéticas que afetam as células normais. No entanto, este conceito tem sido expandido para incorporar as mudanças epigenéticas, que juntamente com as alterações estruturais na molécula de DNA, podem alterar o padrão de expressão de genes importantes para o desenvolvimento tumoral (KIM; HAHN, 2007; KANWAL; GUPTA, 2012).

O termo epigenética define o estudo de mudanças na expressão gênica por meio de modificações químicas no DNA e organização da cromatina que ocorrem sem alterar a sequência do DNA e que são herdáveis durante a divisão celular (SCHÜBELER; ELGIN, 2005; SAWAN et al., 2008). A metilação de citosinas, juntamente com as modificações pós-transcrionais de histonas (SHARMA; KELLY; JONES, 2010) e a regulação por pequenos RNAs (LOPEZ et al., 2009) são considerados mecanismos efetores do controle epigenético da expressão gênica.

Dentre as modificações epigenéticas, a metilação do DNA é uma dos mais estudadas por estar envolvida em vários processos biológicos importantes, dentre eles a inativação do cromossomo X e o *imprinting* genômico. O processo de metilação ocorre por meio de uma modificação covalente causada pela adição de grupos metil (CH_3) na posição 5 do anel pirimídico da molécula de citosina, gerando uma 5-metil-citosina. Este processo ocorre em dinucleotídeos em um contexto CpG e requer a atividade enzimática das DNA metiltransferases (DNMTs), que utiliza a S-adenosil metionina (SAM) como doadora do grupo metil (ROBERTSON, 2005; TABY; ISSA, 2010).

Estima-se que o genoma humano contenha aproximadamente 28 milhões de CpGs e a distribuição desses dinucleotídeos CpGs não sejauniforme (ESTELLER;

HERMAN, 2002; STIRZAKER et al., 2014). Estes dinucleotídeos estão distribuídos por todo o genoma incluindo o corpo de genes, regiões intergênicas e regiões repetitivas (DNA satélites e retrotransposons) (PARK et al., 2011; STIRZAKER et al., 2014). As regiões ricas em dinucleotídeos CpGs são denominadas ilhas CpG e estima-se que 60% dos genes humanos estejam associados com essas ilhas (LAIRD, 2003; BERNSTEIN; MEISSNER; LANDER, 2007; JONES, 2012). Uma ilha CpG é definida como um fragmento de DNA maior do que 500pb, com um conteúdo de C+G maior do que 55% e onde a razão entre o número de sítios CpG observado/esperado é superior a 0,65 (TAKAI; JONES, 2002). A localização destas ilhas ocorre preferencialmente na região 5' dos genes (região promotora, sendo que algumas estendem-se até o primeiro exon) e normalmente tais ilhas não se encontram metiladas em células normais (ESTELLER, 2007; HAN; ZHAO, 2009). Regiões localizadas em até 2 kb *up* ou *downstream* das ilhas CpGs e que apresentam uma densidade relativamente baixa de CpGs são conhecidas como ilhas CpGs marginais (*CpG island shores*) e parecem ter um papel importante na regulação da expressão gênica e também na transcrição alternativa de RNAs (IRIZARRY et al., 2009). Além dessa de ilhas e *shores*, tem sido também relatada a importâncias das *shelves,* regiões de 2 a 4kb *up* ou *downstream* aos *CpG island shores* (BIBIKOVA et al., 2011).

Acredita-se que um dos mecanismos envolvidos no controle da expressão gênica ocorra pela interferência no início da trascrição, uma vez que a presença do grupo metil na citosina seria capaz de interferir diretamente na interação de fatores de transcrição à sua região regulatória nos promotores (ROBERTSON, 2005; GUIL; ESTELLER, 2009). Outro mecanismo descrito envolve a regulação indireta por meio do recrutamento de proteínas que se ligam à sequências CpG metiladas (MBPs – *methyl-CpG-biding domain proteins*) que por sua vez recrutam desacetilases de histonas (HDACs) e proteínas remodeladoras de cromatina, resultando na condensação da cromatina e ausência de expressão (IACOBUZIO-DONAHUE, 2009).

O estabelecimento e a manutenção da metilação do DNA são regulados pela família DNMTs, formada por cinco membros identificados como DNMT1, DNMT2/ TRDMT1, DNMT3A, DNMT3B e DNM3L (GROS et al., 2012). A DNMT1 é considerada a mais abundante em mamíferos, sendo a responsável por copiar os sítios hemi-metilados das novas fitas de DNA e manter os padrões de metilação do DNA durante a replicação. As enzimas DNMT3A e 3B são expressas principalmente em células embrionárias e são responsáveis pela metilação de sítios não-metilados no DNA,

em um processo chamado metilação *de novo* (LAIRD, 2003; SUBRAMANIAM, 2014; TABY; ISSA, 2010). As enzimas DNMT2 e 3L não apresentam domínios regulatórios, entretanto, a primeira enzima apresenta uma fraca atividade enzimática, enquanto a DNMT3L é requerida no processo de metilação de loci regulados por *imprinting* em células germinativas (SCHMITT; JELTSCH, 2003; CHENG; BLUMENTHAL, 2008; ESPADA; ESTELLER, 2010; HERMANN; SUBRAMANIAM, 2014).

No processo tumoral, as principais alterações epigenéticas conhecidas englobam a hipermetilação de regiões promotoras de genes supressores tumorais, hipometilação genômica global, hipometilação gene-específica de oncogenes, alterações nos padrões de modificações das histonas além de alterações no padrão de expressão de microRNAs (FEINBERG, 2007; TABY; ISSA, 2010).

As alterações no padrão de metilação são comuns em células tumorais e pelo fato de serem observadas frequentemente em lesões benignas ou em estágios tumorais iniciais, as alterações epigenéticas podem ser consideradas como eventos primários na transformação de células normais (RODRÍGUEZ-PAREDES; ESTELLER, 2011). A perda da metilação do DNA foi a primeira alteração epigenética identificada no câncer (revisado por FEINBERG e TYCKO, 2004). Do ponto de vista funcional, a hipometilação pode ter um papel na transformação de células normais por estar associada com a instabilidade genômica, ativação gênica, perda do *imprinting* genômico e ativação de elementos transponíveis (ESTELLER, 2008; BERDASCO; ESTELLER, 2010). A hipermetilação do DNA ocorre em ilhas CpGs e, de modo geral, está associada com o silenciamento gênico (SAWAN et al., 2008). Esta alteração contribui para o desenvolvimento e progressão do câncer, principalmente por inativar genes supressores tumorais, além do ganho de metilação de genes específicos envolvidos na regulação do ciclo celular, no reparo a danos no DNA, apoptose, diferenciação, angiogênese, metástase e invasão (COSTELLO; PLASS, 2001; GOODMAN; WATSON, 2002; SHARMA; KELLY; JONES, 2010). Além desses processos já bem descritos, alguns relatos mostram que alterações na metilação em regiões associadas a ilhas CpGs marginais estão envolvidas na reprogramação epigenética do câncer (DOI et al., 2009; OGOSHI et al., 2011).

Em relação ao câncer de tireoide, grandes esforços têm sido direcionados nos últimos anos para a compreensão dos mecanismos e da relevância de padrões de metilação aberrantes neste tipo tumoral. A Tabela 3 resume os relatos em literatura que abordaram a investigação de alterações epigenéticas em carcinomas de tireoide. Esses

resultados mostram alterações no padrão de metilação de importantes genes de reparo a danos do DNA, supressores tumorais, genes envolvidos no controle de ciclo celular e funcionamento normal da glândula tireoide.

Uma grande parte do estudos publicados sobre a avaliação da metilação em câncer de tireoide foi realizado em carcinomas bem diferenciados. Hu et al. (2006b) demonstraram que a metilação de região promotora dos genes *TIMP3*, *DAPK*, *SLC5A8* e *RARβ2* está associada com a mutação V600E em *BRAF* e agressividade tumoral em pacientes com carcinoma papilífero. Resultados semelhantes foram descritos para os genes *TIMP3* e *RARβ2,* além de uma correlação negativa entre metilação de *RASSF1A* e a mutação em *BRAF* em CPT (BRAIT et al., 2012).

A metilação do promotor em *RASSF1A* é um dos eventos epigenéticos mais comunsem cânceres humanos e leva ao silenciamento desse gene (PFEIFER; DAMMANN, 2005). Apesar de presente nos CPTs, a hipermetilação de *RASSF1A* é observada com mais frequência em carcinomas foliculares de tireoide além de estar presente em adenomas (XING et al., 2004). Estes dados sugerem que a hipermetilação de *RASSF1A* é considerada um evento inicial no desenvolvimento do câncer de tireoide (XING et al., 2004; NAKAMURA et al., 2005).

Outro supressor tumoral importante envolvido no processo de tumorigênese de tireoide é o gene *PTEN*. Esse gene codifica uma proteína que age como antagonista da via PI3K e é frequentemente mutado ou sua expressão é perdida no câncer de tireoide (BRZEZIANSKA; PASTUSZAK-LEWANDOSKA, 2011). A metilação aberrante da região promotora do gene *PTEN* foi observada principalmente em adenomas e carcinomas foliculares (83% e 84% das amostras, respectivamente) quando comparadas a carcinomas papíliferos (47%) (ALVAREZ-NUÑEZ et al., 2006). A presença de hipermetilação do gene *PTEN* também foi observada em carcinomas anaplásicos de tireoide em uma frequência maior do que a encontrada em carcinomas foliculares e lesões benignas. A hipermetilação de *PTEN* foi também associada com alterações genéticas na via PI3K/AKT, sugerindo que a inativação do gene causada pela metilação pode deixar de regular negativamente a via de sinalização já ativada pelas mutações e contribuir para a progressão do câncer de tireoide (HOU; JI; XING, 2008).

Tabela 3. Resumo dos relatos publicados em literatura envolvendo alterações epigenéticas em amostras de câncer de tireoide e lesões benignas.

Tamanho da amostra	**Gene(s) Estudado(s)**	**Abordagem metodológica**	**Resultados obtidos**	**Referência**
6 CPTs	*MET*	Sequenciamento	Ausência de metilação.	SCARPINO et al., 2004
12 CPTs e 1 células de Hurthle	*RUNX3*	COBRA	Hipermetilção em 10 CPTs.	KO et al., 2012
70 CPTs, 12 CFTs e 7 AFTs e 7N	*MLH1* e *MGMT*	MSP	Metilação em 44% dos PTCs, 33% dos FTCs e 64% AFTs (*MLH1*); 64% dos PTCs, 67% dos FTCs e 57% AFTs (*MGMT*). Ausência de relação entre mutações e metilação.	SANTOS et al., 2013
3 CMTs, 10 CFTs, 12 CPTs e 6 CATs	*RASSF2*, *RASSF3*, *RASSF4*, *RASSFA*, *RASSF5C*, *WW45*, *MST1*e *MST2*	COBRA Sequenciamento	Aumento de metilação em *RASSF2* em CPT, CFT e CAT. Significante aumento em pacientes > 60 anos.	SCHAGDARSURENGIN et al., 2010
24 adenomas 23 CPTs, 4 CFTs, 5CMTs, 20 nódulos hiperplásicos, 6 tireoidites	*RASSF1A*, *TSHR*, *S100*, *RARβ2*, *DAPK*, *p16*, *CDH1*, *CALCA*, *TIMP3*, *TGFβ*, *GSTpi*	qMSP	Hipermetilação de dois ou mais genes em 25% das hiperplasias, 38% dos adenomas e 48% dos cânceres. Correlação mutação de *RARβ2*.	HOQUE et al., 2005
33 CPTs, 31CFTs, 20 AFTs	*TRα* e *TRβ*	MSP	Hipermetilação de *TRβ* nos tumores, com prevalência em CFT.	JOSEPH et al., 2007
19 PTCs, 3 fvPTCs, 5 FTCs, 3 células Hurthle, 1 ATC, 19 benignos	*RIZ1*	MSP	Metilação em 100% das amostras tumorais estudadas.	LAL et al., 2006
38 CPTs	23 genes de reparo	MSP	Hipermetilação em *hMLH1*, *PCNA* e *OGG1* e associação com metástase em linfonodos. Associação de *hMLH1* e mutação em *BRAF*.	GUAN et al., 2008
42 N, 42 CPTs, 4 CFTs, 5 CMTs, 12 CAT, 23 HTTs, 3 AFTs	*RASSF1A* e *NORE1A*	MSP	Hipermetilação em *RASSF1A* em CPT (32%), CFT (100%), CMT (40%), AFT (33%) e HTT (25%).	NAKAMURA et al., 2005
45 CPTs	*ARHI*, *MEST*, *CDH1*, *p16INK4A*, *KCNQ1*, *RASSF1A*, *SLC5A8*, *VHL*	MSP e Sequenciamento	Média maior de MI em genes de região regulada por *imprinting* (*ARHI*, *p16INK4A*, *MEST* e *KCNQ1*).	CZARNECKA et al., 2011
19 CPTs	*CITED1*	Sequenciamento	Hipometilação associada com aumento de expressão.	SASSA et al., 2011
5 VDE-CPTs e 7 CPTs	E-caderina	MSP	Metilação parcial em 60% VDE e 71% CPT.	ROCHA et al., 2001
138 CPTs	*TIMP3*, *SLC5A8*, *DAPK* e *RARβ2*	qMSP	Metilação de *RARβ2* associada com tabagismo.	KISELJAK-VASSILIADES; XING,

				2011
9 adenomas, 13 CFTs, 35 CPTs, 7 CATs	*SLC26A4*	MSP e Sequenciamento	Hipermetilação em adenoma (44%), CFT (46%), CPT (71%) e CAT (71%).	XING et al., 2003b
13 CPTs, 10 CFTs, 9 CATs, 6 CMTs, 10 AFT e 12 bócios	*RASSF1A*, *p16INK4A*, *TSHR*, *MGMT*, *DAPK*, *ERα*, *ERβ*, *RARβ*, *PTEN*, *CD26*, *RB*, *SLC5A8*, *UCHL1*, *DLC1*, *TIMP3*, *SLIT2*, *GSTP1*	MSP	*RASSF1A*, *p16INK4A*, *TSHR*, *MGMT*, *DAPK*, *ERα*, *ERβ*, *RARβ*, *PTEN*, *CD26*, *SLC5A8* e *UCHL1* metilados em CAT.	SCHAGDARSURENGIN et al., 2006
40 CPTs	*TMS1*	MSP	Metilação em 33% das amostras	SIRAJ et al., 2011
11 CPTs e 2 CFTs	24 genes supressores tumorais	MS-MLPA e MSP	Metilação em *CASP8*, *RASSF1* e *NIS* é um evento precoce e independente do tipo tumoral.	STEPHEN et al., 2011

qMSP – *Real Time Quantitative Methylation Specific PCR*; MSP – *Methylation Specific PCR*; CPT – Carcinoma papilífero de tireoide; CFT – Carcinoma folicular de tireoide; AFT – Adenoma folicular de tireoide; CMT – Carcinoma medular de tiroide; HTT – Tumor trabecular hialinizante*;* MI – Índice de metilação (MI = (M)/(M+U), onde M= concentração alelo metilado e U= concentração alelo não metilado); VDE-PTC – variante difusa esclerosante de CPT; CAT – Carcinoma anaplásico de tireoide; MS-MLPA – *Methylation Specific Multiplex Ligation-dependent Probe Amplification*; COBRA – *Combined Bisulfite Restriction Analysis.*

O funcionamento normal das células da glândula tireoide requer um complexo mecanismo regulatório (KONDO et al., 2008) e genes necessáriospara o funcionamento das células normais da tireoide frequentemente têm uma diminuição de sua expressão com a progressão tumoral (RUSSO et al., 2011). Foram relatados padrões alterados de metilação em ilhas CpGs de regiões promotoras dos genes *NIS* e *TSHR* (XING, 2007b). O gene *TSHR* foi encontrado hipermetilado em amostras de câncer papilífero e folicular (XING et al., 2003a), assim como a hipermetilação em *SLC26A4*, onde o ganho de metilação que foi progressivamente maior nos adenomas seguidos de CFTs e semelhante entre CPTs e CATs (XING et al., 2003b). A mutação V600E em *BRAF* em carcinoma papilífero também foi associada com a redução de expressão de genes críticos no metabolismo de iodo (DURANTE et al., 2007). Em resumo, o silenciamento de genes específicos envolvidos no funcionamento da tireoide geralmente ocorre com a progressão e desdiferenciacão do câncer de tireoide e a metilação desses genes pode estar envolvida no mecanismo de patogênese e progressão tumoral (XING, 2007b).

Apesar da importância do conhecimento da metilação dos genes relacionados ao desenvolvimento do câncer, os estudos investigando a metilação do DNA em carcinomas papilíferos são, em sua maioria, restritos a abordagens de genes candidatos.

Embora essas técnicas sejam capazes de evidenciar o padrão de metilação dos genes particulares (SIEGMUND; LAIRD, 2002), não são capazes de avaliar o padrão global de metilação. Nos últimos anos, tecnologias para análise de metilação global têm permitido um grande avanço na área da epigenômica.

Em 2011, Hou et al. avaliaram as alterações epigenéticas globais associadas com a mutação V600E em duas linhagens de carcinoma papilífero de tireoide que passaram pelo processo de *knockdown*com shRNA (Short Hairpin RNA). Um grande número de genes considerados importantes nesse processo foi encontrado hipo ou hipermetilado, além de demonstrar o papel dos genes *HMGB2* e *FDG1* no controle da proliferação e invasão celular, respectivamente (HOU et al., 2011).

O uso da metodologia de análises globais também foi utilizado para identificar assinaturas moleculares entre diferentes subtipos do câncer de tireoide (Tabela 4). Rodríguez-Rodero et al. (2013) usando a plataforma 27K da Illumina analisaram dois carcinomas papilíferos, dois carcinomas foliculares, dois carcinomas anaplásicos e dois carcinomas medulares, além de duas amostras normais e quatro linhagens celulares. Os autores encontraram uma assinatura epigenética no carcinoma papilífero e folicular (262 e 352 genes hipermetilados, além de hipometilação em, 13 e 21 genes, respectivamente). A análise dos carcinomas anaplásicos e medulares revelou um maior conjunto de genes hipometilados (280 e 393, respectivamente) quando comparado ao número de genes hipermetilados (86 no carcinoma anaplásico e 131 no carcinoma medular). Os autores ainda encontraram vários potencias genes supressores tumorais e oncogenes regulados por metilação aberrante nos tecidos estudados.

Utilizando a plataforma 27k da Illumina, Kikuchi et al. (2013) analisaram 14 amostras de carcinomas papilíferos e relataram um perfil de metilação diferencial em amostras com a mutação no genes *BRAF* e *RAS*. Os autores também mostraram diminuição na expressão de seis genes encontrados hipermetilados (*HIST1H3J*, *POU4F2*, *SHOX2*, *PHKG2*, *TLX3* e *HOXA7*) em linhagens celulares de carcinoma de tireoide, que quando tratadas com 5-aza- 2´deoxicitidina e/ou tricostatina A, voltaram a expressar esses genes, com exceção do gene *SHOX2*. Recentemente, Ellis et al. (2014) avaliaram 51 CPTs (plataforma 450k da Illumina)e demonstraram que a variante folicular apresenta um perfil de metilação distinto da variante clássica e que existe também uma diferença entre os perfis de metilação das amostras de acordo com o status de mutação em *BRAF*, *RAS* e *RET/PTC*.

Tabela 4. Resumo dos estudos globais de alterações epigenéticas em amostras de câncer de tireoide.

Amostras	Sondas hipometiladas	Sondas hipermetiladas	Plataforma	Validação	Análise Integrada*	Referência
2 linhagens derivadas de CPT	10 genes	59 genes	12K Human CpG-island Array chip (Microarray Center, University Health Network, Toronto, ON, Canada)	QMSP nas mesmas linhagens utilizadas	Não	HOU et al., 2011
2 CPTs, 2 CFTs, 2 CATs, 2 CMTs, 2 NT, 4 linhagens	CPTs - 14 CFTs - 24 CATs - 328 CMTs - 490 linhagens derivadas de CPT e CFT - 25 linhagens derivadas de CMT e CAT - 598	CPTs - 309 CFTs - 408 CATs -114 CMTs -148 linhagens derivadas de CPT e CFT - 334 linhagens derivadas de CMT e CAT - 198	Infinium HumanMethylation27k Illumina	Pirosequenciamento amostras independentes	Dados expressão GEO	RODRIGUEZ-RODERO et al., 2013
14 CPTs 10NT	PTCs - 0 genes	PTCs - 25 genes em 3 ou + amostras	Infinium HumanMethylation27k Illumina	Pirosequenciamento amostras independentes	Não	KIKUCHI et al., 2013
51 CPTs 8 NT	CPT clássico -2796 fvCPT - 405	CPT clássico – 1023 fvCPT- 164	Infinium HumanMethylation450k Illumina	-	Não	ELLIS et al., 2014
42 CPTs, 5 fvCPT, 18 CFTs, 18 AFT	CPTs - 53 CFTs - 83 AF - 9	CPTs - 39 CFTs - 460 FA - 89	Infinium HumanMethylation27k Illumina	Sequenciamento amostras grupo teste e independentes	Dados expressão de subgrupo de 31 amostras	MANCIKOVA et al., 2014

CPT – Carcinoma papilífero de tireoide; CFT – Carcinoma folicular de tireoide; AFT – Adenoma folicular de tireoide; CMT – Carcinoma medular de tiroide; fvCPT – Variante folicular do carcinoma papilífero de tireoide; NT – amostra normal de tireoide,QMSP - Quantitative methylation-specific PCR.* Análise integrada dos dados de metilação com dados de expressão.

Em outra análise recente, Mancikova et al. (2014) analisaram cerca de 27.000 CpGs em 83 tumores (47 carcinomas papilíferos, 18 foliculares e 18 adenomas) e realizaram uma análise integrada entre os dados de metilação com dados de expressão de transcritos em um subgrupo de 31 amostras publicados anteriormente pelo grupo. Foi demonstrada alteração no perfil de metilação segundo o tipo histológico do tumor e com mutação em *BRAF* e *RAS*, além de genes importantes no processo tumoral cuja expressão estava associada com metilação.

Uma abrangente análise do genoma de 496 amostras de carcinoma papilífero de tireoide publicado pelo TCGA (*The Cancer Genomic Atlas*) elucidou o papel de muitas alterações que estão envolvidas no desenvolvimento e progressão do câncer de tireoide (Cancer Genome Atlas Research Network, 2014). As análises de variantes genômicas, expressão de transcritos e metilação do DNA mostraram a existência de diferentes *drivers* moleculares. *Drivers* refere-sea mutações em genes que conferem uma vantagem no crescimento da célula tumoral e é selecionada positivamente pelo microambiente tumoral (STRATTON; CAMPBELL; FUTREAL, 2009). A partir dos dados da metilação obtidos, uma análise de clusterização não supervionada permitiu a identificação de quatro clusters distintos do carcinoma papilífero (classificados como Folicular, Ilhas CpGs metiladas, Clásico 1 e Clássico 2) e dois meta-clusters maiores de acordo com as mutações *drivers* encontradas, incluindo a V600E em *BRAF* e *RAS*.

Embora o carcinoma papilífero de tireoide tenha sido muito estudado, o número de investigações epigenéticas neste e em outros subtipos histológicos ainda é limitado. Além disso, a maioria dos estudos utiliza uma plataforma que apresenta uma menor cobertura. Nós utilizamos uma plataforma de array com grande cobertura de CpGs do genoma cujos resultados tem potencial para revelar marcadores moleculares confiáveis.

2. OBJETIVOS

2.1 Geral

Identificar o perfil de metilação em lesões da glândula tireoide na busca de marcadores moleculares diagnósticos e prognósticos úteis na prática clínica.

2.2 Específicos

- Analisar o perfil de metilação em lesões benignas da tireoide, carcinomas papilíferos, foliculares, pouco diferenciados e anaplásicos da tireoide e tecido não neoplásico adjacente, com o intuito de identificar sequências diferencialmente metiladas;
- Confirmar o perfil de metilação em amostras independentes do *array* utilizando banco de dados externos;
- Desenvolver um algoritmo classificador molecular com potencial uso diagnóstico de carcinomas de tireoide;
- Identificar vias de sinalização alteradas e possíveis alvos para intervenção terapêutica;
- Correlacionar, quando possível, os dados obtidos com parâmetros clínico-histopatológicos na busca de marcadores prognósticos e estratificação de risco de pacientes com comprometimento linfonodal.

3. MATERIAL E MÉTODOS

3.1 Casuística

Esse projeto foi aprovado pelo Comitê de Ética em Pesquisa da Fundação Antônio Prudente – A.C. Camargo Cancer Center (CEP nº 475.385) (Anexo 1). As amostras de tumores primários foram coletadas durante a congelação na cirurgia entre os anos de 2000 e 2013 e armazenadas no Banco de Tumores da Instituição. Os pacientes assinaram o Termo de Consentimento Livre e Esclarecido autorizando o uso do material biológico para pesquisa.

Neste estudo, foram selecionadas 91 amostras de lesões tireoidianas (LT) e 51 amostras de tecidos normais adjacentes (TN) ao tumor.

Foram incluídos casos que apresentavam qualidade e quantidade de material suficientes no Biobanco da instituição e em que houvesse dados clínicos e histopatológicos completos. Para os CPT, foram utilizados os seguintes critérios de exclusão: a impossibilidade de obtenção de informações clínico-patológicas relevantes; apresentação de histórico de neoplasias malignas prévias (com exceção de carcinoma basocelular de pele); ablação parcial de tireoide [tireoidectomia parcial (TP) ou tireoidectomia total (TT) sem tratamento com radioiodo (RI), supressão inadequada de TSH (do inglês, *Thyroid Stimulating Hormone)* por terapia com tiroxina sintéticae estimativa de seguimento clínico inferior a cinco anos até o final do estudo, com exceção de pacientes que sofreram recorrência. Para a obtenção das demais neoplasias, foi considerada a impossibilidade de obtenção de informações clínico-patológicas relevantes e a apresentação de histórico de neoplasias malignas prévias.

3.1.1 Caracterização das amostras

As amostras do grupo teste foram compostas por 91 LT (17 LBTs, 60 CPTs, 10 CFT/CCHs, 4 CPDT/CATs) e 51 TN (provenientes de tecidos adjacentes de CPTs) e entre essas amostras, 141 passaram pelos critérios de qualidade das análises de *array* (1 amostra TN foi removida), os quais estão descritos no Apêndice 2. A Tabela 5 apresenta a caracterização dos pacientes com CPT, CFT, CCH, CPDT e CAT envolvidos nesse estudo. Entre os pacientes com lesões benignas (8 adenomas, 6 bócios e 3 tireoidites), a maioria era

do sexo feminino (71%) e com mais de 45 anos de idade (59%). A mediana do tamanho dos adenomas incluídos no estudo foi de 1,35cm.

Nos casos dos carinomas, o desfecho clínico foi definido como: (1) Boa evolução clínica (BEC): nenhuma suspeita de doença ativa por exames de imagem e mensuração de Tg sérica. (2) Evolução clínica ruim (ECR): pacientes com recidiva (doença recorrente ou persistente após tratamento com radioiodo, confirmado por análise histopatológica) e/ou morreram em decorrência da doença.

Tabela 5. Caracterização dos pacientes e dos carcinomas de tireoide selecionados para o estudo.

Características	CPT		Outros Subtipos	
	N	%	N	%
Idade				
<45 anos	37	61,67	4	28,57
≥45 anos	23	38,33	10	71,43
Sexo				
Feminino	44	73,33	10	71,43
Masculino	16	26,67	4	28,57
Histologia (excluindo CPT)				
CFT	-	-	8	57,14
CCH	-	-	2	14,29
CPDT	-	-	1	7,14
CAT	-	-	3	21,43
Variante predominante (CPT)				
Clássica	47	78,33	-	-
Folicular	10	16,67	-	-
Rara	3	5,00	-	-
Dimensão tumor primário				
Mediana (intervalo) cm	1,3 (0,5-5,5)	-	2,3 (0,9-13)	-
mCPT(≤1cm)	25	41,67	-	-
CPT (>1cm)	35	58,33	-	-
Extensão extratireoidiana				
Não	30	52,63	7	53,85
Sim	27	47,37	6	46,15
Ni	3	-	1	-
Invasão angiolinfática				
Sanguínea	2	3,39	5	38,46
Linfática	3	5,08	1	7,7
Ambas	1	1,7	2	15,38
Não	53	89,83	5	38,46
Ni	1	-	1	-
Invasão Perineural				

Não	42	93,33	10	23,08
Sim	3	6,67	3	76,92
Ni	15		1	-
Acometimento linfonodal				
Não (cN0, pN0)	32	53,33	9	69,23
Sim (pN1)	28	46,67	4	30,77
Ni	-	-	1	-
Recorrência				
Não	43	73,33	5	71,43
Sim	16	26,67	2	28,57
Ni*	1	-	7	-
Morte				
Não	59	98,33	10	71,43
Sim	1	1,67	4	28,57
Tempo de seguimento (meses)#	83,8 (1,1-142,9)	-	63,3º (4,0-139,4)	-

Legenda: CPT = carcinoma papílifero de tireoide; mCPT= microcarcinoma papilífero de tireoide;CFT = carcinoma folicular de tireoide; CCH = carcinoma células de Hürthle; CPDT = carcinoma pouco diferenciado de tireoide; CAT = carcinoma anaplásico de tireoide; NI= não informado; * 1 CFT com seguimento perdido, 1 CPT, 2 CFT sem seguimento de 5 anos e 4 carcinomas não diferenciados com doença agressiva e morte antes do diagnóstico de recorrência. #dados obtidos até agosto de 2014. º somente para CFT.

3.2 Extração de DNA

Todas as amostras foram histologicamente avaliadas antes da extração dos ácidos nucleicos para confirmar a presença de tecido tumoral (aproximadamente 100%) ou normal. Os ácidos nucleicos foram extraídos pela equipe do Laboratório de Genômica e Biologia Molecular do Centro de Pesquisa - A.C. Camargo Cancer Center.

A extração do DNA genômico das amostras tumorais e normais foi baseada em protocolos convencionais incluindo a degradação enzimática com proteinase K *(Promega Corporation, Madison, WI, USA)* (10mg/mL), seguida da purificação com solventes orgânicos (fenol/clorofórmio) e tratamento com RNase (*Epicentre Biotechnologies, Madison, WI, USA*). Foram utilizadas amostras de DNA de boa qualidade, avaliads por eletroforese em gel de agarose 1%. As amostras de DNA foram armazenadas a -20°C até o momento do uso.

3.3 Análise do perfil de metilação

Para a análise do perfil de metilação foi utilizada a *Plataforma Infinium® Human Methylation450 BeadChip* (Illumina, San Diego, CA, USA). Essa plataforma interroga mais de 480.000 sítios de metilação por amostra com a resolução de um único nucleotídeo,

apresenta uma cobertura de 96% das ilhas CpGs descritas no genoma e 98,9% dos RefGenes, além de ilhas CpGs estendidas (0 a 4Kb flanqueando as ilhas CpGs).

A plataforma utiliza os ensaios *Infinium* I(Figura 2A) e *Infinium* II (Figura 2B). No ensaio *Infinium* I, duas sondas são utilizadas para interrogar o locus CpG, uma sonda para CpG metilado e uma para CpG não metilado. Nesse modelo, a região 3´ da sonda é desenhada para parear com a base citosina "protegida" (*design* metilado) ou parear coma base timina resultado da conversão por bissulfito e amplificação (*design* não metilado). No ensaio *Infinium* II apenas uma sonda por locus CpG é utilizada, sendo a região 3´ desta complementar a base anterior ao sítio de interesse (C pareado a G) e a extensão resulta na adição de uma guanina ou adenina marcada complementar a citosina (*design* metilado) ou timina (*design* não metilado) (BIBIKOVA et al., 2011).

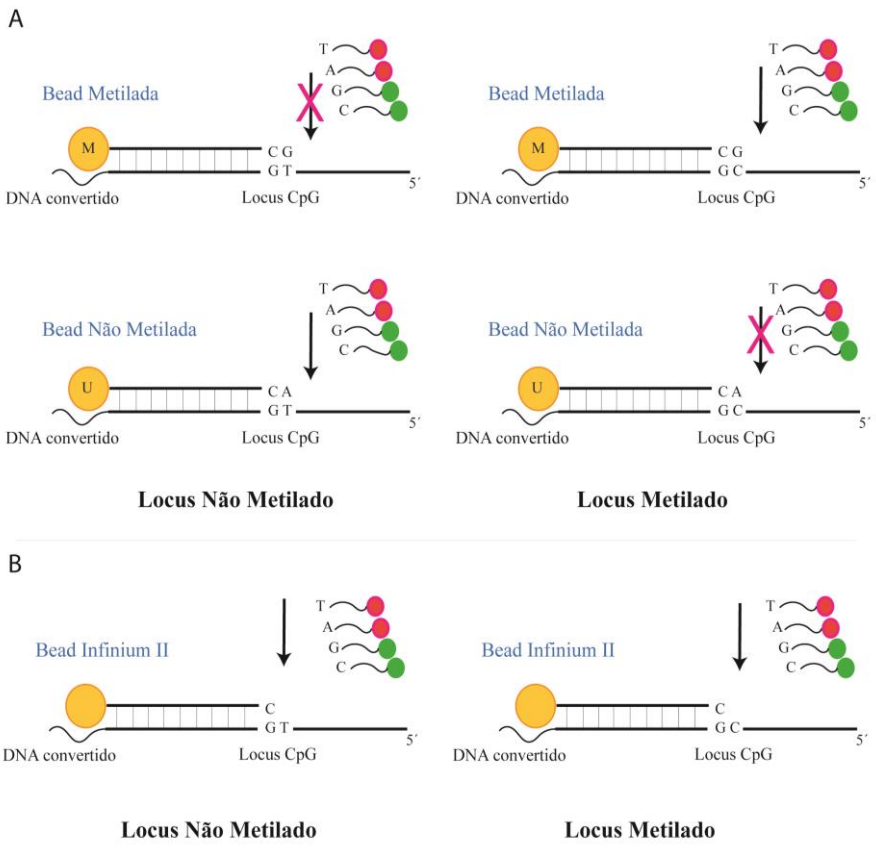

Fonte: modificado Bibikova *et al*., 2011

Figura 2. Química utilizada na Plataforma Human Methylation450 BeadChip (Illumina). **A.** Química *Infinium* I. **B.** Química *Infinium* II.

3.3.1 Quantificação das amostras de DNA

As amostras dos tecidos primários foram quantificadas com o Kit *Qubit® dsDNA BR Assay no Qubit® 2.0 Fluorometer*. Esse método permite a quantificação precisa das amostras, requerida para o início da análise do perfil de metilação. Inicialmente, foi feita uma diluição da solução corante fluorescente em um tampão Qubit® dsDNA BR em uma concentração 1:200.Para calibrar o equipamento, foram utilizadas duas amostras padrão Qubit® dsDNA BR (10µL) adicionadas a 190µL da solução diluída. As soluções de leitura das amostras do estudo foram preparadas com 199µL da solução diluída e 1µL de DNA de cada amostra. Todas as amostras foram homogeneizadas por 3 segundos em vórtex e incubadas em temperatura ambiente por 2 minutos sendo, em seguida, realizadas as quantificações.

3.3.2 Modificação do DNA por bissulfito de sódio

O DNA foi modificado com o *EZ DNA Methylation-Gold™ Kit* (*Zymo Research, Irvine, CA, USA)* com modificações do protocolo original (Illumina) para um melhor rendimento das reações. O primeiro passo consistiu na desnaturação do DNA pela adição de 130µL de *CT Conversion Reagent*em 20µL de DNA (500ng). O DNA foi convertido pela incubação das amostras em termociclador com as seguintes condições: 16 ciclos de 95ºC por 30 segundos e 50ºC por 1 hora seguidas de uma etapa de 4^0C por 10 minutos.

Os passos seguintes consistiram na adição de 600µL de *M-Binding Buffer* na coluna *Zymo-Spin™ IC Column* e transferência do volume (150µL) incubado contendo o DNA. As amostras foram centrifugadas em velocidade máxima por 30 segundos sendodescartado o resíduo que passou pelas colunas. Cem µL de *M-Wash Buffer* foram adicionados a coluna sendo repetidas as etapas de centrifugação e descarte. A desulfonação do DNA foi realizada pela adição de 200µL de *M-Desulphonation Buffer* e incubação a temperatura ambiente por 15 minutos, seguidos por centrifugação durante 30 segundos a 5000g e descarte. Em seguida, foram realizadas duas etapas adicionais de lavagem com 200µL de *M-Wash Buffer* e centrifugação por 30 segundos a 5000g e descarte. A recuperação do DNA modificado foi realizada pela adição de 12µL de *M-Elution Buffer* na matriz da coluna e centrifugação por 5 minutos a 5000g.

3.3.3 Preparação das lâminas de *microarray*

Amplificação do DNA. Após a modificação do DNA por bissufito de sódio, foi utilizado4μL da amostra para a desnaturação e amplificação do DNA. Inicialmente, foram adicionados ao DNA modificado, 20μL do reagente *Multi-Sample Amplification 1 Mix* e 4μL de NaOH 0,1N. As amostras foram então homogeneizadas em vórtex por 1600rpm por 1 minuto, centrifugadas a 280xg por 1 minuto e incubadas a temperatura ambiente por 10 minutos. A próxima etapa consistiu na adição de 68μL de *Random Primer Mix* e 75μL de *Multi-Sample Amplification Master Mix* ao mix preparado anteriormente. Após homogeneização por inversão e centrifugação por 280xg por 1 minuto as amostras foram incubadas a 37^0C (no *Illumina Hybridization Oven*) por aproximadamente 20 horas (não excedendo 24 horas).

Fragmentação e Precipitação do DNA. O DNA amplificado na etapa anterior foi fragmentado por um processo enzimático *end-point* para evitar uma fragmentação excessiva. A reação ocorreu pela adição de 50μL de *Fragmentation solution*.As amostras foram homogeneizadas em vórtex a 1600rpm por 1 minuto e centrifugadas a 50xg por 1 minuto. Em seguida as amostras foram incubadas a 37^0C por 1 hora. Para a precipitação do DNA foram adicionados 100μL de *Precipitation Solution* a cada amostra e estas foram homogeneizadas em vórtex a 100rpm por 1 minuto. Procedeu-se a incubaçãoa 37^0C por 5 minutos e em seguida centrifugação a 50xg (22^0C) por 1 minuto. Foram então adicionados 300μL de 2-propanol 100% e as amostras foram mantidas a 4^0C por 30 minutos e, então, centrifugadas a 3000xg por 20 minutos. Após a centrifugação, o sobrenadante foi removido por inversão em papel absorvente e a placa permaneceu na posição invertida à temperatura ambiente por uma hora para secagem do sedimento.

Ressuspensão do DNA e Hibridação MultiBead Chip. Nessa etapa, foram adicionados 46μL de *Ressuspension, Hybridization* and *Wash solution* ao DNA precipitado, a placa foi selada e as amostras mantidas a 48^0C por uma hora a 37^0C (no Illumina *Hybridization Oven*). Posteriormente as amostras foram homogeneizadas em vórtex a 1800rpm por 1 minuto. Para o passo de hibridação, a *BeadChip Chamber gasket* foi encaixada em uma *BeadChip Chamber* e então 400μL de *Humidifying Buffer* foram adicionados em cada *HybChamber Reservoir*. A tampa da *BeadChip Chamber* foi fechada e travada, sendo mantida em temperatura ambiente (no máximo uma hora) até o momento da adição das *BeadsChips.* As amostras ressuspendidas foram desnaturadas a 95^0C por 20 minutos e então mantidas a temperatura ambiente por mais

30 minutos. Cada *BeadChip*foi colocada no *HybChamber Insert* imediatamente antes do seu uso e 15µL de cada amostra ressuspendida foi pipetada nas seções especificadas do *BeadChip*. Os insertos contendo as *BeadChip* foram colocados no *llumina HybChamber* montadoanteriormente. As *BeadChip* foram então incubadas a 48^{0}C por pelo menos 16 horas (não excedendo 24 horas).

Lavagem. Nesse processo, as *BeadChips* foram preparadas para dar início ao processo *X Stain BeadChip*. As *BeadChips* retiradas do forno de hibridação e mantidas à temperatura ambiente por 30 minutos. O selo de cobertura da lâmina foi retirado cuidadosamente e as *BeadChips* foram lavadas com 200mL de PB1 durante 1 minuto (reagente usado para preparar as *BeadChips* para hibridação).

Extensão Single-Base. Nessa etapa o DNA não hibridado e o DNA hibridado de uma maneira inespecífica foram retirados da lâmina por lavagem e ocorreu a extensão de iniciadores hibridados com a incorporação de nucleotídeos marcados. Inicialmente, a lâmina que passou pelo processo anterior de lavagem foi colocada em uma *Flow-Through Chamber* (mantida a 44^{0}C) e incubada com *Ressuspension*, *Hybridization* and *Wash solution* por 30 segundos por 5 vezes. As seguintes soluções foram posteriormente usadas para incubação: 450µL de *X Stain BeadChip solution 1* por 10 minutos, 450µL de *X Stain BeadChip solution 2* por 10 minutos, 200µL de *Two-Color Extension Master Mix* por 15 minutos, 450µL de formamida 95% /1mM EDTA por 1 minuto; esse último processo foi repetido uma vez e então seguiu-se uma incubação de 5 minutos. O passo seguinte consistiu em iniciar a rampa de temperatura da *Chamber Rack* (32^{0}C), adicionar 450µL de *X Stain BeadChip solution 3*, incubação de 1 minuto e repetição dessa última etapa.

Marcação da BeadChip. A partir do momento que a temperatura *Chamber Rack* estabilizou em 32^{0}C, foram adicionados 250µL de *Superior Two-Color Master Mix*, seguidos de uma incubação por 10 minutos, adição de 450µL de X *Stain BeadChip solution 3* e incubação por 1 minuto, esse último passo foi repetido por mais uma vez e então após 5 minutos todas as etapas foram reiniciadas por mais 4 vezes.

Lavagem e secagem. A última etapa da leitura consistiu em uma lavagem em 310mL de PB1 por 10 vezes e uma incubação nesse mesmo reagente por mais 5 minutos, seguida de uma segunda lavagem em *X Stain Bead Chip solution 4* com o mesmo processo acima. As lâminas então foram mantidas em dessecador a vácuo (675mm Hg) por 50-55 minutos. Amostras

pareadas (tecido tumoral e tecido normal adjacente) foram processadas no mesmo *chip* a fim de evitar variação entre experimentos. Procedeu-se o escaneamento das lâminas.

Captura e Análise dos Dados. A captura das imagens foi realizada no *HiScan Systems* (Illumina). Os dados obtidos da leitura dos canais vermelho e verde são convertidos em um sinal de metilado e não metilado. Após a geração desse sinal um valor β entre 0 e 1 foi fornecido, onde o valor 1 significa totalmente metilado. O cálculo do valor de β utilizado na Plataforma *Infinium® Human Methylation450 BeadChip* é realizado pela fórmula abaixo:

$$\beta = \frac{\mathrm{Max}(\mathrm{M}, 0)}{(\mathrm{Max}(\mathrm{M}, 0) + \mathrm{Max}\ (\mathrm{U}, 0) + 100}$$

Onde: M - sinal da sonda para CpG metilado
U - sinal da sonda para CpG não metilado

3.4 Análises dos dados dos *arrays* de metilação

3.4.1 Controle de qualidade

O controle de qualidade dos dados brutos obtidos da leitura dos *arrays* foi avaliado pelo programa R versão 3.0.2 (R Core Team, 2013) e o pacote de análise do Bioconductor *WateRmelon* (SCHALKWYK et al., 2013).

O primeiro passo das análises incluiu a filtragem das sondas mapeadas em regiões contendo SNPs (*Minor Allele Frequence* >5% para todas as populações de acordo com o banco de dados 1000 Genomas (*www.1000genomes.org/)*), nos cromossomos X e Y e sondas que co-hibridizam em sequências alternativas homó ogas (≥ 49 pares de base) (CHEN et al., 2013). Também foram removidas sondas que apresentaram valores de p>0,05 e contagem de beads < 3 em 5% das amostras.

A checagem do controle de qualidade foi realizada por meio da distribuição dos sinais obtidos para sondas metiladas e não metiladas e do uso da análise multivariada MDS (*Multidimensional Scaling*).

3.4.2 Análise das sondas diferencialmente metiladas

O próximo passo na análise foi o ajuste do viés da cor, normalização entre as amostras pelo método quantile e entre sondas pelo método BMIQ (*Beta-Mixture Quantile Normalization*). Nessa etapa, o algoritmo normaliza a distribuição das sondas do tipo 2 (*Infinium II*) de acordo com as características de distribuição dos valores de beta das sondas tipo 1 (*Infinium I*), além de eliminar o enriquecimento desse tipo de sonda, causado pela baixa dinâmica das sondas tipo 2 (TESCHENDORFF et al., 2013).

Para checar os possíveis efeitos nos resultados causados pela posição das amostras nos *arrays* (*batch effects*), os valores de beta foram transformados logariticamente em valores M. Esse valor, quando comparado ao valor de beta, é mais confiável estatisticamente, uma vez que apresenta uma maior homocedasticidade, ou seja, os dados são mais homogêneos e menos dispersos (DU et al., 2010). Para essa análise foi utilizado o pacote do Bioconductor *sva* (LEEK et al., 2012) que por meio de um regressão linear extrai os coeficientes de acordo com os tipos de tecidos analizados (grupos tumorais, normal ou benigno). Dessa maneira, as alterações de metilação encontradas são devido ao tipo de tecido, ajustadas de acordo com o gênero e idade dos pacientes.

O pacote *limma* (RITCHIE et al., 2015) foi utilizado para identificar o perfil diferencial de metilação entre os grupos amostrais e as sondas foram obtidas após correlação do P-valor por Bonferroni ($p<0.05$). As posições diferencialmente metiladas (DMPs – *Differentially Methylated Positions*) foram identificadas com valor de P ajustado < 0,05 e delta-beta ($\Delta\beta$) < -0.20 ou > +0.20. As sondas foram anotadas de acordo com os dados fornecidos pela *Illumina*, usando o genoma hg19 como referência.

Para realizar as análises comparativas, as amostras tumorais foram divididas em 3 grupos: Grupo 1, composto por 60 amostras de CPT; Grupo 2, composto por 8 CFT e 2 CCH e grupo 3, composto por carcinomas não diferenciados de tireoide (3 CAT e 1 CPDT). O Grupo 4 foi composto por lesões benignas de tiroiede (n=17) e o Grupo 5 por amostras não neoplásicas (n=50).

Os dados gerados acima foram utilizados em duas diferentes etapas de análise e os critérios utilizados para cada uma estão descritos a seguir.

3.5 Construção de algoritmos classificadores diagnóstico

A busca de marcadores diagnósticos para o carcinoma de tireoide foi baseada inicialmente na identificação de sondas diferencialmente metiladas (de acordo com valor de P ajustado e Δβ descritos). Para essa finalidade, foram realizadas três comparações: (a) todos os tumores em relação ao grupo LBT, (b) CFT/CCH em relação à TN e (c) CPT em relação à TN (Figura 3).

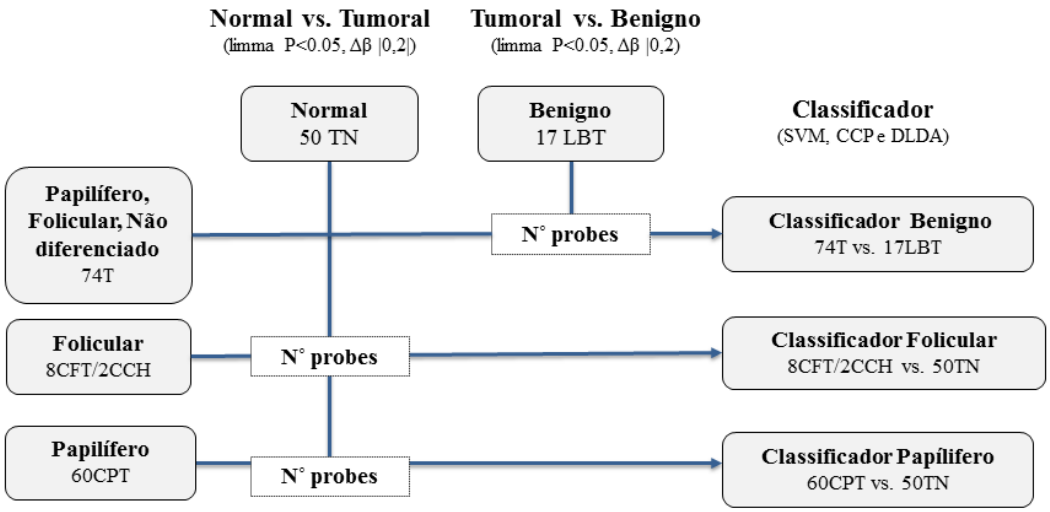

Figura 3: Comparações utilizadas para a identificação de sondas utilizadas na construção dos classificadores diagnósticos. CPT: carcinoma papilífero de tireoide; CFT: carcinoma follicular de tireoide; CCH: carcinoma de células de Hürtle; TN: tireoide não neoplásica; LBT: lesões benignas de tireoide; Δβ: delta beta.

Os dados obtidos das comparações descritas acima foram confirmados utilizando dados externos. Para isso, dados normalizados de *microarray* de metilação de amostras de TN, LBT, CPT e CFT, utilizando a mesma plataforma do presente estudo, foram obtidos do banco de dados público *Gene Expression Omnibus* (GEO) (http://www.ncbi.nlm.nih.gov/gds). A pesquisa foi realizada em Fevereiro de 2015 com as palavras chaves: thyroid cancer e GPL13534. Os dados foram publicados por TIMP *et al*. (2014) e depositados com o ID GSE53051. Para identificar as sondas diferencialmente metiladas presentes nos dados externos, foi aplicado o teste F de Levene para assumir ou não variâncias iguais entre os grupos comparados (teste t não pareado). A significância foi considerada quando P <0,05. Foi utilizado somente o valor de P, não sendo considerado os valores de Δβ. As sondas confirmadas em cada comparação foram avaliadas pela curva ROC (*Receiver Operating*

Characteristic) (AUC), para os dados gerados no estudo atual e externo. A construção do classificador foi realizada apenas com sondas de área abaixo da curva ROC (AUC) acima de 0,75 para diferenciar LBT de outros tumores e de 0,90 para diferenciar CPT e CFT de TN, com intervalo de confiança (IC) de 95%. As sondas selecionadas nessa etapa foram submetidas a uma análise de regressão linear (método *Stepwise*) e as cinco sondas não redundantes com melhores posições para cada classificador foram selecionadas.

Os classificadores baseados nos dados de *microarray* das cinco sondas escolhidas para cada classificador no método acima foram gerados por métodos lineares de reconhecimento de padrão (*Support Vector Machine (SVM)*, *Compound Covariate Predictor (CCP)* e *Diagonal Linear Discriminant Analysis (DLDA)*) avaliando os valores de metilação de cada região selecionada. O desempenho dos classificadores gerados foi descrito em termos de sensibilidade, especificidade, valor preditivo positivo (VPP) e valor preditivo negativo (VPN) na validação cruzada por Leave-One-Out (LOOCV).

Foram construídos três classificadores baseados nos valores de metilação de nove sondas que apresentaram o melhor desempenho nos métodos lineares de reconhecimento. O primeiro classificador foi delineado com o objetivo de separar lesões benignas de malignas, o segundo para discriminar carcinomas foliculares e o terceiro distinguir os carcinomas papilíferos de tireoide dos tecidos normais de tireoide.

O algoritmo classificador desenvolvido para CPT foi aplicado em um conjuto de amostras obtidas de bancos de dados externos e onde havia informação sobre o acometimento linfonodal. Nessa análise, foram comparadas as amostras de CPT provenientes de pacientes sem lesão linfonodal (n=265; N0, pacientes com classificação Nx foram incluídos nesse grupo) e com lesão linfonodal (n=214; N+ ao diagnóstico) obtidas do banco de dados TCGA (*The Cancer Genome Atlas* disponível em http://tcga-data.nci.nih.gov/. Acesso em Junho/2014). Os dados de metilação (*Plataforma Infinium® Human Methylation450 BeadChip)* de 479 amostras no nível 3 (processadas e normalizados) foram obtidos a partir da opção "*Thyroid Carcinoma*" no portal TCGA.

3.6 Avaliação de diferenças biológicas entre as lesões tireoideanas e tecidos normais

Para essa etapa foram analisadas as diferenças de metilação (de acordo com valor de P ajustado e Δβ) entre os grupos de amostras (LBT *vs* NT; CPT *vs* NT; CFT/CHH *vs* NT e CPDT/CAT *vs* NT).

Foi realizada a análise de agrupamento hierárquico não supervisionado com o objetivo de observar se os diferentes tipos histológicos do carcinoma de tireoide conferiam uma variação do perfil de metilação global. Nessa etapa foram utilizadas sondas com intervalo interquartil> 0,2. Foi utilizada a métrica *One minus* com método de ligação completa.

Os genes diferencialemente metilados encontrados nas comparações entre os grupos foram utilizados para as análises funcionais *in silico* pelo programa *Ingenuity Pathway Analysis* (IPA), entre elas a análise de vias canônicas. Para essa análise foram removidas sondas que não foram mapeadas próximas ou em genes conhecidos. Foram selecionados genes que apresentaram pelo menos uma sonda mapeada somente em região promotora.

O perfil de metilação obtido por *microarray* foi avaliado de acordo com o desfecho clínico, comparando os casos de pacientes com carcinomas bem diferenciados (CPT e CFT) de boa evolução clínica com os casos de PDTC/ATC agrupados com casos de carcinoma bem diferenciados que apresetaram recidiva (48 BEC vs 22 ECR). Nessa análise foram obtidas posições diferencialmente metiladas utilizando P<0,001 sem correção e Δβ < -0,10 ou > +0,10 (utilizando o pacote *limma* do Bioconductor). Foram selecionadas cinco sondas que apresentaram AUC>0,80 e o classificador prognóstico foi construído com o método DLDA.

3.7 Análise Estatística

Foi utilizado para análises estatísticas o programa SPSS (*Statistics Packet for Social Sciences*), versão 21.0 (SPSS, Chicago, IL, USA), o programa BRB Array Tools (v. 4.4.0; http://linus.nci.nih.gov/BRB-ArrayTools.html), além do software R e pacotes do Bioconductor (descrito acima).

4. RESULTADOS

Os resultados do presente estudo serão apresentados em três capítulos descritos a seguir. Os dados filtrados e normalizados obtidos dos *arrays* de metilação foram utilizados para as análises realizadas nos artigos descritos nos Capítulos 2 e 3. A representação gráfica da localização das sondas diferencialmente metiladas escolhidas para a construção dos classificadores diagnósticos está apresentada nos Apêndice 1. Os resultados das etapas de Controle de qualidade e Caracterização das sondas diferencialmente metiladas estão apresentados nos Apêndices 2 e 3, respectivamente. As tabelas mostrando os genes que apresentaram um maior ganho e maior perda de metilação nas amostras tumorais/lesões benignas quando comparadas as amostras normais (Todos os tumores *vs* LBT, LBT *vs* NT; CPT *vs* NT; CFT/CHH *vs* NT e CPDT/CAT *vs* NT) estão apresentadas no Apêndice 4.

Capítulo 1 – Review Paper

Epigenetic alterations in well-differentiated thyroid cancer

Mariana Bisarro dos Reis, Caroline Moraes Beltrami, Silvia Regina Rogatto*

Mariana Bisarro dos Reis - Department of Genetics, Biosciences Institute, UNESP, Sao Paulo State University, Botucatu, Sao Paulo, Brazil/ AC Camargo Cancer Center, São Paulo, SP, Brazil - marianabisarro@yahoo.com.br

Caroline Moraes Beltrami - CIPE - AC Camargo Cancer Center, São Paulo, SP, Brazil - caroline_beltrami@hotmail.com

Silvia Regina Rogatto* - AC Camargo Cancer Center, São Paulo, SP, Brazil/ Department of Urology, Faculty of Medicine, UNESP, Sao Paulo State University, Botucatu, SP, Brazil – silvia.rogatto2@gmail.com

*Author to whom correspondence should be addressed:

Silvia Regina Rogatto, Professor

Dept Urologia. Faculdade de Medicina – UNESP, Botucatu - São Paulo, SP – Brazil,

Zip Code: 18618-970

Telephone: +55-14-38116436, Fax: +55-14-38116271

E-mail: rogatto@fmb.unesp.br, silvia.rogatto@cipe.accamargo.org.br.

To be submitted: *Epigenetics and Chromatin (Impact Fator: 4.46)*

ABSTRACT

Epigenetics has been defined as alterations in gene function that are mitotically and or meiotically heritable with no change in DNA sequence. The predominant epigenetic modifications include posttranslational changes of histones, and covalent modifications of DNA bases and non-coding RNAs. DNA methylation regulates critical cellular process including transcription and chromosome stability, both events, when deregulated are associated with cancer development and progression. This review is focused on the involvement of methylation and microRNA epigenetic mechanisms in thyroid carcinogenesis. Well-differentiated thyroid carcinomas comprise papillary and follicular carcinomas, the most common subtypes of this cancer. Methylation of thyroid-specific genes, including *NIS* and *TSHR* involved in PI3K and MAPK pathways, as well as *RASSF1A* and *PTEN* tumor suppressor genes and altered expression of microRNAs are common alterations in these carcinomas. Novel technologies using genome-wide approaches have contributed to reveal new epigenetically regulated genes involved in molecular biology of thyroid cancer. The comprehensive analysis of genetic mutations, DNA methylation alteration as well as microRNA expression in thyroid carcinomas is critical to understand the crosstalk between these alterations and gene regulation contributing to the development of diagnostic and prognostic tools and new therapeutic strategies.

Keywords: DNA methylation, microRNA expression, thyroid carcinoma, genome-wide studies

INTRODUCTION

Thyroid cancer (TC) is the most common endocrine gland malignancy and its incidence has increased in the last decades [1]. Well-differentiated carcinomas are derived from follicular cells and represent the majority of diagnosed thyroid carcinomas [2]. Among these, the papillary (PTC) and follicular thyroid carcinomas (FTC) are the most common histological subtypes representing 80-85% and 10-15% of the cases, respectively [3].

Genetic and epigenetic alterations in TC have been described as associated with the tumor development and progression. Mutations in effectors of the mitogen-activated protein kinase (MAPK) and phosphatidylinositol 3-kinase (PI3K-AKT) pathways have been frequently described as associated with TC. Rearrangements involving *RET* gene (such as *RET/PTC*), *RAS* and *BRAF* mutations are reported in more than 70% of the PTC cases [3,4]. The *BRAFV600E* mutation is reported in 40-45% of the PTC cases and is the most common genetic alteration, leading to a constitutively activation of *BRAF* and subsequent activation of downstream signaling transduction pathway.

In addition to genetic, epigenetic events have been investigated in an attempt to understand other mechanisms involved in well differentiated thyroid carcinoma. Changes in the DNA methylation pattern of important genes involved in DNA damage repair, cell cycle control, tumor suppression, as like as in the normal thyroid gland have been described [5,6,7].

Similarly to other tumors, the development and progression of thyroid cancer are consequences of both, complex epigenetic and genetic alterations. In this review, we described the most relevant epigenetic alterations in well differentiated thyroid cancer, focusing the discussion in DNA methylation and microRNAs, especially in papillary thyroid carcinoma.

Epigenetic alterations as a mechanism of gene regulation

Epigenetic is defined as the study of alterations in gene regulation that are inheritable but not involve changes in DNA sequence [8,9]. The term “epigenetic” was firstly described by Waddington [10] as “the causal mechanisms between genes and their products, bring about phenotypic effects”. Cytosine DNA methylation along with the chromatin modification [11] and regulation by noncoding RNAs [12] are considered effector mechanisms of epigenetic control of gene expression.

The most studied epigenetic mechanism is the DNA methylation which involves the addition of a methyl group to the 5′ position of cytosine, predominantly in the context of CpG

dinucleotides [13]. These CpGs are non-randomly distributed across the genome including gene promoter regions, gene body regions, intergenic regions as well as in repetitive sequences (satellite DNA and retrotransposons) [14, 15]. The regions rich in CpGs are known as CpG islands and about 60% of human genes have these islands [13, 16, 17].

In tumor process, hypermethylation of CpG islands is a well-recognized epigenetic event [18]. Abnormal gain of DNA methylation often occurs in specific genes and this change can be associated with gene expression loss (reviewed by 19). DNA hypomethylation also contributes to tumorigenesis (Figure 1). Functionally, global loss of DNA methylation may play a role in the transformation of normal cells associated with gene activation, loss of genomic imprinting and activation of DNA repetitive elements resulting in an enhanced chromosomal instability [20, 21].

In addition, alterations in microRNA expression pattern also play an important role in cancer development [22, 23]. MicroRNAs (miRNAs) are small, non-coding RNAs that control the expression of their target genes, causing either degradation or inhibition of translation [24, 25]. In tumor cells, microRNAs may function as oncogenes or tumor suppressor genes, depending on their expression and target genes [26]. The target genes control multiple biological process including embryogenesis, development timing, stem cell division, apoptosis, angiogenesis and other cancer-associated processes [27, 28]. Furthermore, like classical genes, microRNAs can be subjected to epigenetic alterations including DNA methylation [29].

EPIGENETIC ALTERATIONS IN THYROID CANCER

DNA Methylation

Gene promoter hypermethylation and inativation of tumor supressor genes are important mechanisms described in thyroid cancer [30-33]. Hu et al. [34] reported that aberrant gain of methylation in *TIMP3, DAPK*, *SLC5A8* and *RARβ2* promoter regions are associated with the *BRAFV600E* mutation and aggressiveness in papillary thyroid carcinoma. The authors found a strong association between DNA methylation in these four tumor suppressor genes and classical and tall-cell PTC and aggressiveness of PTC. Similar results were reported in PTC for *RARβ2* and *TIMP3* genes added to an inverse correlation between *RASSF1A* methylation and the presence of *BRAF* mutation [35].

The *RASSF1A* promoter methylation is one of the most common epigenetic events in human cancers leading to a gene silencing [36]. Although described as altered in PTC,

RASSF1A hypermethylation is observed more frequently in FTC and in adenomas [37]. Brown et al. [38] reported *RASSF1A* promotor methylation in follicular thyroid lesions including hyperplasia (61% of cases), adenoma (90%) and FTC (70%). Moreover, *RASSF1A* methylation was reported in a frequency of 93% of benign lesions and 76% of PTC samples [39]. Thus, *RASSF1A* hypermethylation might be an initial event associated with the development of TC [37, 40].

A second tumor suppressor gene frequently reported as involved in thyroid tumorigenesis is *PTEN,* which is often mutated or downexpressed. The encoded protein acts as an antagonist of PI3K pathway [41]. Aberrant methylation of the *PTEN* promoter region has been observed mainly in follicular adenomas and carcinomas (83% and 84% samples, respectively) when compared to papillary carcinomas (47%) [42]. *PTEN* hypermethylation (Figure 1) has also been described in anaplastic thyroid carcinoma (ATC) in higher frequency when compared to follicular carcinomas and benign lesions [43]. The *PTEN* hypermethylation was also associated with genetic alterations in PI3K/AKT pathway, suggesting that gene inactivation caused by methylation can stimulate signaling pathways already activated by mutations and thus contributing to the progression of thyroid cancer [43].

In addition to *PTEN*, altered methylation pattern in other genes involved in the initiation or transduction of the signaling of the PI3K/Akt and MAPK pathway have been described. The tumor suppressor RASAL1 (*RAS protein activator like-1*) acts as a negative modulator of the PI3K and MAPK pathways. Reduced expression of *RASAL1* gene mediated through CpG methylation was described in several tumors with aberrant increased activity of RAS signaling pathway [44]. In thyroid cancer, 12 known negative modulators of the RAS pathway (*NF1*, *SPRY1*, *SPRY2*, *SPRED1*, *SPRED2*, *RKIP*, *DUSP5*, *DUSP6*, *TSC1*, *TSC2*, *LKB1)* including *RASAL1* were screened using a panel of 12 human-derived thyroid cancer cell lines [45]. Only *DAB2IP* and *RASAL1* genes were underexpressed in the tumor cell lines. Particularly, *RASAL1* expression was absent in tumor cells in contrast with normal tissues or normal thyroid cell lines. The authors also found that *RASAL1* gene was hypermethylated predominantly in FTC and anaplastic TC compared with benign thyroid lesions and PTC. Thus, based on these findings, *RASAL1* alterations were suggested to affect the regulation of the PI3K pathway over the MAPK pathway, acting as a major tumor suppressor gene in thyroid carcinomas [45].

Lin et al. [46] proposed that *MIG6* acts as a tumor suppressor gene in PTC, regulating negatively MAPK pathway. The authors showed that the promoter methylation was

associated with *MIG6* down expression and with high levels of EGFR and ERK phosphorylation. In a functional analysis, the increased expression of *MIG6* inhibited the proliferation and Mig-6 knockdown promoting the invasion of PTC cells. More recently, Lee et al. [47] investigated the DNA methylation pattern of MAPK signal-inhibiting genes. The promoter region of *DUSP4* and *DUSP6* were unmethylated and the genes were expressed. In contrast, *SERPINA5* was methylated in a PTC1 cell line and in 83% of the tumor tissues (63 of the 76 cases). In addition, *SERPINA5* promoter methylation was also associated with *BRAF* mutation.

By using cDNA transfection in WRO thyroid cell line, Kondo et al. [48] demonstrated that the restoration of FGFR2-IIIb isoform expression was able to interfere in the BRAF phosphorylation and to decrease the MAPK activation. The treatment with 5′-aza-deoxycytidine restored the expression of *FGFR2 IIIb* in WRO and TPC-1 thyroid cell lines suggesting that methylation is a mechanism of *FGFR2* regulation and consequently is involved in MAPK control [48].

It is well established that PI3K and MAPK pathways can interact in multiple ways. Epigenetic control of key members of these pathways adds another layer of complexity. All these data indicate that aberrant methylation of key tumor suppressor genes may play a pivotal role in thyroid carcinogenesis.

In addition to tumor suppressor genes, the mismatch repair genes have been described as hypermethylated in thyroid carcinomas. Guan et al. [49] analyzed the methylation pattern in 23 genes including *MLH1* (21% of the PTC samples showed aberrant methylation), *PCNA* (13%) and *OGG1* (5% of PTC samples). The authors reported that *MLH1* methylation was associated with lymph node metastasis and *BRAFV600E* mutation. No differences in *MLH1* and *MGMT* methylation patterns were observed in PTC, FTC and benign follicular thyroid adenomas [50]. However, samples with mutations in *BRAF*, *IDH1* and *NRAS* showed decreased *MLH1* expression.

The normal function of the thyroid gland cells requires a complex regulatory mechanism [51]. It has been reported that genes involved in iodide uptake and thyroid hormones synthesis also present aberrant methylation in their promoter regions (Figure 1). The *TSHR* gene was reported to be hypermethylated in papillary (59% of samples) and follicular thyroid cancer (47%), while normal and benign samples were unmethylated [52]. A progressive *SLC26A4* hypermethylation was described from adenomas to FTC, while methylation patterns were similar between PTC and anaplastic thyroid carcinoma (ATC) [53].

Although evaluating a limited number of cases, Stephen et al. [54] found altered methylation in sodium/iodide symporter *(NIS)* gene in PTC (11 cases), FTC (2 cases) and benign lesions (3 cases) compared with normal tissues (5 cases). The *NIS* gene promoter methylation was also reported in cold thyroid nodules. An association of mRNA downexpression was found in 50% of hypermethylated samples [55].

These findings suggest that methylation of specific genes involved in the thyroid function leading to gene downregulation may play a role in tumor development and progression. Khan et al [56] described an association between the hypermethylation of *TSHR* gene promotor and *BRAFV600E* mutation. *TSHR* hypermethylation was detected in 73.3% of 15 *BRAF*-mutated tumors (12 PTC, 2 FTC and 1 with rare histology). The presence of *BRAF* mutation was also related to *NIS* down-expression, mediated by *DNMT1*. In 30 PTC samples, Choi et al. [57] found significant *NIS* mRNA and protein downregulation in cases harboring the *BRAFV600E* mutation. The authors also found a negative correlation between *NIS* and *DNMT1* expression in *BRAF* mutated cases and associated the high expression of *DNMT1* with epigenetic silencing of *NIS*.

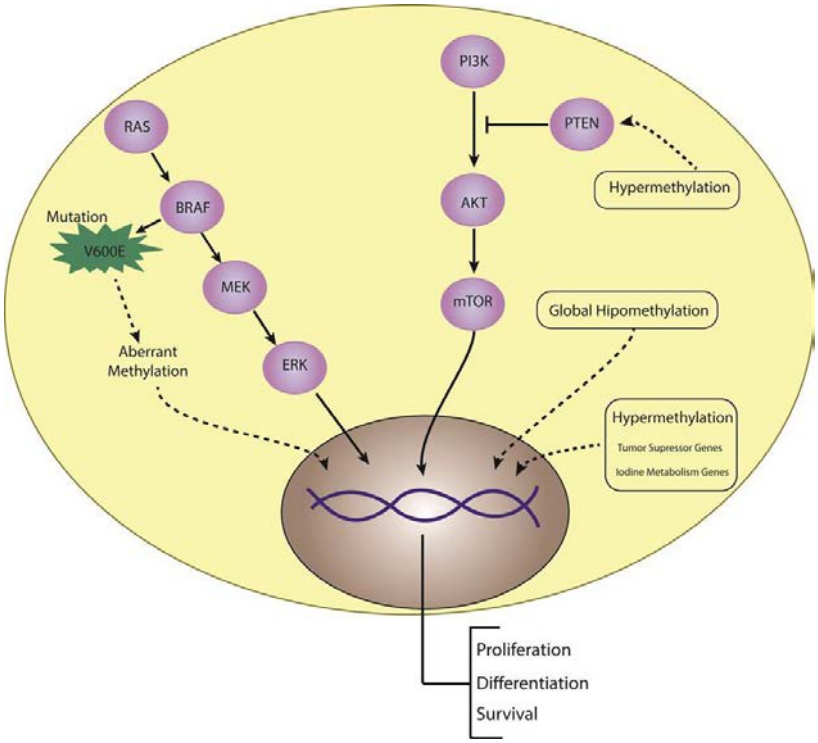

Figure 1. Methylation changes are part of the global alterations found in thyroid cancer. Global hypomethylation and hypermethylation of tumor suppressor genes and those involved in iodine metabolism are found in well-differentiated thyroid cancer. Mutation in *BRAF* is associated with several genes with altered methylation pattern in PTC. In addition, *PTEN* hypermethylation is related with PI3/AKT pathway activation.

In summary, several genes with altered methylation patterns have been described in well differentiated thyroid carcinoma. These genes presenting tumor suppressor functions are involved in the normal function of thyrocytes or associated with pathways involved in thyroid carcinogenesis. However these studies investigating the DNA methylation are mostly restricted to candidate gene approaches. Only recently large-scale studies addressing the gene methylation profile have been reported in TC, and most of them evaluated PTC samples. To our knowledge, there are six reports describing epigenetic profiles in thyroid carcinomas. In 2011, Hou *et al*. [58] assessed the global epigenetic alterations associated with *BRAFV600E* mutation in two papillary thyroid carcinoma cell lines through the process with shRNA knockdown for this mutation. Using this strategy, the authors described 10 hypo- and 59 hypermethylated genes in both cell lines after the *BRAF* knockdown and the involvement of *HMGB2* and *FDG1* genes in proliferation and cell invasion control, respectively [58].

More recently, global DNA methylation analysis has been applied to identify molecular signatures in different subtypes of thyroid cancer. Rodríguez-Rodero et al. [59]

using the 27K platform (Illumina) analyzed two PTC, two FTC, two anaplastic carcinomas, two medullary carcinomas, two normal samples and four cell lines. The authors found an epigenetic signature in papillary and follicular carcinomas (262 and 352 hypermethylated genes and 13 and 21 hypomethylated genes, respectively). The comparison of these findings with the alterations found in medullary and anaplastic tumors, revealed 155 and 210 hypermethylated genes and 13 and 21 hypomethylated genes exclusively in PTC and FTC, respectively. The authors found several potential tumor suppressor genes (*ADAMTS8* and *HOXB4* in PTC and *ZIC1* and *KISS1R* in FTC) and oncogenes (*INSL4* and *DPPA2* for MTC and *TCL1B* and *NOTCH4* in anaplastic carcinomas) confirmed as altered by methylation in thyroid carcinomas.

Using the 27K platform (Illumina), Kikuchi et al. [60] described a differential methylation profile in in 14 PTC samples according to *BRAF* and *RAS* mutations. Six hypermethylated genes (*HIST1H3J*, *POU4F2*, *SHOX2*, *PHKG2*, *TLX3* e *HOXA7*) presented down expression in TC cell lines. After the treatment with 5-aza-2´deoxycytidine and/or trichostatin A, the cells lines restored the expression of these genes, except *SHOX2*.

The methylome (27K platform, Illumina) was evaluated in 83 tumors (47 PTC, 18 FTC and 18 adenomas) and the results were integrated with transcripts expression data from 31 samples [61]. The authors found a methylation profile according to the histological subtype and the *BRAF* and *RAS* mutation.

Recently, Ellis et al. [62] evaluated 51 PTC (450K platform, Illumina) demonstrating a global hypomethylation compared with normal tissues (91% of differentially methylated sites had methylation loss). The follicular variant showed distinct methylation profile in comparison with the classical variant as well as difference between the methylation profile according to the *BRAF*, *RAS* and *RET*/*PTC* mutation (3.6 fold more differentially methylated compared with wild-type tumors).

In addition, a comprehensive analysis of the genome in more than 400 papillary thyroid carcinoma samples from TCGA project [63] revealed the involvement of several alterations associated with the development and progression of the disease. Analysis of genomic variants, transcripts expression and DNA methylation revealed potential molecular drivers. An unsupervised clustering analysis with methylation data revealed four clusters of papillary carcinoma classified as Follicular, methylated CpG Islands, Classical 1 and Classical 2. In addition, two meta-clusters were identified according the *BRAFV600E* and *RAS* mutations. The samples with RAS mutations showed two different clusters, one with

lower number of methylation changes termed Meth-follicular and other, Meth-CpG Island cluster, with large number of CpG hypermethylated in CpG islands and CpG shore regions.

Although epigenetic alterations based on genome-wide methods have been described in well-differentiated thyroid carcinomas, a better understanding of the molecular alterations is necessary to guide the development of meaningful markers for early diagnosis, prognosis and prediction of response to therapies in thyroid carcinoma.

microRNA expression in thyroid cancer

In well-differentiated thyroid carcinomas, mostly PTC, numerous miRNAs have been described with altered expression. The miRNA genetic signature based on expression levels has been used to differentiate distinct variants of PTC and FTC cases. In PTC, up-regulation of miR-21, 146b, 155, 181a, 181b, 221 and 222 among others have been described [64-68]. In particular, the expression levels of miR-21, 146b, 181b, 221 and 222 were able to distinguish PTC from follicular adenomas and multinodular goiters [69]. The authors observed differences in the miRNA expression levels in the classical variant (miR-146b) and tall cell variant (miR-146b, -21 and -222) when compared with the follicular variant of papillary carcinoma [69].

Alterations in the microRNA expression were also associated with the mutational status of PTC. The upregulation of miR-221 and miR-222 were found in samples with *BRAF* and *RAS* mutation whereas the overexpression of miR-146b was observed in cases carrying *RAS* mutation [65]. The miR-221 expression was also associated with *BRAF* mutation in addition to extrathyroidal invasion, lymph node metastasis and cases with advanced stage of disease [70]. Recently, by using deep-sequencing, Mancikova et al. [71] found down regulation of miR-7 and -204 in PTC harboring the *BRAF* V600E mutation.

To understand the role of microRNAs in thyroid carcinogenesis, many studies have been focused on functional assays to identify the targets of these molecules. It was suggested that miR-221 was associated with the control of cell proliferation in PTC cell lines [66]. In addition, miR-221 and -222 potentially regulate the cell cycle targeting the *CDKN1B* transcript, which codifies the $p27^{kip1}$ protein [72]. The authors showed that these miRs targeted the 3'UTR of *CDKN1B* resulting in reduced protein levels, which regulates the cell proliferation in thyroid cells.

The miR-181b, also upregulated in PTC, directly targets *CYLD* gene, which is associated with apoptosis [73]. High expression level of miR-21 was associated with cell proliferation and invasion, with a negative correlation with expression of *PDCD4* gene [74]. Using *in silico* analysis, Jazdzewski et al. [75] showed that the 3'UTR of *THRβ* gene contains binding sites for several microRNAs with aberrant expression in PTC. The authors used the cell line CAKI-2 derived from kidney carcinoma and demonstrated a direct interaction between *THRβ* and miR-21 and -146a. The down expression of this gene was detected when cells were transfected with miR-21, -146a and -221.

In follicular thyroid carcinoma, Weber et al. [76] reported the up regulation of miR-192, miR-197, miR-328 and miR-346 when compared with follicular adenomas. The overexpression of miR-197 and -346 were associated with cell proliferation. In addition, it was found down expression of two predict targets of each miR (miR-197: *ACVR1* and *TSPAN3*; miR-346: *EFEMP2* and *CFLAR*). Upregulation of the miR-187, -224, -155, -222, and -221 were observed in conventional follicular carcinomas (CFC), whereas in oncocytic follicular carcinomas (OFC), up regulation of miR-187, -221, -339, -183, -222, and -197 were observed when compared with hyperplastic nodules. The authors also analyzed a panel of miRs in a small number of fine-needle aspiration biopsies and observed a high accuracy to detect cancer samples [65]. A higher expression of miR-96, -182, -183, -221, -222, -449a and -874 and low expression of miR-542, -574, -455, and -199a were detected in follicular carcinomas (OFC and CFC) when compared with normal tissues. In addition, it was observed that miR-885 is potential novel marker for OFC [77].

Notwithstanding altered microRNA expression is well established in cancer, the molecular mechanisms underlying the regulation of these miRNAs are not completely understood. In general, miRs are mapped in regions involved in amplification and deletions as well as in breakpoints associated with other structural alterations as translocations [78, 79]. Moreover, similar to genes that encode proteins, microRNAs are transcribed by genes that are targets for the epigenetic events and also acts modulating the gene expression (Figure 2). In 2011, Kunej et al. [80] reported that that more than one hundred miRNAs are regulated by epigenetic mechanisms. The first epigenetically regulated microRNA described was the miRNA-127 in bladder cancer cells [81]. After this discovery, several studies demonstrated alterations in methylation pattern of microRNAs in gastric carcinoma [82], lung adenocarcinoma [83], gliobastoma [84] and colon cancer [85]. In thyroid carcinoma, this is a relatively unexplored field. So far, only the study published by TCGA group showed

microRNA genes controlled by epigenetic mechanisms [63]. They reported that miR-21, miR-146b, and miR-204 genes are aberrantly methylated in PTC and associated with altered expression of these microRNAs.

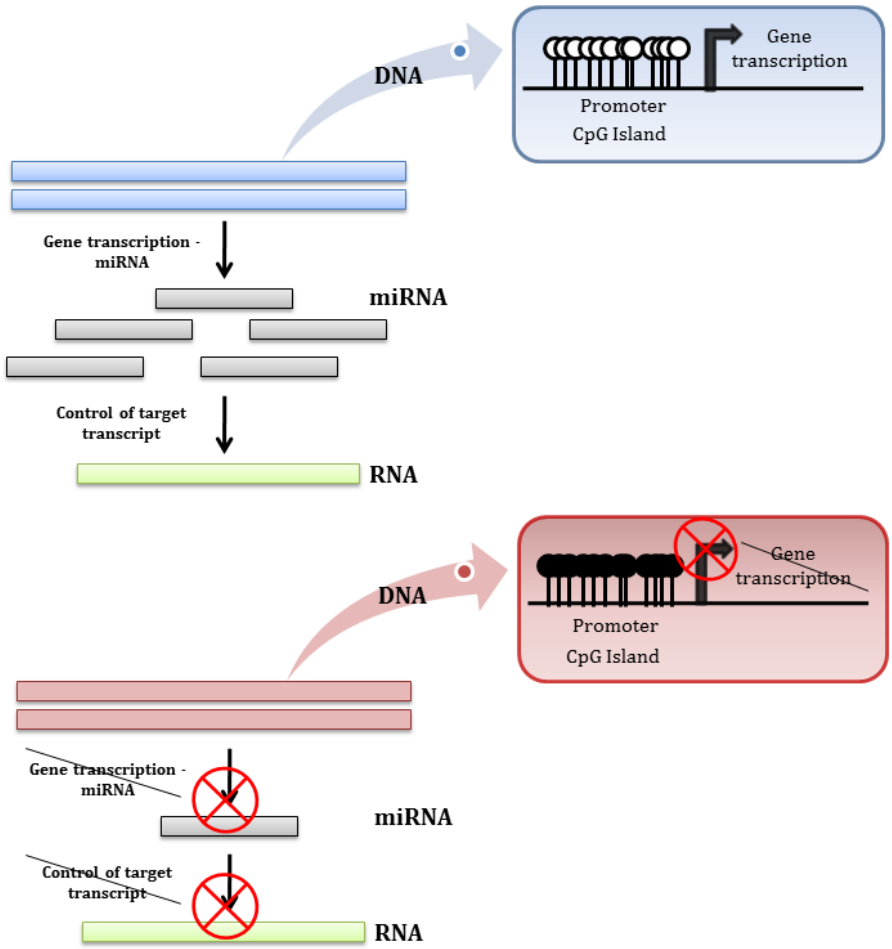

Figure 2. Expression of microRNA can be controlled by epigenetic mechanisms, such as cytosine methylation in promoter CpG island. Hypomethylated CpG island on promoter region of microRNA gene leads to microRNA expression. Conversely, hypermethylation of these CpG islands impairs the microRNA expression.

CONCLUSION

As highlighted in this review, changes in DNA methylation and microRNA expression play a role in the development of thyroid carcinoma. However, a complete understanding of these alterations in TC remains to be clarified. Recent reports addressing the gene methylation profiling in appropriated number of samples have contributed to reveal important drivers with

aberrant methylation in thyroid cancer. Two lines of evidence point out the relevance of microRNAs in TC. First, the recurrent altered expression in several miRs that regulate several transcripts TC-associated and, second, the recent finding of methylation in miRs. From this perspective, future studies are necessary to better understand the mechanisms involved in thyroid carcinogenesis. Future exploratory research should focus on characterization of aberrant DNA methylation and microRNA and how this knowledge could guide clinic management of well differentiated thyroid carcinomas.

FUNDING

This study was supported by grants from the National Institute of Science and Technology in Oncogenomics (Fundação de Amparo à Pesquisa do Estado de São Paulo –FAPESP Grant 2008/57887–9, Conselho Nacional de Desenvolvimento Científico e Tecnoló ́ico Grant CNPq 573589/08–9 and fellowship CNPq (140819/2011-8).

Disclosure Summary: The authors have nothing to disclose.

REFERENCES

[1] Siegel RL, Miller KD, Jemal A. Cancer statistics. CA Cancer J Clin. 2015;65(1):5-29.

[2] Elisei R, Pinchera A. Advances in the follow-up of differentiated or medullary thyroid cancer. Nat Rev Endocrinol. 2012; 3;8(8):466-75

[3] Xing M. Molecular pathogenesis and mechanisms of thyroid cancer. Nat Rev Cancer. 2013; 13(3):184-99.

[4] Nikiforov YE, Nikiforova MN. Molecular genetics and diagnosis of thyroid cancer. Nat Rev Endocrinol. 2011; 7(10):569-80.

[5] Czarnecka K, Pastuszak-Lewandoska D, Migdalska-Sek M, Nawrot E, Brzezinski J, Dedecjus M, et al. Aberrant methylation as a main mechanism of TSGs silencing in PTC. Front Biosci (Elite Ed). 2011; 3:137-57.

[6] Schagdarsurengin U, Richter AM, Hornung J, Lange C, Steinmann K, Dammann RH. Frequent epigenetic inactivation of RASSF2 in thyroid cancer and functional consequences. Mol Cancer. 2010; 9:264.

[7] Galrão AL, Sodré AK, Camargo RY, Friguglietti CU, Kulcsar MA, Lima EU, et al. Methylation levels of sodium-iodide symporter (NIS) promoter in benign and malignant thyroid tumors with reduced NIS expression. Endocrine. 2013; 43(1):225-9.

[8] Schübeler D, Elgin SC. Defining epigenetic states through chromatin and RNA. Nat Genet. 2005; 37:917-8.

[9] Sawan C, Vaissière T, Murr R, Herceg Z. Epigenetic drivers and genetic passengers on the road to cancer. Mutat Res. 2008; 642(1-2):1-13.

[10] Waddington CH. The epigenotype. 1942. Int J Epidemiol. 2012 Feb;41(1):10-3.

[11] Sharma S, Kelly TK, Jones PA. Epigenetics in cancer. Carcinogenesis. 2010; 31(1):27-36.

[12] Lopez J, Percharde M, Coley HM, Webb A, Crook T. The context and potential of epigenetics in oncology. Br J Cancer. 2009; 100(4):571-7.

[13] Jones PA. Functions of DNA methylation: islands, start sites, gene bodies and beyond. Nat Rev Genet. 2012; 13(7):484-92.

[14] Park YJ, Claus R, Weichenhan D, Plass C. Genome-wide epigenetic modifications in cancer. Prog Drug Res. 2011; 67:25-49.

[15] Stirzaker C, Taberlay PC, Statham AL, Clark SJ. Mining cancer methylomes: prospects and challenges. Trends Genet. 2014; 30(2):75-84.

[16] Bernstein BE, Meissner A, Lander ES. The mammalian epigenome. Cell. 2007; 128:669-81.

[17] Laird PW. The power and the promise of DNA methylation markers. Nat Rev Cancer. 2003; 3:253-66.

[18] You JS, Jones PA. Cancer genetics and epigenetics: two sides of the same coin? Cancer Cell. 2012; 22(1):9-20.

[19] Baylin SB, Jones PA. A decade of exploring the cancer epigenome - biological and translational implications. Nat Rev Cancer. 11(10):726-34.

[20] Berdasco M, Esteller M. Aberrant epigenetic landscape in cancer: how cellular identity goes awry. Dev Cell. 2010; 19(5):698-711.

[21] Esteller M. Epigenetics in cancer. N Engl J Med. 2008; 358(11):1148-59.

[22] Feinberg AP. Phenotypic plasticity and the epigenetics of human disease. Nature. 2007; 447:433-40.

[23] Taby R, Issa JP. Cancer epigenetics. CA Cancer J Clin. 2010; 60(6):376-92.

[24] Krol J, Loedige I, Filipowicz W. The widespread regulation of microRNA biogenesis, function and decay. Nat Rev Genet. 2010; 11(9):597-610.

[25] Choi JD, Lee JS. Interplay between Epigenetics and Genetics in Cancer. Genomics Inform. 2013; 11(4):164-73.

[26] Kasinski AL, Slack FJ. Epigenetics and genetics. MicroRNAs en route to the clinic: progress in validating and targeting microRNAs for cancer therapy. Nat Rev Cancer. 2011; 11(12):849-64**.**

[27] Chhabra R, Saini N. MicroRNAs in cancer stem cells: current status and future directions. Tumour Biol. 2014;35(9):8395-405.

[28] Hayes J, Peruzzi PP, Lawler S. MicroRNAs in cancer: biomarkers, functions and therapy. Trends Mol Med. 2014; 20(8):460-9.

[29] Davis-Dusenbery BN, Hata A. Mechanisms of control of microRNA biogenesis. J Biochem. 2010; 148(4):381-92.

[30] Huang Y, de la Chapelle A, Pellegata NS. Hypermethylation, but not LOH, is associated with the low expression of MT1G and CRABP1 in papillary thyroid carcinoma. Int J Cancer. 2003;104:735-44.

[31] Lal G, Padmanabha L, Smith BJ, Nicholson RM, Howe JR, O'Dorisio MS, et al. RIZ1 is epigenetically inactivated by promoter hypermethylation in thyroid carcinoma. **Cancer**. 2006; 107:2752-9.

[32] Yin DT, Wu W, Li M, Wang QE, Li H, Wang Y, et al. DKK3 is a potential tumor suppressor gene in papillary thyroid carcinoma. Endocr Relat Cancer. 2013; 20(4):507-14.

[33] Qiang W, Zhao Y, Yang Q, Liu W, Guan H, Lv S, et al. ZIC1 is a putative tumor suppressor in thyroid cancer by modulating major signaling pathways and transcription factor FOXO3a. J Clin Endocrinol Metab. 2014; 99(7):E1163-72.

[34] Hu S, Liu D, Tufano RP, Carson KA, Rosenbaum E, Cohen Y, et al. Association of aberrant methylation of tumor suppressor genes with tumor aggressiveness and BRAF mutation in papillary thyroid cancer. Int J Cancer. 2006; 119:2322-9.

[35] Brait M, Loyo M, Rosenbaum E, Ostrow KL, Markova A, Papagerakis S, et al. Correlation between BRAF mutation and promoter methylation of TIMP3, RARβ2 and RASSF1A in thyroid cancer. Epigenetics. 2012; 7(7):710-9.

[36] Pfeifer GP, Dammann R. Methylation of the tumor suppressor gene RASSF1A in human tumors. Biochemistry (Mosc)**.** 2005; 70:576-83.

[37] Xing M, Cohen Y, Mambo E, Tallini G, Udelsman R, Ladenson PW, et al. Early occurrence of RASSF1A hypermethylation and its mutual exclusion with BRAF mutation in thyroid tumorigenesis. Cancer Res. 2004; 64:1664-8.

[38] Brown TC, Juhlin CC, Healy JM, Prasad ML, Korah R, Carling T. Frequent silencing of RASSF1A via promoter methylation in follicular thyroid hyperplasia: a potential early epigenetic susceptibility event in thyroid carcinogenesis. JAMA Surg. 2014; 149(11):1146-52.

[39] Mohammadi-as J, Larijani B, Khorgami Z, Tavangar SM, Haghpanah V, Kheirollahi M, et al. Qualitative and quantitative promoter hypermethylation patterns of the P16, TSHR, RASSF1A and RARβ2 genes in papillary thyroid carcinoma. Med Oncol. 2011; 28(4):1123-8

[40] Nakamura N, Carney JA, Jin L, Kajita S, Pallares J, Zhang H, et al. RASSF1A and NORE1A methylation and BRAFV600E mutations in thyroid tumors. Lab Invest. 2005; 85:1065-75.

[41] Brzezianska E, Pastuszak-Lewandoska D. A minireview: the role of MAPK/ERK and PI3K/Akt pathways in thyroid follicular cell-derived neoplasm. Front Biosci (Landmark Ed). 2011; 16:422-39.

[42] Alvarez-Nuñez F, Bussaglia E, Mauricio D, Ybarra J, Vilar M, Lerma E, et al. PTEN promoter methylation in sporadic thyroid carcinomas. Thyroid. 2006. 16:17-23.

[43] Hou P, Ji M, Xing M. Association of PTEN gene methylation with genetic alterations in the phosphatidylinositol 3-kinase/AKT signaling pathway in thyroid tumors. Cancer. 2008; 113(9):2440-7.

[44] Jin H, Wang X, Ying J, Wong AH, Cui Y, Srivastava G, et al. Epigenetic silencing of a Ca(2+)-regulated Ras GTPase-activating protein RASAL defines a new mechanism of Ras activation in human cancers. Proc Natl Acad Sci U S A. 2007; 104:12353-8

[45] Liu D, Yang C, Bojdani E, Murugan AK, Xing M. Identification of RASAL1 as a major tumor suppressor gene in thyroid cancer. J Natl Cancer Inst. 2013; doi: 105(21):1617-27.

[46] Lin CI, Du J, Shen WT, Whang EE, Donner DB, Griff N, et al. Mitogen-inducible gene-6 is a multifunctional adaptor protein with tumor suppressor-like activity in papillary thyroid cancer. J Clin Endocrinol Metab. 2011; 96(3):E554-65.

[47] Lee EK, Chung KW, Yang SK, Park MJ, Min HS, Kim SW, et al. DNA methylation of MAPK signal-inhibiting genes in papillary thyroid carcinoma. Anticancer Res. 2013; 33:4833-9.

[48] Kondo T, Zheng L, Liu W, Kurebayashi J, Asa SL, Ezzat S. Epigenetically controlled fibroblast growth factor receptor 2 signaling imposes on the RAS/BRAF/mitogen-activated protein kinase pathway to modulate thyroid cancer progression. Cancer Res. 2007; 67:5461-70.

[49] Guan H, Ji M, Hou P, Liu Z, Wang C, Shan Z, et al. Hypermethylation of the DNA mismatch repair gene hMLH1 and its association with lymph node metastasis and T1799A BRAF mutation in patients with papillary thyroid cancer. Cancer. 2008; 113(2):247-55.

[50] Santos JC, Bastos AU, Cerutti JM, Ribeiro ML. Correlation of MLH1 and MGMT expression and promoter methylation with genomic instability in patients with thyroid carcinoma. BMC Cancer. 2013; 13:79.

[51] Kondo T, Asa SL, Ezzat S. Epigenetic dysregulation in thyroid neoplasia. Endocrinol Metab Clin North Am. 2008; 37(2):389-400.

[52] Xing M, Usadel H, Cohen Y, Tokumaru Y, Guo Z, Westra WB, et al. Methylation of the thyroid-stimulating hormone receptor gene in epithelial thyroid tumors: a marker of malignancy and a cause of gene silencing. Cancer Res. 2003; 63:2316:21.

[53] Xing M, Tokumaru Y, Wu G, Westra WB, Ladenson PW, Sidransky D. Hypermethylation of the Pendred syndrome gene SLC26A4 is an early event in thyroid tumorigenesis. Cancer Res. 2003; 63:2312-5.

[54] Stephen JK, Chitale D, Narra V, Chen KM, Sawhney R, Worsham MJ. DNA methylation in thyroid tumorigenesis. Cancers (Basel). 2011; 3(2):1732-43.

[55] Neumann S, Schuchardt K, Reske A, Reske A, Emmrich P, Paschke R. Lack of correlation for sodium iodide symporter mRNA and protein expression and analysis of sodium iodide symporter promoter methylation in benign cold thyroid nodules. Thyroid. 2004;14(2):99-111.

[56] Khan MS, Pandith AA, Masoodi SR, Wani KA, Ul Hussain M, Mudassar S. Epigenetic silencing of TSHR gene in thyroid cancer patients in relation to their BRAF V600E mutation status. Endocrine. 2014; 47(2):449-55.

[57] Choi YW, Kim HJ, Kim YH, Park SH, Chwae YJ, Lee J, et al. B-RafV600E inhibits sodium iodide symporter expression via regulation of DNA methyltransferase 1. Exp Mol Med. 2014; 46:e120.

[58] Hou P, Liu D, Xing M. Genome-wide alterations in gene methylation by the BRAF V600E mutation in papillary thyroid cancer cells. Endocr Relat Cancer. 2011; 18(6):687-97.

[59] Rodríguez-Rodero S, Fernández AF, Fernández-Morera JL, Castro-Santos P, Bayon GF, Ferrero C, et al. J Clin Endocrinol Metab. 2013;98(7):2811-21.

[60] Kikuchi Y, Tsuji E, Yagi K, Matsusaka K, Tsuji S, Kurebayashi J, et al. Aberrantly methylated genes in human papillary thyroid cancer and their association with BRAF/RAS mutation. Front Genet. 2013; 4:271.

[61] Mancikova V, Buj R, Castelblanco E, Inglada-Pérez L, Diez A, de Cubas AA, et al. DNA methylation profiling of well-differentiated thyroid cancer uncovers markers of recurrence free survival. Int J Cancer. 2014; 135(3):598-610.

[62] Ellis RJ, Wang Y, Stevenson HS, Boufragech M, Patel D, Nilubol N, et al. Genome-Wide Methylation Patterns in Papillary Thyroid Cancer Are Distinct Based on Histological Subtype and Tumor Genotype. J Clin Endocrinol Metab. 2014; 99(2):E329-37.

[63] Cancer Genome Atlas Research Network. Integrated genomic characterization of papillary thyroid carcinoma. Cell. 2014; 159(3):676-90.

[64] He H, Jazdzewski K, Li W, Liyanarachchi S, Nagy R, Volinia S, et al. The role of microRNA genes in papillary thyroid carcinoma. Proc Natl Acad Sci U S A. 2005; 102:19075-80.

[65] Nikiforova MN, Tseng GC, Steward D, Diorio D, Nikiforov YE. MicroRNA expression profiling of thyroid tumors: biological significance and diagnostic utility. J Clin Endocrinol Metab. 2008; 93(5):1600-8.

[66] Pallante P, Visone R, Ferracin M, Ferraro A, Berlingieri MT, Troncone G, et al. MicroRNA deregulation in human thyroid papillary carcinomas. Endocr Relat Cancer. 2006; 13:497–508.

[67] Tetzlaff MT, Liu A, Xu X, Master SR, Baldwin DA, Tobias JW, et al. Differential Expression of miRNAs in Papillary Thyroid Carcinoma Compared to Multinodular Goiter Using Formalin Fixed Paraffin Embedded Tissues. Endocr Pathol. 2007; 18:163–73.

[68] Chen YT, Kitabayashi N, Zhou XK, Fahey TJ III, Scognamiglio T. MicroRNA analysis as a potential diagnostic tool for papillary thyroid carcinoma. Mod Pathol. 2008; 21(9):1139-46.

[69] Sheu SY, Grabellus F, Schwertheim S, Worm K, Broecker-Preuss M, Schmid KW. Differential miRNA expression profiles in variants of papillary thyroid carcinoma and encapsulated follicular thyroid tumours. Br J Cancer. 2010; 102(2):376-82.

[70] Zhou YL, Liu C, Dai XX, Zhang XH, Wang OC. Overexpression of miR-221 is associated with aggressive clinicopathologic characteristics and the BRAF mutation in papillary thyroid carcinomas. Med Oncol. 2012; 29(5):3360-6..

[71] Mancikova V, Castelblanco E, Pineiro-Yanez E, Perales-Paton J, de Cubas AA, Inglada-Perez L, et al. MicroRNA deep-sequencing reveals master regulators of follicular and papillary thyroid tumors. Mod Pathol. 2015. [Epub ahead of print]

[72] Visone R, Russo L, Pallante P, De Martino I, Ferraro A, Leone V, et al. MicroRNAs (miR)-221 and miR-222, both overexpressed in human thyroid papillary carcinomas, regulate p27Kip1 protein levels and cell cycle. Endocr Relat Cancer. 2007; 14:791-8.

[73] Li D, Jian W, Wei C, Song H, Gu Y, Luo Y, et al. Down-regulation of miR-181b promotes apoptosis by targeting CYLD in thyroid papillary cancer. Int J Clin Exp Pathol. 2014; 7:7672-80.

[74] Zhang J, Yang Y, Liu Y, Fan Y, Liu Z, Wang X, et al. MicroRNA-21 regulates biological behaviors in papillary thyroid carcinoma by targeting programmed cell death 4. J Surg Res. 2014; 189(1):68-74.

[75] Jazdzewski K, Boguslawska J, Jendrzejewski J, Liyanarachchi S, Pachucki J, Wardyn KA, et al. Thyroid hormone receptor beta (THRB) is a major target gene for microRNAs deregulated in papillary thyroid carcinoma (PTC). J Clin Endocrinol Metab. 2011; 96(3):E546-53.

[76] Weber F, Teresi RE, Broelsch CE, Frilling A, Eng C. A limited set of human MicroRNA is deregulated in follicular thyroid carcinoma. J Clin Endocrinol Metab. 2006; 91:3584-91.

[77] Dettmer M, Vogetseder A, Durso MB, Moch H, Komminoth P, Perren A, et al. MicroRNA expression array identifies novel diagnostic markers for conventional and oncocytic follicular thyroid carcinomas. J Clin Endocrinol Metab. 2013; 98(1):E1-7.

[78] Croce CM. Causes and consequences of microRNA dysregulation in cancer. Nat Rev Genet. 2009 Oct;10(10):704-14.

[79] Zhang L, Huang J, Yang N, Greshock J, Megraw MS, Giannakakis A, et al. microRNAs exhibit high frequency genomic alterations in human cancer. Proc Natl Acad Sci U S A. 2006;103(24):9136-41.

[80] Kunej T, Godnic I, Ferdin J, Horvat S, Dovc P, Calin GA Epigenetic regulation of microRNAs in cancer: an integrated review of literature. Mutat Res. 2011 Dec 1;717(1-2):77-84.

[81] Saito Y, Liang G, Egger G, Friedman JM, Chuang JC, Coetzee GA, et al. Specific activation of with downregulation of the proto-oncogene BCL6 by chromatin-modifying drugs in human cancer cells. Cancer Cell. 2006 Jun;9(6):435-43.

[82] Steponaitiene R, Kupcinskas J, Langner C, Balaguer F, Venclauskas L, Pauzas H, et al. Link Epigenetic silencing of miR-137 is a frequent event in gastric carcinogenesis. Mol Carcinog. 2015 [Epub ahead of print]

[83] Nadal E, Chen G, Gallegos M, Lin L, Ferrer-Torres D, Truini A, et al. Epigenetic inactivation of microRNA-34b/c predicts poor disease-free survival in early-stage lung adenocarcinoma. Clin Cancer Res. 2013; 19(24):6842-52.

[84] Chiou GY, Chien CS, Wang ML, Chen MT, Yang YP, Yu YL, et al. Epigenetic regulation of the miR142-3p/interleukin-6 circuit in glioblastoma. Mol Cell. 2013; 52(5):693-706.

[85] Tanaka T, Arai M, Wu S, Kanda T, Miyauchi H, Imazeki F, et al. Epigenetic silencing of microRNA-373 plays an important role in regulating cell proliferation in colon cancer. Oncol Rep. 2011; 26(5):1329-35.

Capítulo 2 – Research Paper

DNA methylation profiling reveals potential differential diagnostic markers in thyroid benign lesions and carcinomas

Mariana Bisarro dos Reis[1,2], Mateus de Camargo Barros Filho[2], Caroline Moraes Beltrami[2], Fábio Albuquerque Marchi[2], Hellen Kuasne[2,5], Clovis Antonio Pinto[3] , Srikant Ambatipudi[4], Zkenko Herceg[4], Luiz Paulo Kowalski[5], Silvia Regina Rogatto[2,6]*

1 Genetics Graduation Program, Biosciences Institute, UNESP, Sao Paulo State University, Botucatu, Sao Paulo, Brazil

2 International Research Center,A.C .Camargo Cancer Center, São Paulo, SP, Brazil;

3 Department of Pathology, A.C. Camargo Cancer Center, São Paulo, SP, Brazil;

4 Epigenetics Group; International Agency for Research on Cancer (IARC), Lyon, France;

5 Department of Head and Neck Surgery and Otorhinolaryngology, A. C. Camargo Cancer Center, São Paulo, SP, Brazil.

6 Department of Urology, Faculty of Medicine, UNESP, Sao Paulo State University, Botucatu, SP, Brazil.

***To whom correspondence should be addressed at:**

Silvia Regina Rogatto, PhD

Dept Urologia. Faculdade de Medicina – UNESP, Botucatu - São Paulo, SP – Brazil

CEP: 18618-970; Telephone: +55-14-38116436, Fax: +55-14-38116271;

E-mail: rogatto@fmb.unesp.br, silvia.rogatto@cipe.accamargo.org.br.

Keywords: thyroid cancer, DNA methylation, diagnostic markers

The Journal of Clinical Endocrinology & Metabolism (to be submitted) (FI 6.310)

Abstract

Context: Thyroid cancer (TC) is the most common endocrine-related cancer with growing worldwide incidence. High accuracy in diagnosing thyroid tumors, particularly follicular subtypes, is still a challenge. Molecular testing for epigenetic alterations associated with malignancy is a potential tool for differential diagnosis in thyroid carcinoma.

Objective: This study was designed to reveal potential diagnostic markers in thyroid carcinomas.

Design: Genome-wide methylation profiling technology (Illumina Infinium Human Methylation 450K arrays) was applied in 50 non-neoplastic tissues, 17 benign lesions, 60 papillary (PTC), 10 follicular, 1 poorly differentiated and 3 anaplastic carcinomas. Differentially methylated probes detected in the internal dataset were confirmed in a cross validation study analysis. The differentially methylated CpGs were tested for their ability to correctly diagnose benign lesions and carcinomas by using logistic regression, receiver operating characteristic curves (ROC) and linear prediction methods.

Results: Global hypomethylation was observed in thyroid cancer compared to benign lesions. Hypermethylation was more frequently detected in follicular carcinomas and hypomethylation in papillary carcinomas when compared to non-neoplastic tissues. Aberrant methylation in nine *loci* (*SLC22A18*/*SLC22A18AS, SCNN1A, DCUN1D3, ELOVL5, ELK3, EHF, SOX10, LTK* and one CpG probe mapped outside of a known gene) showed sensitivity of 91.9% and specificity of 76.5% for discriminating benign lesions from thyroid carcinomas. Furthermore, we demonstrated that 3 of 9 *loci* could be also used for stratifying patients with PTC according to the risk of developing lymph node metastasis.

Conclusions: Three epigenetic classifiers with high performance to be used as diagnostic tool in TC were described. We also pointed out three potential markers able to stratify PTC patients according to lymph nodes involvement.

Introduction

Thyroid follicular epithelial cell-derived carcinomas are the most common endocrine malignancies, accounting for 90-95% of thyroid cancer (TC) cases (Elisei and Pinchera, 2012). Based on histology, these carcinomas are subdivided into well-differentiated, including papillary (PTC) and follicular (FTC) thyroid carcinomas, poorly differentiated (PDTC) and undifferentiated (anaplastic – ATC) thyroid carcinomas (Kondo, Ezzat and Asa, 2008).

TC represents approximately 5% of clinically palpable thyroid nodules (Hegedüs, 2004). Fine-needle aspiration (FNA) is the gold standard for screening and diagnosis of thyroid nodules (Schneider and Chen, 2013) and despite of the accuracy of this method, about 17% of the aspirations are classified as having indeterminate cytology (Wang et al., 2011). According to The Bethesda System for Reporting Thyroid Cytopathology, cytologically indeterminate thyroid nodules comprehend Follicular Neoplasms/ Suspicious for Follicular Neoplasm (FN/SFN) and Atypia of Undetermined Significance/Follicular Lesion of Undetermined Significance (AUS/FLUS). Thyroidectomy is commonly recommended for indeterminate or suspicious lesions and these patients underwent to surgery, in the most of times, only for diagnosis purposes. Nevertheless, the majority of these lesions will prove to be benign at surgical intervention (Yang et al., 2007; Wang et al., 2011).

Several molecular tests have been proposed aiming to improve the accuracy of indeterminate FNA cytology and avoid unnecessary and potentially harmful surgery for patients. These studies show a panel of alterations including *BRAF* and *RAS* point mutations and *PAX8/PPARγ* and *RET/PTC* rearrangements with a great potential to identify malignancies in indeterminate thyroid nodules (Cantara et al., 2010; Moses et al., 2010; Nikiforov et al., 2011; Ohori et al., 2010). Although these markers have high specificity and positive predictive value, many tumors are negative for these mutations, resulting in elevated number of false-negative results. Therefore, a differential diagnosis of indeterminate lesions is still necessary.

The use of markers based on gene expression (Chudova et al., 2010) and miRNAs (Nikiforova et al., 2008) for the differential diagnosis of thyroid tumors have been described for FNA and surgical samples. However, diagnostic approaches based on DNA analysis are desirable due to higher DNA stability. In this context, DNA methylation have been considered an attractive epigenetic diagnostic tool and preliminary data in literature have

shown differential gene methylation in TC samples, suggesting that these alterations may potentially be a useful for thyroid cancer diagnosis (Hu et al., 2006; Zhang et al., 2014).

Herein, based on DNA methylation analysis using a global approach we developed a diagnostic classifier for thyroid cancer by combining analysis on an internal dataset with a large sample cohort and external data validation.

Material and Methods

Clinical Samples

A total of 141 thyroid surgical samples were obtained from patients who underwent to surgery at A.C. Camargo Cancer Center (São Paulo, SP, Brazil). The samples comprised 17 benign thyroid lesions (BTL) consisted of follicular adenoma (8), nodular goiter (6) and lymphocytic thyroiditis samples (3), 74 thyroid carcinomas, including 60 papillary (PTC), 8 follicular (FTC), 2 Hürthle cell (HCC), 1 poorly differentiated (PDTC) and 3 anaplastic carcinomas (ATC); and 50 surrounding histologically nonmalignant tissue (NT) from PTC samples. The frozen samples were histologically evaluated by experienced pathologists. In case of discrepancies, a final consensus was reached by three specialized pathologists from A.C. Camargo Cancer Center. The Institutional Ethics Committee (Protocol n° 475.385) approved the study. The patients were advised about the procedures and authorized the research by signing an informed consent. Supplemental Table 1 summarizes the clinical and histopathological data of the cases included in the study.

DNA extraction and bisulfite conversion

After macrodissection, genomic DNA from frozen thyroid tissue was isolated using phenol–chloroform method followed by quantification by *Qubit® dsDNA BR Assay no Qubit® 2.0* Fluorometer (Life Technologies - Carlsbad, CA, USA). Bisulfite conversion of 500 ng of genomic DNA of each sample was performed using *EZ DNA Methylation-Gold™ Kit* (*Zymo Research, Irvine, CA, USA)* according to the manufacturer's recommendations and with the modifications proposed by Illumina.

DNA methylation analysis

The Infinium Methylation 450K assay was performed according to Illumina's standard protocol. Briefly, 4μL (~166ng) of bisulfite converted DNA was whole genome amplified followed by enzymatic fragmentation, precipitation and re-suspension. The resuspended samples were hybridized to Human Methylation 450 BeadChip (Illumina, San Diego, CA, USA) and arrays were stained and scanned with the Illumina HiScan system. The level of methylation at each CpG site was scored as β values ranging between 0 and 1, with 0 indicating unmethylated and 1, completely methylated.

Data quality control, preprocessing and data analysis

Data from Infinium methylation assay were analyzed using a combination of R and Bioconductor packages. To exclude technical and biological biases in further analyses, probes mapped on X and Y chromosomes, those overlapped with known single nucleotide polymorphisms (SNPs), as well as the cross-reactive probes (Chen *et al*., 2013) were excluded. Probes were filtered for low bead count (<3), low quality (p detection >0.05%) and samples having 1% of sites with a detection p-value > 0.05 were also removed using the WaterRmelon package. The data were corrected for color bias and inter sample with quantile normalization. Arrays were also normalized using the beta-mixture quantile normalization (BMIQ) method (Teschendorff *et al.*, 2013) and the batch effects were corrected using Surrogate Variable Analysis (sva) package. Raw microarray and normalized data will be available in Gene Expression Omnibus (http://www.ncbi.nlm.nih.gov/geo/) under specific accession number.

The tumor sample groups were compared using the limma package. The p values for differentially methylated CpG sites were corrected for multiple testing using the Bonferroni correction. The Differentially Methylated Positions (DMPs) were identified with adjusted p value <0.05 and mean delta beta (Δβ) < -0.20 or > +0.20. The probes were annotated according to the data provided by Illumina and HUGO Gene Nomenclature Committee (HGNC).

DNA Methylation Classifier

Methylation classifiers for thyroid lesions were constructed based on DMPs identified by comparing all tumors samples *vs* benign lesions (BTL classifier), papillary carcinoma *vs* non neoplastic (PTC classifier) tissue, and follicular carcinoma *vs* non neoplastic tissue (FTC classifier). To confirm the list of probes obtained in this step, cross study validation was performed using methylation data of thyroid tissues from Timp et al. (2014) with GEO access ID GSE53051 (Supplementary Material). The ability of molecular methylation markers to predict benign and cancer lesions was tested by carrying out a Receiver Operating Characteristic (ROC) curve analysis reporting probes with area under the curve with CI 95%. The lists of probes for each comparison were filtered by linear regression analysis (Stepwise method). The classifiers were constructed in the training set using combinations of probes and different linear class prediction algorithms including Support Vector Machine, Compound Covariate Predictor and Diagonal Linear Discriminant Analysis. The performance was assessed by Leave-One-Out-Cross-Validation (LOOCV) test. Detailed description of these analyses is found in the Supplementary Methods and Supplementary Figure 1. Algorithm scores were associated with the presence of lymph node metastasis using linear-by-linear association test.

Statistical analysis

Data analyses were performed using the R and Bioconductor packages (methylumi, sva and limma). Statistical analysis applied in the discovery of diagnostic markers was performed using SPSS (v. 21.0; SPSS, Chicago, IL, USA) and BRB ArrayTools (v. 4.4.0; http://linus.nci.nih.gov/BRB-ArrayTools.html).

Results

Differentially Methylated CpGs and Cross-Study Validation

The analysis comparing 74 TC with BTL samples revealed 2,517 differentially methylated probes, being 2,383 hypomethylated and 134 hypermethylated. The comparison of PTC with NT showed a list of 3,015 differentially methylated probes, being 2,773 hypomethylated and 242 hypermethylated (Supplementary Table 2). In contrast, FTC compared with NT showed higher frequency of hypermethylated probes (4,100 hyper *vs* 1,475 hypomethylated) (Supplementary Table 2).

To confirm our findings, a cross-study validation test was performed using the methylation microarray data from 82 samples obtained in GEO database (12 NT, 32 BTL, 20 PTC and 18 FTC/HCC). Eighty percent of the probes were confirmed in TC compared with BTL samples (76% hypomethylated and 4% hypermethylated), 73% in FTC *versus* NT (19% hypomethylated and 54% hypermethylated) and 96% in PTC *versus* NT comparison (88% hypomethylated and 8% hypermethylated) (Supplementary Figure 2).

Molecular diagnostic algorithm based on DNA methylation

Differentially methylated probes detected in our study and confirmed by external data validation were further filtered by ROC curve and linear regression analysis. Methylation status of genes distributed across the whole genome to predict the ability of these biomarkers in classifying TC from BTL/NT was used. Non-redundant probes on linear regression analysis are showed in Table 1. The performance of one to five probes combination for each classifier was evaluated with three different linear class prediction methods (SVM, CCP and DLDA) (Supplementary Table 3). Figure 1 shows the mean AUC for each classifier using the internal and external data.

Three-probe based classifiers were selected among nine aberrantly methylated loci (*SLC22A18*/*SLC22A18AS, SCNN1A, DCUN1D3, ELOVL5, ELK3, EHF, SOX10, LTK* and one CpG locus mapped outside of a known gene) to discriminate initially BTL from TC and, subsequently, PTC and FTC from NT (internal data illustrated in Figure 2 and external data in Supplemental Figure 4)

Table 1. Non-redundant probes detected by multivariable analysis used to develop the diagnostic algorithms.

Analysis	Probe ID	Region	Gene Symbol	Internal Data			External Data (GEO GSE53051)			Input order*
				delta β	P# Value	AUC (CI 95%)	delta β	P ° Value	AUC (CI 95%)	
TC versus BTL	cg18419977	Body	*SLC22A18AS*	-0.32	1E-11	0.96 (0.92-1.00)	-0.24	3E-07	0.85 (0.75-0.94)	1
	cg26244013	Body	*SCNN1A*	-0.29	1E-08	0.95 (0.91-1.00)	-0.23	5E-08	0.85 (0.76-0.94)	2
	cg06533895	5'UTR	*DCUN1D3*	-0.32	0.0305	0.94 (0.89-1.00)	-0.18	3E-06	0.85 (0.76-0.94)	3
	cg14116056	Body	*DPY19L1*	-0.32	3E-08	0.96 (0.92-1.00)	-0.26	2E-10	0.89 (0.82-0.97)	4
	cg25096745	Body	*CD44*	-0.33	4E-07	0.97 (0.94-1.00)	-0.22	8E-07	0.85 (0.75-0.94)	5
FTC versus NT	cg23109891	Body	*SOX10*	0.48	2E-23	1.00 (1.00-1.00)	0.30	5E-08	0.98 (0.93-1.00)	1
	cg27141871	-	-	0.26	3E-13	1.00 (1.00-1.00)	0.22	3E-08	0.98 (0.94-1.00)	2
	cg03321553	TSS200	*LTK*	0.24	2E-20	1.00 (1.00-1.00)	0.18	1E-07	0.97 (0.92-1.00)	3
	cg05643964	Body	*LIME1*	0.34	7E-22	1.00 (1.00-1.00)	0.24	1E-06	0.98 (0.93-1.00)	4
	cg27254040	Body	*NRXN1*	-0.29	7E-22	1.00 (1.00-1.00)	-0.16	0.0026	0.97 (0.92-1.00)	5
	cg24202916	-	-	-0.28	6E-07	0.96 (0.91-1.00)	-0.30	9E-09	1.00 (0.98-1.00)	6
	cg14669515	5'UTR	*SPSB1*	0.29	2E-11	1.00 (0.99-1.00)	0.43	5E-11	0.98 (0.93-1.00)	7
	cg24119869	TSS200	*KIR3DX1*	-0.27	9E-10	0.99 (0.98-1.00)	-0.16	2E-05	0.97 (0.92-1.00)	8
	cg10791422	TSS200	*MRGPRD*	-0.22	9E-11	0.99 (0.98-1.00)	-0.23	6E-10	1.00 (1.00-1.00)	9
	cg20703581	-	-	-0.21	7E-09	1.00 (0.99-1.00)	-0.18	3E-05	0.98 (0.93-1.00)	10

	cg13225830	-	-	0.24	1E-07	0.98 (0.95-1.00)	0.25	3E-09	1.00 (1.00-1.00)	11
	cg04720596	TSS1500	*FSD1*	-0.24	1E-11	0.99 (0.97-1.00)	-0.19	1E-06	0.99 (0.95-1.00)	12
	cg20789620	TSS1500	*FSD1*	-0.22	8E-06	0.96 (0.91-1.00)	-0.22	2E-11	1.00 (1.00-1.00)	13
	cg14624546	5'UTR	*ST5*	0.29	4E-10	0.99 (0.97-1.00)	0.29	3E-08	1.00 (0.98-1.00)	14
	cg24168221	TSS1500	*CST9*	-0.35	1E-12	1.00 (1.00-1.00)	-0.37	4E-07	0.97 (0.91-1.00)	15
	cg02482730	Body	*SEPT9*	0.32	0.0002	0.98 (0.93-1.00)	0.28	8E-09	0.97 (0.92-1.00)	16
	cg03478630	-	-	-0.21	2E-06	0.98 (0.96-1.00)	-0.27	8E-06	0.96 (0.90-1.00)	17
	cg22033362	-	-	-0.20	7E-12	0.97 (0.91-1.00)	-0.16	8E-10	1.00 (1.00 -1.00)	18
	cg00923634	Body	*MAN1C1*	0.25	2E-08	1.00 (0.98-1.00)	0.30	2E-08	0.97 (0.91-1.00)	19
	cg05006231	-	-	0.26	1E-07	1.00 (0.99-1.00)	0.22	9E-07	1.00 (0.98-1.00)	20
	cg16498391	Body	*SLMO1*	0.28	3E-09	1.00 (0.99-1.00)	0.29	2E-13	1.00 (1.00-1.00)	21
	cg13337655	-	-	0.26	1E-09	1.00 (0.99-1.00)	0.30	4E-12	1.00 (0.98-1.00)	22
	cg04888174	-	-	-0.25	5E-12	1.00 (0.99-1.00)	-0.18	3E-08	0.98 (0.94-1.00)	23
	cg00241002	TSS200	-	-0.28	5E-13	1.00 (0.99-1.00)	-0.40	2E-09	0.98 (0.94-1.00)	24
	cg20817941	1stExon	*CTSK*	0.29	3E-15	1.00 (1.00-1.00)	0.18	2E-08	0.98 (0.941-1.00)	25
	cg14014720	Body	*DAPK1*	0.22	2E-09	0.99 (0.97-1)	0.43	6E-08	0.98 (0.93-1.00)	26
	cg27038348	1stExon	*RBP3*	-0.26	8E-13	1.00 (1.00-1.00)	-0.18	2E-07	0.98 (0.94-1.00)	27
	cg08610426	5'UTR	*IZUMO1*	0.27	1E-10	0.99 (0.98-1.00)	0.32	6E-10	0.99 (0.97-1.00)	28
PTC	cg08597067	Body	*ELOVL5*	0.37	2E-29	0.99 (0.97-1.00)	0.38	3E-09	0.97 (0.91-1.00)	1

versus NT	cg01291854	5'UTR	*ELK3*	-0.43	5E-28	0.99 (0.99-1.00)	-0.25	3E-05	0.97 (0.92-1.00)	2
	cg05503887	TSS1500	*EHF*	-0.27	2E-15	0.94 (0.90-0.987)	-0.28	8E-08	0.97 (0.91-1.00)	3
	cg06533895	5'UTR	*DCUN1D3*	-0.39	4E-19	0.99 (0.97-1.00)	-0.31	3E-07	0.98 (0.94-1.00)	4
	cg02819992	-	-	-0.43	3E-29	0.99 (0.97-1.00)	-0.34	4E-07	0.96 (0.90-1.00)	5
	cg00610577	Body	*ETV6*	-0.37	2E-20	0.96 (0.92-1.00)	-0.49	3E-09	0.97 (0.91-1.00)	6

Legend: [#] Bonferroni correction adjusted P value ˚ P value of unpaired t test ***** Input order for linear class prediction algorithms

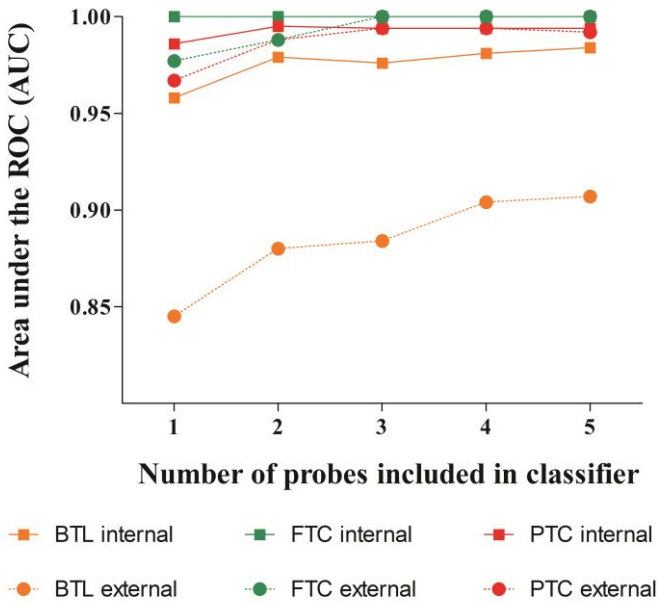

Figure 1. Mean area under the curve of the receiver operating characteristic (ROC) of three class prediction methods, according to the number of methylated markers included in the construction of the classifiers. The top five probes for each comparison were selected after linear regression analysis.

The combined application of the three probes methylation classifiers for thyroid lesions is shown on Figure 3. Using internal data (Figure 3A), the first classifier (design to recognize BTL) was able to discriminate 11 of 17 BTL, which the indication would be only watchful waiting. For the remaining cases, by adding the second classifier (designed to recognize FTC), surgery would be indicated for 17 of 74 malignant tumors (all FTC/HCC and PDTC/ATC cases and 3 PTC) and four BTL samples. Finally, the third classifier (designed to recognize PTC) would indicate surgery for 51 PTC. Two BTL and six PTC were negative for all steps of the algorithm, which the indication would be the watchful waiting. The algorithm correctly classified the NT samples.

Using the same application model for external data (Figure 3B), surgery would be indicated for six benign lesions and only three malignant lesions would be classified as negative for all tests and thus indicated for watchful waiting. Classification according to histological type in internal and external data is detailed in Supplementary Table 5.

These classifiers using the methylation pattern of selected probes allowed the correct classification of carcinomas and benign lesions with sensitivity of 91.9% and specificity of 76.5%. By applying the same algorithm in an external set of samples, high sensitivity and specificity (92.1% and 81.3%, respectively) was also observed (Table 2).

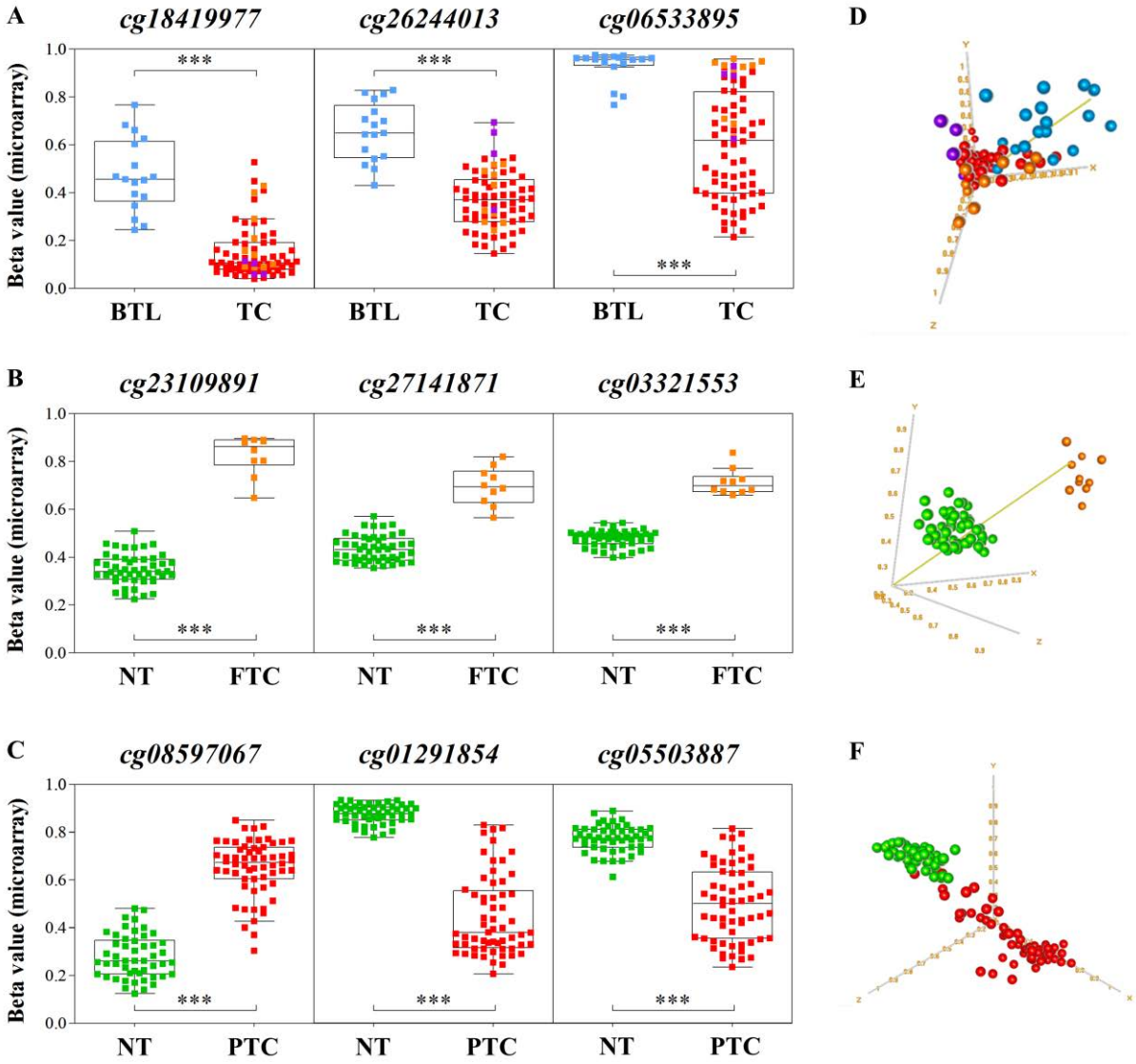

Figure 2. Diagnostic model for thyroid lesions using the methylation data obtained in the present study. **A.** The overall methylation pattern **(**Beta values) of the top 3 probes for benign classifier, **B.** follicular classifier and **C.** papillary classifier. **D.** Three dimensional graph plotting methylation pattern for benign lesions**, E**. for follicular carcinomas and **F**. papillary carcinomas. **Abbreviation.** NT: non neoplastic thyroid tissue; BTL: benign thyroid lesions; TC: thyroid carcinomas; PTC: papillary thyroid carcinoma; FTC: follicular thyroid carcinoma.

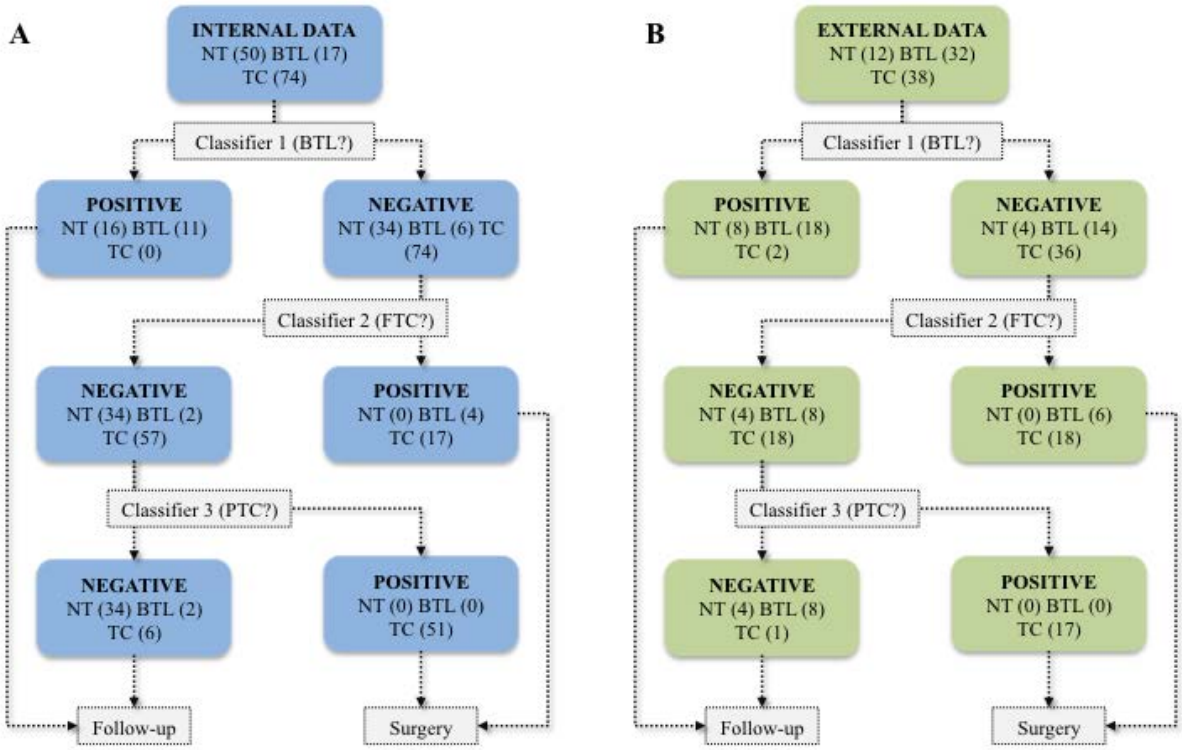

Figure 3. Flowchart showing the application and global performance of the three classifiers developed to differentiate benign lesions and thyroid carcinomas. **A.** Summary of the sample classification obtained in the training set (internal data). **B.** Summary of the classification of samples obtained using the external data (GEO data set) **Abbreviation.** NT: non neoplastic thyroid tissue; BTL: benign thyroid lesions; TC: thyroid carcinomas; PTC: papillary thyroid carcinoma; FTC: follicular thyroid carcinoma.

Table 2. Classification of global performance using the data obtained in this study (internal and external data of the 3 methylated *loci* classifier.

Metric	Internal Data		External Data	
	Estimate	**CI (95%)**	**Estimate**	**CI (95%)**
Sensitivity	91.9%	83.2-97.0	92.1%	78.6-98.3
Specificity	76.5%	50.1-93.2	81.3%	63.6-92.8
PPV	94.4%	86.4-98.5	85.4%	70.8-94.4
NPV	68.4%	43.5-87.4	89.7%	72.7-97.8

Abbreviation. PPV= positive predictive value; NPV= negative predictive value; CI= confidence interval.

Risk score based on methylation signature is a prognostic factor

The PTC classifier, comprising 3 *loci*, was tested as a lymph node metastasis predictor in a external dataset of 479 PTC samples (TCGA). Scores values obtained by SVM method were homogenously stratified in five risk subclasses (very low, low, intermediate, high and very high). A linear association with the risk of lymph node involvement was revealed, ranging from 0% in very low group risk to 66% in very high group risk (linear by linear association test P<0.001) (Figure 4).

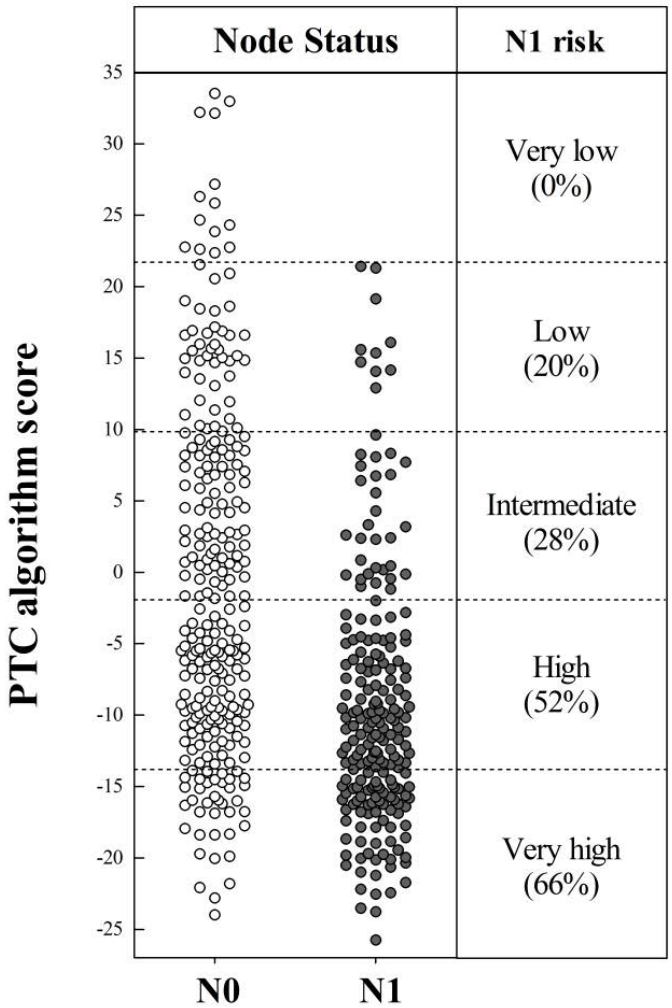

Figure 4. Lymph node metastasis risk according to the PTC algorithm score. The figure demonstrates a linear association of risk of lymph node involvement according to algorithm score values in papillary thyroid cancer patients using external data (TCGA).
Abbreviation. N0: without lymph node involvement, N1: presence of lymph node metastasis

Discussion

Despite the significant reduction of unnecessary thyroid surgeries by using FNA in thyroid nodule diagnosis, only 34% of samples with indeterminate diagnostic will prove to be malignant in post-surgical histological analysis (Xing et al., 2013), since most of the cases are cytological benign lesions (Hegedüs, 2004; Mazzaferri, 1993). Thus, the differential diagnosis of thyroid nodule is still a challenge in some cases, especially in lesions with follicular pattern (Suster, 2006).

In this study, using a comprehensive genome-wide profiling technology, capable to detect methylation pattern with single-site resolution, we determined the methylation changes in thyroid tumor samples compared to benign lesions. In addition, the methylation profiling was also assessed in papillary and follicular carcinomas in relation to non-neoplastic tissues revealing multiple CpG with aberrant methylation. Notably, a robust classifier combining the methylation patterns in 9 *loci* was identified in a training set of 141 thyroid surgical samples with high performance to discriminate TC from normal and benign samples.

Previous studies evaluated the potential of DNA methylation markers for differential diagnosis in thyroid lesions. Gauchotte et al. (2013) failed to classify the thyroid carcinomas based on the *RARB2* methylation patterns, since aberrant methylation was observed only in anaplastic carcinomas. In contrast, the average methylation status of 5 CpG sites of Galectin-3 gene was able to distinguish papillary and anaplastic cancer from the non- neoplastic thyroid tissues (Keller et al., 2013). Recently, Zane et al. (2013) suggested that a panel including circulating cell-free DNA, *SLC5A8* and *SLC26A4* hypermethylation, and *BRAFV600E* mutation analysis could be used as a tool diagnosis of TC, however the methylation analysis only included papillary TC samples. Mohammadi-asl et al. (2011) also distinguished PTC carcinomas applying a cutoff for hypermethylation levels of *P16*, *TSHR* and *RASSF1A* genes. Most of these studies were designed including only PTC samples, which limit their clinical application, since the FTC is the subtype presenting more difficulties at diagnosis, even for experienced pathologists (Franc et al., 2003).

Evaluation of *CALCA*, *TIMP3*, *DAPK*, *CDH1* and *RARB2* serum methylation levels was proposed as a diagnostic tool for TC. Hu et al. (2006), testing these genes, evaluated 53 FNAs obtained from 31 PTC, 7 FTC and 15 benign lesions and found a preoperative diagnostic accuracy of 77%, a high positive predictive value (96%) and

negative predictive value of 60%. More recently, aberrant methylation *CALCA*, *TIMP3, DAPK1*, *RARB* and *RASSF1A* genes revealed a diagnostic accuracy of 63.69% in papillary carcinomas and benign lesions, increasing this value to 85.71% for training and 79.74% for test group with concomitant detection of *BRAF* mutation (Zhang et al., 2014). Higher diagnostic accuracy was observed by combining the methylation markers and detection of *BRAF* mutation, but only for PTC samples, since follicular carcinomas are negative for this mutation.

Single biomarkers can render false positive and false negative results, thus they are often inadequate for clinical recommendation. Large-scale approaches have contributed to reveal potential biomarkers in various cancers. The best example is Mamaprint test approved by FDA, an algorithm to predict prognosis in breast cancer, which evaluates the expression levels of 70 genes resulted from a large-scale transcriptome analysis (van' t Veer et al., 2002). A previous prospective and multicenter study evaluated 265 selected FNAs thyroid samples with indeterminate diagnosis using a gene-expression classifier composed of 167 genes. The algorithm was able to identify nodules as suspicious with high sensitivity (92%), but with low specificity (52%) (Alexander et al., 2012). Other studies confirmed the potential of this classifier (Duick et al., 2012; Walsh et al., 2012), but also raised questions of the application of this test in the clinical practice (McIver et al., 2014). In addition, Chudova et al. (2010) in their seminal study using a diagnostic test based on gene-expression classifier in TC pointed the need of a high number of genes combined in a classifier in order to achieve a high accuracy test (Chudova et al., 2010). Various studies have also investigated the immunhistochemical expression pattern of proteins to be used in the diagnosis of thyroid carcinomas (Ozolins et al., 2012; Ratour et al., 2013; Zhang et al., 2015).

It is well recognized that DNA-based molecular biomarkers are very attractive, part due to the robustness and stability of these biomarkers, and part due to the fact that analyses involving gene and protein expression have more pitfalls for this application (Shivapurkar and Gazdar, 2010; Tost, 2010). In the epigenetic field, recent technological advances enable the global analysis of methylation patterns in tumor tissues allowing the detection of a large range of putative epigenetic biomarkers, which allow the detection of more suitable classifiers. In our study, the algorithm designed is promising for application in clinical practice by combining the test stability compared to gene expression-based classifiers and also by comprising a small number of *loc*i (*SLC22A18*/*SLC22A18AS, SCNN1A, DCUN1D3, ELOVL5, ELK3, EHF, SOX10, LTK*

and one CpG locus mapped outside a known gene).

We were able to identify with high sensitivity (91.9%) thyroid cancer cases in a significant number of samples, including those with follicular pattern based on the differential methylation of *SLC22A18*/*SLC22A18AS, SCNN1A, DCUN1D3, ELOVL5, ELK3, EHF, SOX10, LTK* and one CpG locus mapped outside of a known gene. The application of our algorithm allowed the correct classification of all FTC samples, but 4 of 8 follicular adenoma samples (FA, supplementary Table 5) were classified as malignant using FTC classifier. These data suggest that these benign tumors not only show similar cytological features with FTC but also present similar epigenetic changes, which make difficult to fully differentiate these lesions. Conversely, among the malignant lesions misclassified as benign by our algorithm, 3 were classical PTCs (3 of 47) and 3 were follicular variants of PTC (FVPTC, 3 of 10). In fact, difficulties on differential diagnosis involving these variants are commonly reported (Baloch and LiVolsi, 2002; Logani et al., 2000). In our study, 66.67% of these variants were correctly classified, thus our classifier could improve the diagnosis in FNA-cytology.

One of the challenges in developing diagnostic algorithm is to reproduce the performance in a different sample set. Testing our classifier in an independent data set of 82 thyroid tumors and 32 benign lesions obtained from GEO database, only nine samples were misclassified, being 3 (4.2%) tumor samples (2 FTC and 1 PTC) classified as benign and 6 (18.8%) benign lesions classified as malignant, reinforcing the power of our classifier.

The *SCNN1A* gene, included in the algorithm designed to differentiate BTL from TC, encodes the 1 alpha subunit of a sodium channel, non-voltage gated. The expression of the *SCNN1A* gene-encoded protein together with other putative biomarkers were assessed in thyroid tissues arranged in a tissue microarray trying to distinguish benign from malignant thyroid nodules, however this protein was discarded as a good diagnostic marker (Davidov et al., 2014). Despite not having been related to thyroid carcinomas, the aberrant gain of methylation in this gene (along with other biomarkers) proved to be associated with poor prognosis in breast cancer (Roll et al., 2013) and neuroblastoma (Carén et al., 2011). In overall, among the 8 known genes included in the diagnostic algorithm, none of then had been previously associated with thyroid carcinomas.

The *SOX10,* also included in our algorithm, belongs in a family of transcription factors and was found as hypermethylated in folicullar carcinomas in our study. This

gene was reported as oncogene in melanoma (Verfaillie et al., 2015) and hepatocarcinoma (Zhou et al., 2014), but as tumor suppressor gene in Merlin-null schwannoma (Doddrell et al., 2013). Despite of the controversy regarding its function, the protein expression was reported as a sensitive diagnostic marker in salivary adenoid cystic carcinoma and basal-like breast carcinoma (Ivanov et al., 2013) and in desmoplastic melanoma (Palla et al., 2013). Moreover, the downregulation of *SOX10,* inversely correlated with methylation was associated with shorter survival in patients with glioblastoma (Etcheverry et al., 2010). The *SOX10* hypermethylation detected in our study is in agreement with the results reported in digestive tumors (colon, stomach and esophagus) (Tong et al., 2014). *SOX10* hypermethylation revealed to be a potential diagnostic marker in thyroid cancer.

We found the *SLC22A18*/*SLC22A18AS* among the genes identified in our diagnostic classifier. *SLC22A18* is a tumor suppressor gene that shows an imprinting regulation (Cooper et al., 19980). Loss of methylation in the promoter region was previously described in gliomas (Chu et al., 2011). In addition, this gene is one of the 4-genes panel associated with the potential to distinguish Barrett's disease from esophagus adenocarcinoma (Alvi et al., 2014). Remarkably, *SLC22A18* hypomethylation was a classifier member able to discriminate benign lesions from carcinomasin in our study. Furthermore, *EHF* overexpression was associated with poor prognosis in serous ovarian carcinoma (Brenne et al., 2011) and *ELOVL5* upregulation was reported in prostate carcinomas (Romanuik et al., 2009).

Although the mechanisms by which some of these genes are involved in thyroid carcinogenesis or even in other cancer types are not very clear, aberrant methylation of CpG in these loci have the potential to be used as differential diagnosis in thyroid lesions.

Importantly, this algorithm had the ability to identify PTC patients with risk to have lymph nodes involvement. In cases classified with low risk, none of patients presented lymph node metastasis according three differentially methylated loci. The percentage of patients with lymph node metastasis linearly increased according to the algorithm score. Although PTC is an indolent carcinoma, central lymph node (CLN) metastases are common e despite of a well-known independent risk factor in local recurrence, the prophylactic neck dissection is still controversial (Lundgren et al., 2006; Mazzaferri et al., 2009). The usage of the PTC classifier preoperatively herein described has the potential to be introduced in the clinical practice as an auxiliary tool in the

decision of therapeutic central neck dissection.

Taken together, we reported a novel classifier with potential clinical application in distinguish benign from malignant thyroid tumors. Our results can improve the advances in the preoperative screening and is able to determine the stratification risk of lymph node metastasis in papillary thyroid carcinomas.

Acknowlegments

The authors thank the A.C. Camargo Cancer Center Biobank for providing and processing the samples.

Funding

This study was supported by grants from the National Institute of Science and Technology in Oncogenomics (Fundação de Amparo à Pesquisa do Estado de São Paulo –FAPESP Grant 2008/57887–9, Conselho Nacional de Desenvolvimento Científico e Tecnoló́ ico Grant CNPq 573589/08–9) The PhD student (MBR) was supported by fellowship from CNPq (140819/2011-8).

Disclosure Summary: The authors have nothing to disclose.

References

Alexander EK, Kennedy GC, Baloch ZW, Cibas ES, Chudova D, Diggans J, Friedman L, Kloos RT, LiVolsi VA, Mandel SJ, Raab SS, Rosai J, Steward DL, Walsh PS, Wilde JI, Zeiger MA, Lanman RB, Haugen BR. Preoperative diagnosis of benign thyroid nodules with indeterminate cytology. N Engl J Med. 2012; 367(8):705-15.

Alvi MA, Liu X, O'Donovan M, Newton R, Wernisch L, Shannon NB, Shariff K, di Pietro M, Bergman JJ, Ragunath K, Fitzgerald RC. DNA methylation as an adjunct to histopathology to detect prevalent, inconspicuous dysplasia and early-stage neoplasia in Barrett's esophagus. Clin Cancer Res. 2013; 19(4):878-88.

Baloch ZW, Livolsi VA. Follicular-patterned lesions of the thyroid: the bane of the pathologist. Am J Clin Pathol. 2002; 117(1):143-50.

Brenne K, Nymoen DA, Hetland TE, Trope' CG, Davidson B. Expression of the Ets transcription factor EHF in serous ovarian carcinoma effusions is a marker of poor survival. Hum Pathol. 2012; 43(4):496-505.

Cantara S, Capezzone M, Marchisotta S, Capuano S, Busonero G, Toti P, Di Santo A, Caruso G, Carli AF, Brilli L, Montanaro A, Pacini F. Impact of proto-oncogene mutation detection in cytological specimens from thyroid nodules improves the diagnostic accuracy of cytology. J Clin Endocrinol Metab. 2010; 95(3):1365-9.

Carén H, Djos A, Nethander M, Sjöberg RM, Kogner P, Enström C, Nilsson S, Martinsson T. Identification of epigenetically regulated genes that predict patient outcome in neuroblastoma. BMC Cancer. 2011; 11:66.

Chen YA, Lemire M, Choufani S, Butcher DT, Grafodatskaya D, Zanke BW, Gallinger S, Hudson TJ, Weksberg R. Discovery of cross-reactive probes and polymorphic CpGs in the Illumina Infinium HumanMethylation450 microarray. Epigenetics. 2013; 8(2):203-9.

Chudova D, Wilde JI, Wang ET, Wang H, Rabbee N, Egidio CM, Reynolds J, Tom E, Pagan M, Rigl CT, Friedman L, Wang CC, Lanman RB, Zeiger M, Kebebew E, Rosai J, Fellegara G, LiVolsi VA, Kennedy GC. Molecular classification of thyroid nodules using high-dimensionality genomic data. J Clin Endocrinol Metab. 2010; 95(12):5296-304.

Chu SH, Feng DF, Ma YB, Zhang H, Zhu ZA, Li ZQ, Jiang PC. Promoter methylation and downregulation of SLC22A18 are associated with the development and progression of human glioma. J Transl Med. 2011; 9:156.

Cooper PR, Smilinich NJ, Day CD, Nowak NJ, Reid LH, Pearsall RS, Reece M, Prawitt D, Landers J, Housman DE, Winterpacht A, Zabel BU, Pelletier J, Weissman BE, Shows TB, Higgins MJ. Divergently transcribed overlapping genes expressed in liver and kidney and located in the 11p15.5 imprinted domain. Genomics. 1998; 49(1):38-51.

Davidov T, Nagar M, Kierson M, Chekmareva M, Chen C, Lu SE, Lin Y, Chernyavsky V, Potdevin L, Arumugam D, Barnard N, Trooskin S. Carbonic anhydrase 4 and crystallin α-B immunoreactivity may distinguish benign from malignant thyroid nodules in patients with indeterminate thyroid cytology. J Surg Res. 2014; 190(2):565-74.

Doddrell RD, Dun XP, Shivane A, Feltri ML, Wrabetz L, Wegner M, Sock E, Hanemann CO, Parkinson DB. Loss of SOX10 function contributes to the phenotype of human Merlin-null schwannoma cells. Brain. 2013; 136(Pt 2):549-63.

Duick DS, Klopper JP, Diggans JC, Friedman L, Kennedy GC, Lanman RB, McIver B. The impact of benign gene expression classifier test results on the endocrinologist-patient decision to operate on patients with thyroid nodules with indeterminate fine-needle aspiration cytopathology. Thyroid. 2012; 22(10):996-1001.

Elisei R, Pinchera A. Advances in the follow-up of differentiated or medullary thyroid cancer. Nat Rev Endocrinol. 2012; 8(8):466-75.

Etcheverry A, Aubry M, de Tayrac M, Vauleon E, Boniface R, Guenot F, Saikali S, Hamlat A, Riffaud L, Menei P, Quillien V, Mosser J. DNA methylation in glioblastoma: impact on gene expression and clinical outcome. BMC Genomics. 2010; 11:701.

Franc B, de la Salmonière P, Lange F, Hoang C, Louvel A, de Roquancourt A, Vildé F, Hejblum G, Chevret S, Chastang C. Interobserver and intraobserver reproducibility in the histopathology of follicular thyroid carcinoma. Hum Pathol 2003; 34:1092-1100.

Gauchotte G, Lacomme S, Brochin L, Tournier B, Cahn V, Monhoven N, Piard F, Klein M, Martinet N, Rochette-Egly C, Vignaud JM. Retinoid acid receptor expression is helpful to distinguish between adenoma and well-differentiated carcinoma in the thyroid. Virchows Arch. 2013; 462(6):619-32.

Hegedüs L. Clinical practice. The thyroid nodule. N Engl J Med. 2004; 351(17):1764-71.

Hu S, Ewertz M, Tufano RP, Brait M, Carvalho AL, Liu D, Tufaro AP, Basaria S, Cooper DS, Sidransky D, Ladenson PW, Xing M. Detection of serum deoxyribonucleic acid methylation markers: a novel diagnostic tool for thyroid cancer. J Clin Endocrinol Metab. 2006; 91(1):98-104.

Ivanov SV, Panaccione A, Nonaka D, Prasad ML, Boyd KL, Brown B, Guo Y, Sewell A, Yarbrough WG. Diagnostic SOX10 gene signatures in salivary adenoid cystic and breast basal-like carcinomas. Br J Cancer. 2013; 109(2):444-51.

Kondo T, Asa SL, Ezzat S. Epigenetic dysregulation in thyroid neoplasia. Endocrinol Metab Clin North Am. 2008; 37(2):389-400.

Li H, Hong G, Xu H, Guo Z. Application of the rank-based method to DNA methylation for cancer diagnosis. Gene. 2015; 555(2):203-7.

Logani S, Gupta PK, LiVolsi VA, Mandel S, Baloch ZW. Thyroid nodules with FNA cytology suspicious for follicular variant of papillary thyroid carcinoma: follow-up and management. Diagn Cytopathol. 2000; 23(6):380-5.

Lundgren CI, Hall P, Dickman PW, Zedenius J. Clinically significant prognostic factors for differentiated thyroid carcinoma: a population-based, nested case-control study. Cancer. 2006; 106(3):524-31.

Mazzaferri EL, Doherty GM, Steward DL. The pros and cons of prophylactic central compartment lymph node dissection for papillary thyroid carcinoma. Thyroid. 2009; 19(7):683-9.

Mazzaferri EL. Management of a solitary thyroid nodule. N Engl J Med. 1993; 328(8):553-9.

McIver B, Castro MR, Morris JC, Bernet V, Smallridge R, Henry M, Kosok L, Reddi H. An independent study of a gene expression classifier (Afirma) in the evaluation of cytologically indeterminate thyroid nodules. J Clin Endocrinol Metab. 2014; 99(11):4069-77.

Mohammadi-asl J, Larijani B, Khorgami Z, Tavangar SM, Haghpanah V, Kheirollahi M, Mehdipour P. Qualitative and quantitative promoter hypermethylation patterns of the P16, TSHR, RASSF1A and RARβ2 genes in papillary thyroid carcinoma. Med Oncol. 2011; 28(4):1123-8.

Moses W, Weng J, Sansano I, Peng M, Khanafshar E, Ljung BM, Duh QY, Clark OH, Kebebew E. Molecular testing for somatic mutations improves the accuracy of thyroid fine-needle aspiration biopsy. World J Surg. 2010; 34(11):2589-94.

Nikiforova MN, Tseng GC, Steward D, Diorio D, Nikiforov YE. MicroRNA expression profiling of thyroid tumors: biological significance and diagnostic utility. J Clin Endocrinol Metab. 2008; 93(5):1600-8.

Nikiforov YE, Ohori NP, Hodak SP, Carty SE, LeBeau SO, Ferris RL, Yip L, Seethala RR, Tublin ME, Stang MT, Coyne C, Johnson JT, Stewart AF, Nikiforova MN. Impact of mutational testing on the diagnosis and management of patients with cytologically indeterminate thyroid nodules: a prospective analysis of 1056 FNA samples. J Clin Endocrinol Metab. 2011; 96(11):3390-7.

Ohori NP, Nikiforova MN, Schoedel KE, LeBeau SO, Hodak SP, Seethala RR, Carty SE, Ogilvie JB, Yip L, Nikiforov YE. Contribution of molecular testing to thyroid fine-

needle aspiration cytology of "follicular lesion of undetermined significance/atypia of undetermined significance". Cancer Cytopathol. 2010; 118(1):17-23.

Ozolins A, Narbuts Z, Strumfa I, Volanska G, Stepanovs K, Gardovskis J. Immunohistochemical expression of HBME-1, E-cadherin, and CD56 in the differential diagnosis of thyroid nodules. Medicina (Kaunas). 2012; 48(10):507-14.

Palla B, Su A, Binder S, Dry S. SOX10 expression distinguishes desmoplastic melanoma from its histologic mimics. Am J Dermatopathol. 2013; 35(5):576-81.

Pennelli G, Saccani A, Rubello D, Nitti D, Pelizzo MR. Circulating cell-free DNA, SLC5A8 and SLC26A4 hypermethylation, BRAF(V600E): A non-invasive tool panel for early detection of thyroid cancer. Biomed Pharmacother. 2013; 67(8):723-30.

Ratour J, Polivka M, Dahan H, Hamzi L, Kania R, Dumuis ML, Cohen R, Laloi-Michelin M, Cochand-Priollet B. Diagnosis of follicular lesions of undetermined significance in fine-needle aspirations of thyroid nodules. J Thyroid Res. 2013; 2013:250347.

Roll JD, Rivenbark AG, Sandhu R, Parker JS, Jones WD, Carey LA, Livasy CA, Coleman WB. Dysregulation of the epigenome in triple-negative breast cancers: basal-like and claudin-low breast cancers express aberrant DNA hypermethylation. Exp Mol Pathol. 2013; 95(3):276-87.

Romanuik TL, Ueda T, Le N, Haile S, Yong TM, Thomson T, Vessella RL, Sadar MD. Novel biomarkers for prostate cancer including noncoding transcripts. Am J Pathol. 2009 Dec; 175(6):2264-76.

Schneider DF, Chen H. New developments in the diagnosis and treatment of thyroid cancer. CA Cancer J Clin. 2013; 63(6):374-94.

Shivapurkar N, Gazdar AF. DNA methylation based biomarkers in non-invasive cancer screening. Curr Mol Med. 2010; 10(2):123-32.

Suster S.Thyroid tumors with a follicular growth pattern: problems in differential diagnosis. Arch Pathol Lab Med. 2006; 130(7):984-8.

Teschendorff AE, Marabita F, Lechner M, Bartlett T, Tegner J, Gomez-Cabrero D, Beck S. A beta-mixture quantile normalization method for correcting probe design bias in Illumina Infinium 450 k DNA methylation data. Bioinformatics. 2013; 29(2):189-96.

Tong X, Li L, Li X, Heng L, Zhong L, Su X, Rong R, Hu S, Liu W, Jia B, Liu X, Kou G, Han J, Guo S, Hu Y, Li C, Tao Q, Guo Y. SOX10, a novel HMG-box-containing tumor suppressor, inhibits growth and metastasis of digestive cancers by suppressing the Wnt/β-catenin pathway. Oncotarget. 2014; 5(21):10571-83.

Tost J. DNA methylation: an introduction to the biology and the disease-associated changes of a promising biomarker. Mol Biotechnol. 2010; 44(1):71-81.

van 't Veer LJ, Dai H, van de Vijver MJ, He YD, Hart AA, Mao M, Peterse HL, van der Kooy K, Marton MJ, Witteveen AT, Schreiber GJ, Kerkhoven RM, Roberts C, Linsley PS, Bernards R, Friend SH. Gene expression profiling predicts clinical outcome of breast cancer. Nature. 2002; 415(6871):530-6.

Verfaillie A, Imrichova H, Atak ZK, Dewaele M, Rambow F, Hulselmans G, Christiaens V, Svetlichnyy D, Luciani F, Van den Mooter L, Claerhout S, Fiers M, Journe F, Ghanem GE, Herrmann C, Halder G, Marine JC, Aerts S. Decoding the regulatory landscape of melanoma reveals TEADS as regulators of the invasive cell state. Nat Commun. 2015; 6:6683.

Walsh PS, Wilde JI, Tom EY, Reynolds JD, Chen DC, Chudova DI, Pagan M, Pankratz DG, Wong M, Veitch J, Friedman L, Monroe R, Steward DL, Lupo MA, Lanman RB, Kennedy GC. Analytical performance verification of a molecular diagnostic for cytology-indeterminate thyroid nodules. J Clin Endocrinol Metab. 2012; 97(12):E2297-306.

Wang CC, Friedman L, Kennedy GC, Wang H, Kebebew E, Steward DL, Zeiger MA, Westra WH, Wang Y, Khanafshar E, Fellegara G, Rosai J, Livolsi V, Lanman RB. A large multicenter correlation study of thyroid nodule cytopathology and histopathology. Thyroid. 2011; 21(3):243-51.

Yang J, Schnadig V, Logrono R, Wasserman PG. Fine-needle aspiration of thyroid nodules: a study of 4703 patients with histologic and clinical correlations. Cancer. 2007; 111(5):306-15.

Xing M, Haugen BR, Schlumberger M. Progress in molecular-based management of differentiated thyroid cancer. Lancet. 2013; 381(9871):1058-69.

Zane M, Agostini M, Enzo MV, Casal Ide E, Del Bianco P, Torresan F, Merante Boschin I, Keller S, Angrisano T, Florio E, Pero R, Decaussin-Petrucci M, Troncone G, Capasso M, Lembo F, Fusco A, Chiariotti L. DNA methylation state of the galectin-3 gene represents a potential new marker of thyroid malignancy. Oncol Lett. 2013; 6(1):86-90.

Zhang B, Liu S, Zhang Z, Wei J, Qu Y, Wu K, Yang Q, Hou P1, Shi B. Analysis of BRAF(V600E) mutation and DNA methylation improves the diagnostics of thyroid fine needle aspiration biopsies. Diagn Pathol. 2014; 9:45.

Zhang L, Krausz T, DeMay RM. A Pilot Study of Galectin-3, HBME-1, and p27 Triple Immunostaining Pattern for Diagnosis of Indeterminate Thyroid Nodules in Cytology With Correlation to Histology. Appl Immunohistochem Mol Morphol. 2014 Sep 15. [Epub ahead of print]

Zhou D, Bai F, Zhang X, Hu M, Zhao G, Zhao Z, Liu R. SOX10 is a novel oncogene in hepatocellular carcinoma through Wnt/β-catenin/TCF4 cascade. Tumour Biol. 2014; 35(10):9935-40.

Supplementary Data

Sample selection

Fresh-frozen samples from 8 FA, 6 NG, 3 LT, 60 PTC, 8 FTC, 2 HCC, 1 PDTC, 3 ATC and 50 NT were retrospectively selected from patients underwent to surgery at A.C. Camargo Cancer Center (São Paulo, SP, Brazil) between 2000 and 2013 according to the availability of institutional BioBank. The NT samples presented no histological alterations. Among the patients with benign lesions, 71% where female and the majority of them had more than 45 years old (59%).

Confirmation step of differentially methylated probes

Before the construction of the diagnostic algorithm, we performed a cross validation study to confirm the initial list of CpG differentially methylated probes obtained in all comparisons. For this purpose, methylation profile data were screened using GEO Dataset (http://www.ncbi.nlm.nih.gov/gds). Methylation β values (Illumina Beadchip 450k) of 12 NT, 32 BTL, 10 PTC and 18 FTC/HCC were collected and used for this confirmation step. Public database was assessed in February, 2015. Levene statistical test was applied in this dataset and significance was considered with $P < 0.05$ in unpaired t test. Only significant probes (without considering the cutoff of delta β) were used in the diagnostic algorithm.

Development of methylation-based diagnostic algorithm

A ROC curve analysis was performed for each comparison using the β values for confirmed probes detected in our dataset. Probes were selected with area under the curve (AUC) of 0.75 with CI 95% for all tumors vs benign lesions and 0.90 for papillary and follicular carcinomas versus non neoplastic lesions. We applied linear regression analysis (Stepwise method) in β values for 14 probes in BTL classifier, 120

probes for PTC and 212 for FTC classifier, in both, internal and external data. The top 5 positions for each classifier were selected to apply the Support Vector Machine, Compound Covariate Predictor and Diagonal Linear Discriminant Analysis. Performance of the top 9 probes (3 probes for each classifier) was defined as sensitivity, specificity, positive predictive value (PPV), negative predictive value (NPV) for internal and external microarray data.

TCGA data for application of prognostic algorithm

We tested the prognostic potential of our PTC diagnostic algorithm by using external data collected from TCGA (https://tcga-data.nci.nih.gov/tcga/). Methylation data (Platform Infinium® Human Methylation450 BeadChip) of 479 PTC were collected from the "Thyroid Carcinoma" option in TCGA portal. Data were obtained from level 3 (normalized data) and from samples with lymph node status available. For analytical purposes, we grouped Nx and N0 into category without lymph node metastasis and N1, as a category of patients that presented lymph nodes involvement. Algorithm scores were homogenously stratified in five risk subclasses: very low, low, intermediate, high and very high.

Supplementary Table 1. Clinicopathologic characteristics of the patients with PTC, FTC, HCC, PDTC and ATC enrolled in the study.

Characteristics	CPT		Other Subtypes	
	N	%	N	%
Age				
<45 years	37	61,67	4	28,57
≥45 years	23	38,33	10	71,43
Gender				
Female	44	73,33	10	71,43
Male	16	26,67	4	28,57
Histology (excluded PTC)				
FTC	-	-	8	57,14
HCC	-	-	2	14,29
PDTC	-	-	1	7,14
ATC	-	-	3	21,43
Predominant variant (PTC only)				
Classic	47	78,33	-	-

Follicular	10	16,67	-	-
Other	3	5,00	-	-
Tumor dimension (cm)				
Median (interval)	1,3 (0,5-5,5)	-	2,3 (0,9-13)	-
mCPT(≤1cm)	25	41,67	-	-
CPT (>1cm)	35	58,33	-	-
Extrathyroidal extension				
No	30	52,63	7	53,85
Yes	27	47,37	6	46,15
Ni	3	-	1	-
Invasion				
Blood	2	3,39	5	38,46
Lymphatic	3	5,08	1	7,69
Both	1	1,69	2	15,38
No	53	89,83	5	38,46
Ni	1	-	1	-
Perineural invasion				
No	42	93,33	10	23,08
Yes	3	6,67	3	76,92
Ni	15		1	-
Lymph node metastasis				
No (cN0, pN0)	32	53,33	9	69,23
Yes (pN1)	28	46,67	4	30,77
Ni	-	-	1	-
Clinical evolution				
Free of disease	44	73,33	5	71,43
Confirmed recurrence	16	26,67	2	28,57
Ni*	-	-	7	-
Death				
No	59	98,33	10	71,43
Yes	1	1,67	4	28,57
Follow-up (months)#	83,8 (1,1-142,9)	-	63,3[o] (4,0-139,4)	-

Abbreviation. Ni: not informed; cN: no clinical evidence of cancer in the regional lymph nodes; pN0: no pathologically evidence of cancer in regional lymph nodes; pN1: pathological confirmation of cancer in regional lymph nodes.* 1 FTC with lost follow-up, 2 FTC without 5 years of follow-up and 4 non differentiated carcinomas with aggressive disease and death before the recurrence diagnosis. # data up to August, 2014. [o] only for FTC samples.

Supplementary Table 2. List of probes found differentially methylated in three comparisons (TC *vs* BTL, FTC *vs* NT and PTC *vs* NT) evaluated in this study: (Excel format)

Supplementary Table 3. Performance of the probes combination for each classifier using the three linear classification method.

Cassete	nº of probes	Linear Classification Methods								
		CCP			DLDA			SVM		
		Sens	Spec	AUC	Sens	Spec	AUC	Sens	Spec	AUC
Benign?	1	82	92	0.958	82	92	0.958	18	99	0.958
	2	94	92	0.979	94	92	0.979	65	100	0.979
	3	88	87	0.975	88	89	0.977	**65**	**100**	**0.978**
	4	94	85	0.979	94	88	0.982	77	100	0.981
	5	94	84	0.984	94	87	0.984	82	99	0.984
Follicular carcinoma?	1	100	100	1.000	100	100	1.000	90	100	1.000
	2	100	100	1.000	100	100	1.000	100	100	1.000
	3	100	100	1.000	**100**	**100**	**1.000**	100	100	1.000
	4	100	100	1.000	100	100	1.000	100	100	1.000
	5	100	100	1.000	100	100	1.000	100	100	1.000
Papillary carcinoma?	1	92	96	0.986	92	96	0.986	93	96	0.986
	2	90	100	0.995	90	100	0.995	90	100	0.996
	3	88	100	0.994	88	100	0.994	**90**	**100**	**0.995**
	4	83	100	0.994	87	100	0.994	90	100	0.995
	5	88	100	0.994	88	100	0.994	92	100	0.994

Abbreviation. Sens = sensibility; Spec = specificity; AUC = area under curve; CCP = Compound Covariate Predictor; DLDA = Diagonal Linear Discriminant Analysis; SVM = Support Vector Machine. In bold are showed the combinations used for further analysis.

Supplementary Table 4. Classification performance of the methylation-based diagnostic markers according to the histological types.

INTERNAL DATA					EXTERNAL DATA				
Histological diagnosis	**Trio 1+ (BTL)**	**Trio 2+ (FTC)**	**Trio 3+ (PTC)**	**All negative**	**Histological diagnosis**	**Trio 1+ (BTL)**	**Trio 2+ (FTC)**	**Trio 3+ (PTC)**	**All negative**
NT= 50	16	0	0	34	**NT= 12**	8	0	0	4
NG= 6	5	0	0	1	**NG=11**	7	1	0	3
FA= 8	4	4	0	0	**FA= 21**	11	5	0	5
CLT= 3	2	0	0	1	**CLT= 0**	-	-	-	-
FTC= 8	0	8	0	0	**FTC= 10**	2	7	1	0
HCC= 2	0	2	0	0	**HCC= 8**	0	7	1	0
PTC= 47	0	2	42	3	**PTC= 10**	0	1	8	1
FVPTC= 10	0	1	6	3	**FVPTC= 10**	0	3	7	0
RVPTC= 3	0	0	3	0	**RVPTC= 0**	-	-	-	-
PDTC= 1	0	1	0	0	**PDTC= 0**	-	-	-	-
ATC= 3	0	3	0	0	**ATC= 0**	-	-	-	-

Abbreviation. NT= normal thyroid; FA= follicular adenomas; HYP= nodular hyperplasia; NG= nodular goiter; CLT= chronic lymphocytic thyroiditis ; PTC= classical variant papillary thyroid carcinoma; FVPTC= follicular variant papillary thyroid carcinoma; RVPTC= rare variant papillary thyroid carcinoma; PDTC= poor differentiated thyroid carcinomas; ATC= anaplastic thyroid carcinomas; FTC= follicular thyroid carcinomas (FTC); HCC= Hürtle cell carcinomas.

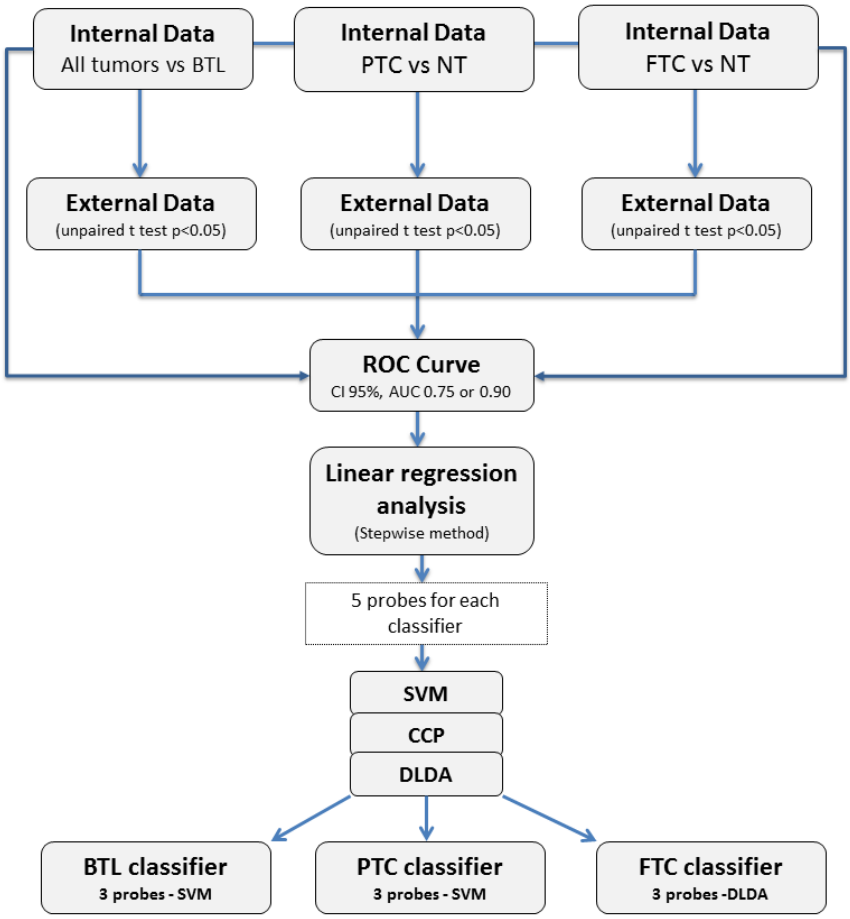

Supplementary Figure 1. Flowchart illustrating the design used in development of the classifier algorithm. Our data was confirmed using GEO database. The ROC curve analysis were performed for internal and external comparison analysis. Probes with AUC established were submitted to linear regression analysis and the combination of top 5 probes for each comparison was evaluated by SVM, CCP and DLDA to create a diagnostic algorithm.

Abbreviation. ROC = Receiver Operating Characteristic; AUC = area under curve; CCP = Compound Covariate Predictor; DLDA = Diagonal Linear Discriminant Analysis; SVM = Support Vector

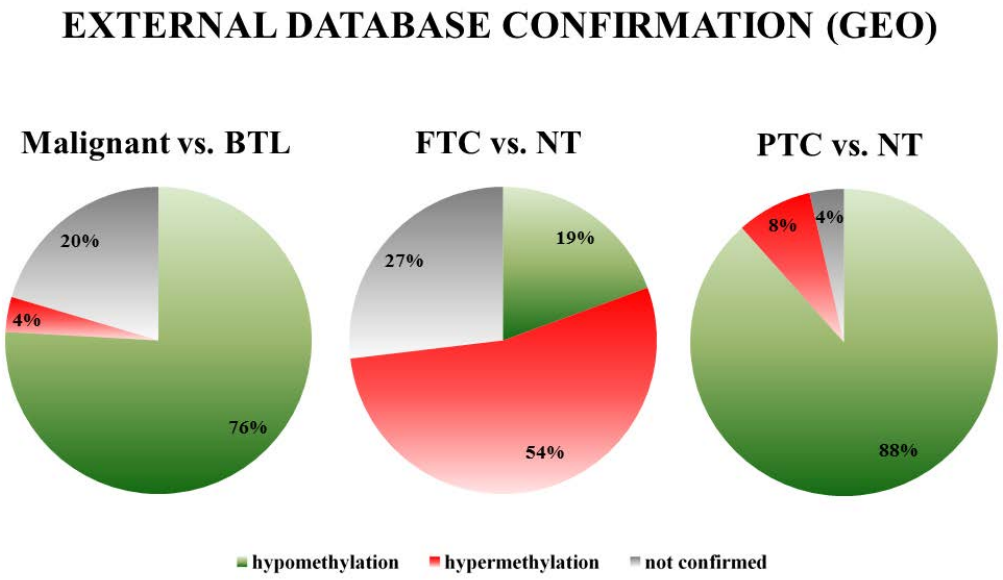

Supplementary Figure 2. Data confirmation of the differentially methylated probes in thyroid lesions by GEO database. Only P value was used for statistical analyses (delta beta cutoff was not evaluated). None of the significant probes presented an inverted methylation direction. Probes not confirmed included those without statistical significance and probes without available beta value in external data. Significant probes for each comparison were used in ROC curve analyses

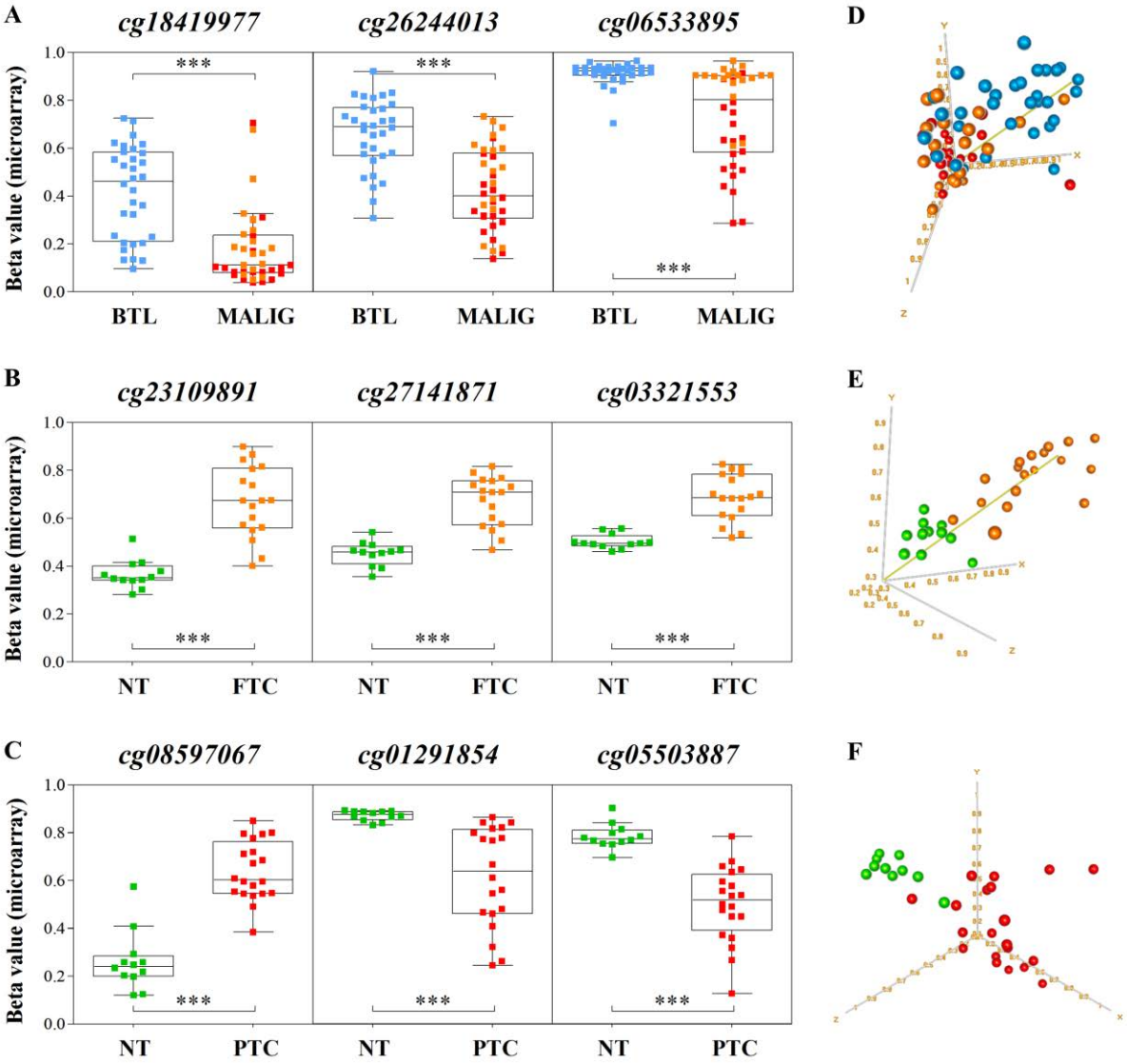

Supplementary Figure 3. Diagnostic model for thyroid lesions using external data (GEO database). **A.** The overall methylation pattern **(**Beta values) of the top 3 probes for benign classifier, **B.** follicular classifier and **C.** papillary classifier. **D.** Three dimensional graph plotting methylation pattern for benign lesions**, E**. for follicular carcinomas and **F**. papillary carcinomas.

Capítulo 3 – Research Paper

Methylation signature according to the histological subtypes of thyroid lesions and its impact in patient outcome

Mariana Bisarro dos Reis[1], Mateus de Camargo Barros Filho[2], Fábio Marchi[2], Caroline Moraes Beltrami[2], Hellen Kuasne[2,5], Clóvis Antônio Lopes Pinto[3],Srikant Ambatipudi[4], Zdenko Herceg[4] , Luiz Paulo Kowalski[2,5], Silvia Regina Rogatto[2,6]*

[1] Genetics Post Graduation Program, Biosciences Institute, UNESP, Sao Paulo State University, Botucatu, Sao Paulo, Brazil

[2] Internacional Research Center - CIPE – A.C. Camargo Cancer Center and National Institute of Science and Technology in Oncogenomics, São Paulo, Brazil

[3] Department of Pathology, A.C. Camargo Cancer Center, São Paulo, SP, Brazil

[4] Epigenetics Group; International Agency for Research on Cancer (IARC), Lyon, France

[5] Department of Head and Neck Surgery and Otorhinolaryngology, A. C. Camargo Cancer Center, São Paulo, SP, Brazil and

[6] Department of Urology, Faculty of Medicine, UNESP - Sao Paulo State University, Botucatu, SP, Brazil.

***To whom correspondence should be addressed at:**

Silvia Regina Rogatto, PhD
Dept Urologia. Faculdade de Medicina – UNESP, Botucatu - São Paulo, SP – Brazil
CEP: 18618-970; Telephone: +55-14-38116436, Fax: +55-14-38116271;
E-mail: rogatto@fmb.unesp.br, silvia.rogatto@cipe.accamargo.org.br.

Key words: methylation profile, thyroid cancer, benign lesions, prognostic markers

Cinical Epigenetics (to be submitted) (FI 6.22)

Abstract

Background: Cumulative evidences have suggested that the deregulation of normal DNA methylation landscape contributes to thyroid cancer development. Thyroid carcinoma (TC) is the most common endocrine gland tumor and papillary TC (PTC) is detected in the majority of the cases (80-85% of cases). To better understand the biology of TC and to identify a prognostic epigenetic signature, we used the genome-wide DNA methylation approach (450k platform, Illumina) in a cohort of 50 non neoplastic thyroid tissues, 17 benign lesions (8 adenomas, 6 goiter and 3 thyroiditis) and 74 thyroid carcinomas (60 PTC, 8 follicular, 2 Hurthle carcinomas, 1 poorly differentiated and 3 anaplastic carcinomas).

Results: A specific epigenetic profile was detected according to the histological subtype. Benign lesions and follicular carcinomas showed a greater number of methylated CpG, whereas hypomethylation was predominant in papillary and undifferentiated carcinomas. Specifically in undifferentiated tumors, the G alpha i signaling pathway was activated (11 genes hypomethylated and 1 hypermethylated). Promoter-based differential methylation (DM) analysis revealed several pathways involved in the etiology of benign and malignant lesions, including dysregulation of retinoic acid metabolism, immune response and cell cycle control. Interestingly, a prognostic classifier based on five hypomethylated probes (cg13237068, cg17765025, cg04473654, cg06042504, cg27500148) was able to predict poor outcome in patients with malignant tumors (Sensitivity: 77.3%; Specificity: 89.6%).

Conclusions: We characterized the methylome of thyroid lesions according to the histological subtypes and identified putative biomarkers regulated by methylation. In addition, a meaningful algorithm based on five probes associated with worse prognosis (recurrence and death by disease) in thyroid carcinoma patients was described.

Introduction

Epigenetics is one of the most promising fields in biomedical research and refers to changes that can alter the transcriptional pattern of a gene without modify the genomic sequence. DNA methylation is a relatively stable epigenetic modification that occurs almost exclusively in CpG context and plays a role in the control of gene expression (Baylin and Jones, 2011). Hypermethylation of promoter CpGs in cancer cells is associated with silencing of tumor suppressor genes (Jones and Baylin, 2002). Loss of 5-methylcitosine is also observed and causes activation of oncogenes or genomic instability in cancer cells (Esteller M, 2006; Feinberg, 2004). In addition to genetic alterations, accumulate evidences reveal that alterations in DNA methylation play an important role in thyroid tumorigenesis (Xing, 2007; Rodríguez-Rodero et al., 2014).

Thyroid cancer (TC) is the most common endocrine cancer (Siegel, 2015) and comprises a group of tumors with remarkably different features. Papillary (PTC) and follicular carcinomas (FTC) are well-differentiated tumors comprising 90% of all TC cases (Elisei and Pinchera, 2012), whilst poorly differentiated (PDTC) and anaplastic thyroid carcinoma (ATC) subtypes are less frequently diagnosed (Siironen et al., 2010). Despite of indolent biological behavior of the well-differentiated carcinomas, these tumors occasionally may give rise to less-differentiated and more aggressive thyroid cancers (Bhaijee and Nikiforov, 2011; Xing, 2013). In addition, well differentiated carcinomas metastasize and a significant number of patients developed recurrence (Aschebrook-Kilfoy et al., 2013; Hay et al, 2002).

DNA methylation in TC has been intensively studied and several markers have been described, however, to our knowledge none of them has been applied in the clinical practice. Graff et al. (1998) was one of the first groups that demonstrated the importance of methylation in TC. The authors evaluated the methylation pattern of *CDH1* in 32 TC (6 PTC, 9 FTC and 5 Hürtle carcinomas, 12 poorly differentiated) showing differences according to the histological subtypes. The association of methylation and prognosis in TC has also been described (Guan et al., 2008; Hu et al., 2006). More recently, the methylation patterns of *SLC5A8* and *SLC26A4* were described as associated with early diagnosis (Zane et al., 2013).

Currently, limited number of genome wide methylation studies has been reported in TC, and most of them are focused in PTC. In a recent publication of The Cancer Genome Atlas project (TCGA), the differential methylation profiles were

revealed in a large cohort of PTC (N=496) using a high-density platform (Illumina Infinium HM 450 array) and combining different genomic approaches (Cancer Genome Atlas Research Network, 2014, 2014). The authors proposed a reclassification of the PTC based on the molecular subtypes and argue that the findings are potentially useful to contribute to the management of the disease. Rodriguez-Rodero et al. (2013) using a low-density platform (Illumina Infinium HM 27K microarray) in a limited number of samples (2 PTC, 2 FTC, 2 medullary and 2 ATC) showed different methylation profiles related with thyroid cancer subtypes. The authors also suggested aberrant methylation patterns in potential tumor suppressor genes and oncogenes, which could be associated with thyroid cancer.

In the present study, we performed a comprehensive characterization of the global methylation (Illumina Infinium HM 450K microarray) in a large cohort of benign and malignant thyroid lesions revealing potential epigenetically regulated biomarkers and pathways involved in thyroid carcinogenesis.

Methods

Patients

Seventeen benign thyroid lesions (BTL); 74 thyroid tumors including 60 PTC, 10 FTC/HCC, 1 PDTC and 3 ATC; and 50 surrounding nonmalignant tissue (NT) of PTC samples were obtained from patients that underwent to surgery at A.C. Camargo Cancer Center (São Paulo, SP, Brazil). This study was approved by the institutional Ethics Committee (Protocol n° 475.385). Patients were advised regarding the procedures and provided written informed consent. Supplemental Table 1 summarizes the clinical and histopathological data.

DNA extraction, bisulfite conversion and DNA methylation analysis

Genomic DNA from frozen thyroid tissue was extracted using phenol-chloroform method and was quantified by Qubit® dsDNA BR Assay (Qubit® 2.0 Fluorometer, Life Technologies - Carlsbad, CA, USA). The DNA (500ng) was bisulfite converted using EZ DNA Methylation-Gold™ Kit (Zymo Research, Irvine, CA, USA) according to the manufacturer's instructions with the modifications described by Illumina.

Genome wide methylation assays were performed using the Human Methylation 450 BeadChip (Illumina, San Diego, CA, USA) as per the manufacturer's recommendations. The data were captured in Illumina HiScan system and the β values ranged from 0 (unmethylated) to 1 (methylated).

Methylation analysis was performed using R language. Quality control parameters were checked, probes were filtered, normalized and a batch effect was assessed. Briefly, cross-reactive probes (≥49 bases), SNPs (MAF>5%), sex-associated probes (Chen *et al*., 2013), low quality probes (p>0,05) and low bead count (<3) in at least 5% of samples were excluded. Data were normalized using the beta-mixture quantile normalization (BMIQ) method (Teschendorff *et al.*, 2013) and the batch effects correction was performed using the surrogate variable analysis (sva) package (Leek et al, 2014). Annotation was performed according to HUGO Gene Nomenclature Committee (HGNC). Differentially hyper- or hypomethylated loci between benign lesions, papillary, follicular/Hürthle and poorly differentiated/anaplastic tumor samples against non-neoplastic tissue were identified using limma package with adjusted P value <0.05 and mean delta beta (Δβ) < -0.20 or > +0.20.

Clustering analysis

Unsupervised hierarchical clustering analysis was performed using complete linkage and one-minus-correlation distance parameters, comprising the most variably methylated probes (8,016 probes with interquartile range (IR) >0.2) with BRB Array Tools v. 4.4.0 software (Biometric Research Branch, National Cancer Institute).

Pathway enrichment analysis

I*n silico* pathway analysis was conducted with Ingenuity Pathway Analysis software (IPA®, QIAGEN Redwood City, www.qiagen.com/ingenuity) and KOBAS (v. 2.0; http://kobas.cbi.pku.edu.cn/home.do) comprising the list of differentially methylated probes obtained in all comparisons (BTL *vs* NT, PTC *vs* NT, FTC/HCC *vs* NT and PDTC/ATC *vs* NT). As an additional criteria, only probes mapped distantly from the transcription start site (TSS) mapped within the interval until 200 bp and 200 to 1500bp upstream of this site and those mapped proximal to the TSS (CpGs located within the 5'UTR and first exon) were included.

DNA methylation-based algorithm to predict thyroid cancer outcome

The differential methylation profiles were evaluated according to patient outcome. For analysis purposes, poorly differentiated and anaplastic carcinomas (death due to the disease) and well-differentiated cases with recurrence (death or recurrence histologically confirmed) were grouped and compared with well-differentiated carcinomas of patients with good clinical outcome (no evidence of active disease in at least five years of follow-up). Differentially methylated probes were firstly selected according to non-adjusted $P<0.001$ and $\Delta\beta < -0.10$ or $> +0.10$ (using limma package). Probes were then filtered by the area under the receiver operating characteristic (ROC) curve (AUC> 0.8) before the construction of a classifier using BRB Array Tools v. 4.4.0 software. Diagonal linear discriminant analysis (DLDA) method was applied adopting recursive feature elimination approach to estimate the optimal number of probes inputted. Classification performance was calculated using leave-one-out cross-validation (LOOCV). Scores obtained by the predictive model were stratified in low (above first quartile), intermediate (interquartile range) and high (under the third quartile) risk categories. Disease-free survival analysis was performed including only well differentiated tumors employing Kaplan–Meier estimator and log-rank test.

Statistical Analysis

Methylation quality control data and differential analysis were performed using R and Bioconductor packages (methylumi, sva, limma). The Bonferroni method was used to adjust P values for multiple comparisons. DNA methylation β-values were graphically represented using heatmap generated by BRB ArrayTools (v. 4.4.0; http://linus.nci.nih.gov/BRB-ArrayTools.html).

Results

Global DNA methylation in thyroid cancer subtypes

Methylation profiles of 91 benign lesions and tumor samples and 50 surrounding nonmalignant tissue were investigated. Unsupervised hierarchical cluster analysis revealed four clusters using the most variable probes of the platform (IR> 0.2), which showed pathological and molecular differences (Figure 1). The cluster 1 was enriched

by follicular adenomas, nodular goiter and minimally invasive follicular carcinomas, the cluster 2 by non-neoplastic thyroid tissues, cluster 3 by papillary thyroid carcinomas and cluster 4 by undifferentiated thyroid cancer and lymphocytic chronic thyroiditis.

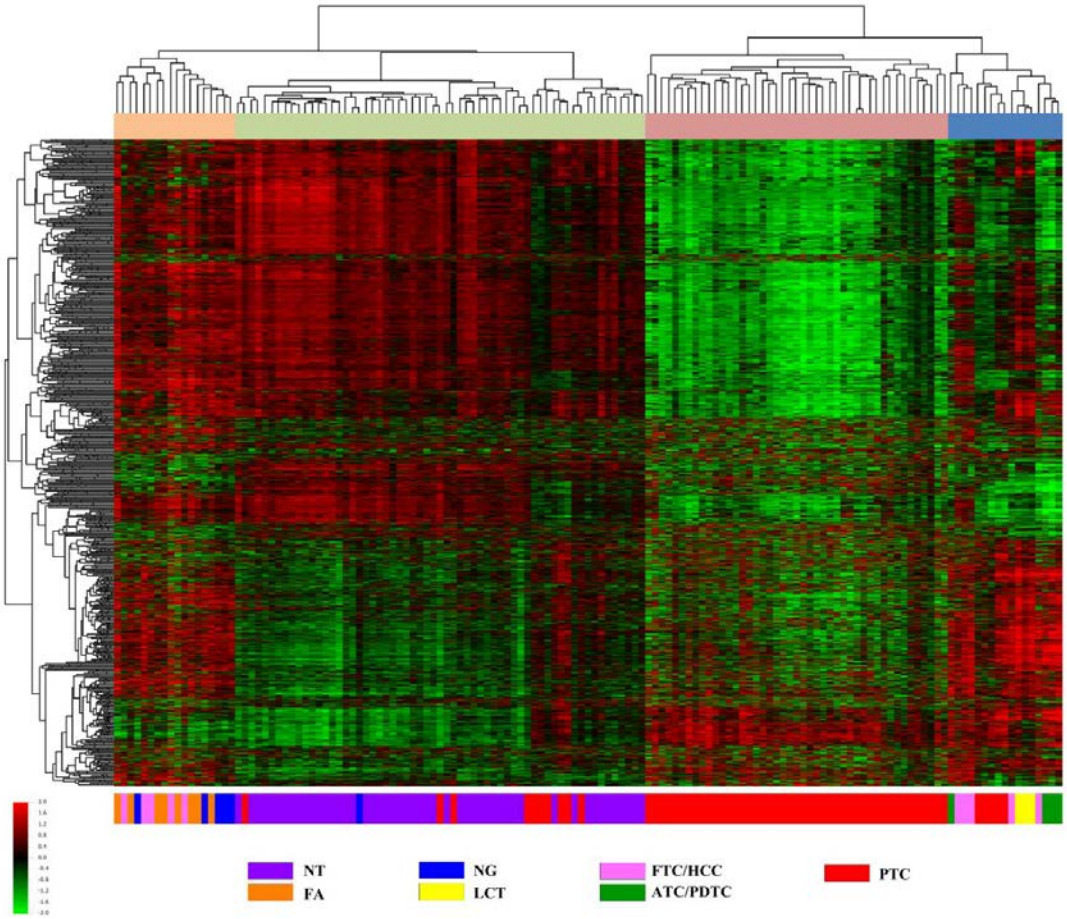

Figure 1. Unsupervised hierarchical clustering of the methylation profiles of thyroid tissues. Four major groups were detected and defined by the most variable probes. The rows correspond to CpG sites, while the columns correspond to samples. **Abbreviation.** NT, non-neoplastic adjacent thyroid tissue; FA, follicular adenoma; NG, nodular goiter; LCT= lymphocytic thyroiditis; FTC, follicular thyroid carcinoma; HCC, Hurthle Cell Carcinoma; ATC, anaplastic thyroid carcinoma; PDTC, poorly differentiated thyroid carcinoma; PTC, papillary thyroid carcinoma.

Comparison of benign lesions and follicular-derived cell carcinomas revealed a progressive number of differentially methylated probes from BLT, PTC, FTC/HCC to PDTC/ATC compared with non-neoplastic thyroid tissues. Using a $|\Delta\beta|$ of 0.2 and adjusted p value of 0.05; 1,753 differentially methylated probes in benign lesions were identified (222 hypomethylated and 1,531 hypermethylated); 3,015 in PTC (2,773 hypo and 242 hypermethylated); 5,575 in FTC (1,475 hypo and 4,100 hypermethylated) and 35,167 in PDTC/ATC (28,252 hypo and 6,195 hypermethylated) (Figure 2A; Supplemental Table 1). Top 10 differentially methylated probes are shown on Table 1.

DNA methylation changes were found in all genomic regions. Hypermethylated CpGs were enriched in CpG island regions in all comparisons; whereas hypomethylation was more frequently observed outside of CpG islands (Figure 2B). In total, 620 hypermethylated probes were exclusively found in BTL, 113 in PTC, 2,244 in FTC/HCC and 5,411 in PDTC/ATC. Similarly, 95 hypomethylated probes were found in BTL, 1,996 in PTC, 465 in FTC/HCC and 26,734 in PDTC/ATC (Figure 2C).

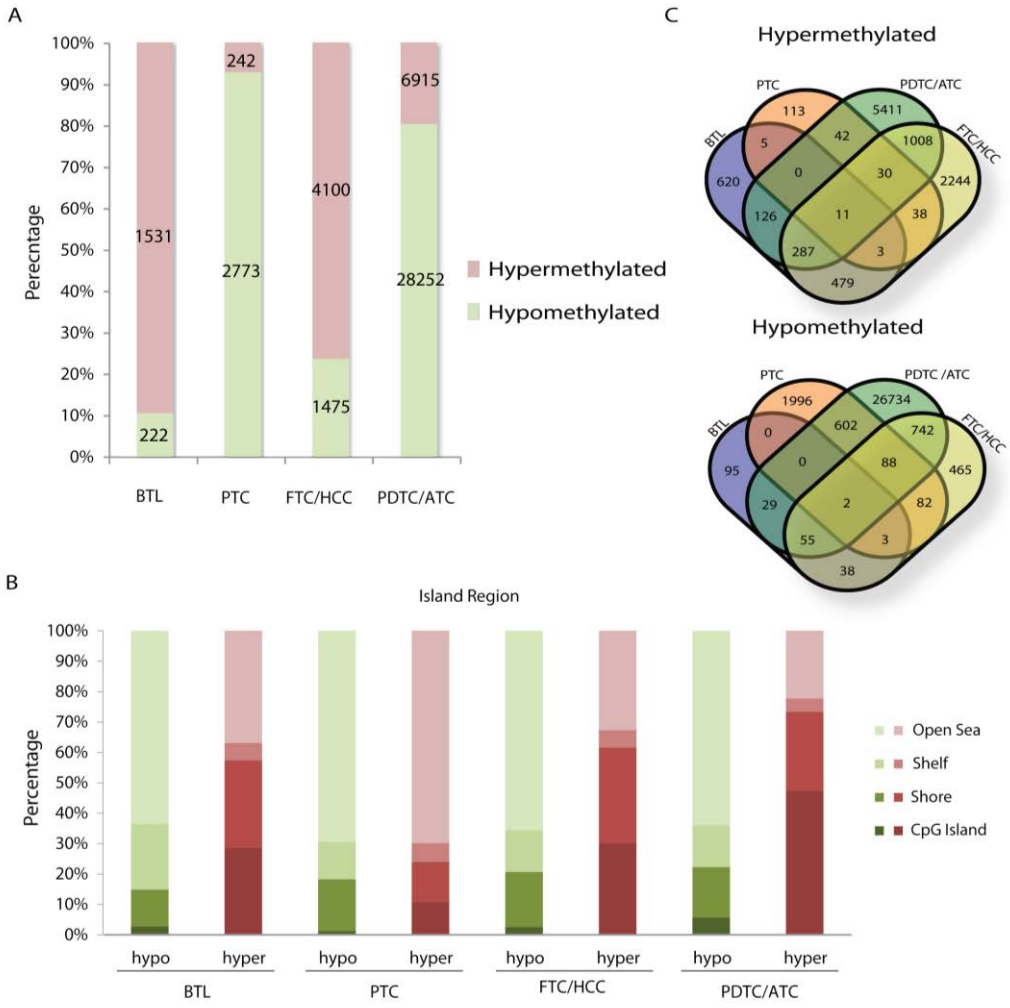

Figure 2. Comparison of CpG site methylation among benign lesions, thyroid carcinomas and surrounding nonmalignant tissues. **A**. Percentage of hypermethylated (red) and hypomethylated (green) probes in BTL, PTC, FTC/HCC and PDTC/ATC. **B**. CpG site proportions by location relative to CpG island regions, according to Illumina 450 K annotation. **C**. Hyper-and hypomethylation according to pathological subtypes revealed common and exclusive alterations. **Abbreviation.** BTL, benign thyroid lesions, follicular thyroid carcinoma; HCC, Hurthle Cell Carcinoma; ATC, anaplastic thyroid carcinoma; PDTC, poorly differentiated thyroid carcinoma; PTC, papillary thyroid carcinoma.

Table 1. Top 10 differentially methylated probes identified in each comparison of thyroid lesions (BTL, FTC, PTC and ATC) with surrounding non-malignant tissues (NT).

Analysis	Probe ID	Region	Gene Symbol	Gene name	delta (lesion-NT)	adj P Val
BTL vs. NT	cg13331354	Body	*SSBP4*	single stranded DNA binding protein 4	0.39	4E-18
	cg10790698	Body	*SSBP4*	single stranded DNA binding protein 4	0.39	2E-20
	cg23483886	Body	*LPCAT1*	lysophosphatidylcholine acyltransferase 1	0.39	6E-17
	cg05578056	Body	*LMF1*	lipase maturation factor 1	0.38	2E-19
	cg18547371	Body	*SSBP4*	single stranded DNA binding protein 4	0.38	1E-18
	cg12019614	Body	*DOCK6*	dedicator of cytokinesis 6	0.38	2E-17
	cg07160992	Body	*AKT1*	v-akt murine thymoma viral oncogene homolog 1	0.36	4E-11
	cg07561894	Body	*SSBP4*	single stranded DNA binding protein 4	0.36	2E-15
	cg23109891	Body	*SOX10*	SRY (sex determining region Y)-box 10	0.36	9E-20
	cg01252526	Body	*WDR90*	WD repeat domain 90	0.36	3E-09
FTC/HCC vs. NT	cg23109891	Body	*SOX10*	SRY (sex determining region Y)-box 10	0.48	2E-23
	cg07160992	Body	*AKT1*	v-akt murine thymoma viral oncogene homolog 1	0.48	2E-13
	cg21851534	3'UTR	*ZZEF1*	zinc finger, ZZ-type with EF-hand domain 1	0.43	1E-16
	cg09557149	Body	*DCTD*	dCMP deaminase	0.43	6E-13
	cg23483886	Body	*LPCAT1*	lysophosphatidylcholine acyltransferase 1	0.42	4E-13
	cg25138553	Body	*HSPG2*	heparan sulfate proteoglycan 2	0.41	1E-13
	cg01252526	Body	*WDR90*	WD repeat domain 90	0.41	5E-08
	cg24628744	TSS1500	*H2AFY*	H2A histone family, member Y	0.41	1E-23
	cg08379987	Body	*TEX26*	testis expressed 26	0.40	8E-20
	cg20191453	Body	*AMT*	aminomethyltransferase	0.40	8E-23
PTC vs. NT	cg20834178	Body	*TBC1D14*	TBC1 domain family, member 14	-0.48	3E-31
	cg11228682	Body	*ATXN1*	ataxin 1	-0.47	5E-29
	cg13606889	Body	*SORL1*	sortilin-related receptor, L(DLR class) A repeats containing	-0.47	4E-29
	cg03301058	Body	*GABRR2*	gamma-aminobutyric acid (GABA) A receptor, rho 2	-0.46	7E-29
	cg13591783	5'UTR	*ANXA1*	annexin A1	-0.45	3E-25
	cg09968361	5'UTR	*SERPINA1*	serpin peptidase inhibitor, clade A (alpha-1 antiproteinase, antitrypsin), member 1	-0.44	7E-29
	cg18458509	Body	*SLC22A18AS*	solute carrier family 22 (organic cation transporter), member 18 antisense	-0.44	7E-30
	cg06778183	Body	*MCTP1*	multiple C2 domains, transmembrane 1	-0.43	6E-29
	cg08908131	Body	*KIAA1598*	KIAA1598	-0.43	2E-24
	cg21638357	Body	*GIGYF1*	GRB10 interacting GYF protein 1	-0.43	2E-26
PDTC/ATC vs. NT	cg16209517	Body	*CIPC*	CLOCK-interacting pacemaker	0.65	3E-15
	cg04915566	5'UTR	*RUNX1*	runt-related transcription factor 1	-0.64	2E-13
	cg01058360	Body	*PRKAG2*	protein kinase, AMP-activated, gamma 2 non-catalytic subunit	-0.63	1E-17
	cg27549186	Body	*TIMP2*	TIMP metallopeptidase inhibitor 2	-0.61	9E-19
	cg17117459	5'UTR	*PARP4*	poly (ADP-ribose) polymerase family, member 4	-0.60	2E-14
	cg08202226	TSS1500	*GATAD2B*	GATA zinc finger domain containing 2B	-0.60	2E-21
	cg17648080	Body	*SMG6*	SMG6 nonsense mediated mRNA decay factor	0.59	2E-18
	cg26554834	Body	*PTPRN2*	protein tyrosine phosphatase, receptor type, N polypeptide 2	-0.59	2E-33

	cg22969397	Body	*CELSR1*	cadherin, EGF LAG seven-pass G-type receptor 1	0.59	3E-14
	cg14178043	Body	*CAPN2*	calpain 2, (m/II) large subunit	0.58	3E-13

Promoter – associated pathways

In silico signaling pathway analyses revealed that hypo and hypemethylated genes in thyroid cancer were involved in different inhibited or activated pathways in benign lesions, papillary, follicular and poorly/anaplastic thyroid carcinomas (Table 2; Supplemental Table 3). Mechanisms involved in the Gαi Signaling in non-differentiated carcinoma were identified as deregulated canonical pathways by IPA and KOBAS software (Figure 3; Supplemental Table 3 and 4). Canonical pathways involving retinoic acid receptors (VDX/RXR) also appeared to be activated in PTC and FTC.

Table 2. Top 10 significant canonical pathways identified in group's comparisons by Ingenuity Pathway Analysis software.

Analysis	Pathway (IPA)	Prediction state (z-score)	Genes found / database	P (Fisher exact test)	P (BH correction)
BTL vs NT	Reelin Signaling in Neurons	-	6/79	0.002	0.438
	eNOS Signaling	inhibited (-1.9)	8/142	0.003	0.438
	Leukocyte Extravasation Signaling	inhibited (-0.7)	9/198	0.006	0.443
	IL-4 Signaling	-	5/76	0.009	0.443
	CCR3 Signaling in Eosinophils	-	6/117	0.014	0.443
	FAK Signaling	-	5/87	0.015	0.443
	L-dopachrome Biosynthesis	-	1/1	0.017	0.443
	RhoA Signaling	inhibited (-2.2)	6/122	0.017	0.443
	Amyotrophic Lateral Sclerosis Signaling	-	5/98	0.025	0.443
	IL-12 Signaling and Production in Macrophages	-	6/135	0.026	0.443
FTC/HCC vs NT	Inhibition of Matrix Metalloproteases	-	6/39	0.014	0.946
	Leukocyte Extravasation Signaling	inhibited (-1.4)	18/198	0.015	0.946
	eNOS Signaling	inhibited (-1.7)	14/142	0.016	0.946
	Tec Kinase Signaling	inhibited (-1.9)	15/158	0.017	0.946
	HGF Signaling	inhibited (-2.1)	11/105	0.020	0.946
	Reelin Signaling in Neurons	-	9/79	0.021	0.946
	FAK Signaling	-	9/87	0.036	0.946
	Fatty Acid α-oxidation	-	3/16	0.047	0.946
	VDR/RXR Activation	activated (0.4)	8/78	0.049	0.946
	Factors Promoting Cardiogenesis in Vertebrates	-	9/92	0.049	0.946
PTC vs NT	TREM1 Signaling	activated (2.8)	8/74	<0.001	0.044

	IL-10 Signaling	-	7/68	<0.001	0.079
	RhoGDI Signaling	inhibited (-2.3)	10/173	0.003	0.192
	Signaling by Rho Family GTPases	activated (2.1)	12/234	0.003	0.192
	The Visual Cycle	-	3/15	0.003	0.192
	LXR/RXR Activation	inhibited (-2.1)	8/121	0.003	0.192
	VDR/RXR Activation	activated (2.2)	6/78	0.005	0.232
	LPS/IL-1 Mediated Inhibition of RXR Function	activated (1.0)	11/219	0.005	0.232
	Integrin Signaling	activated (3.0)	10/201	0.008	0.301
	Role of JAK1 and JAK3 in γc Cytokine Signaling	-	5/63	0.009	0.301
PDTC/ATC vs NT	Agranulocyte Adhesion and Diapedesis	-	58/189	<0.001	0.001
	Atherosclerosis Signaling	-	41/124	<0.001	0.002
	LXR/RXR Activation	inhibited (-1.0)	39/121	<0.001	0.004
	Transcriptional Regulatory Network in Embryonic Stem Cells	-	18/40	<0.001	0.004
	FXR/RXR Activation	-	39/127	<0.001	0.009
	Granulocyte Adhesion and Diapedesis	-	50/177	<0.001	0.009
	GABA Receptor Signaling	-	23/67	<0.001	0.031
	Estrogen Biosynthesis	-	15/37	<0.001	0.033
	Gαi Signaling	activated (2.8)	35/120	<0.001	0.033
	Gαs Signaling	activated (1.0)	32/109	<0.001	0.045

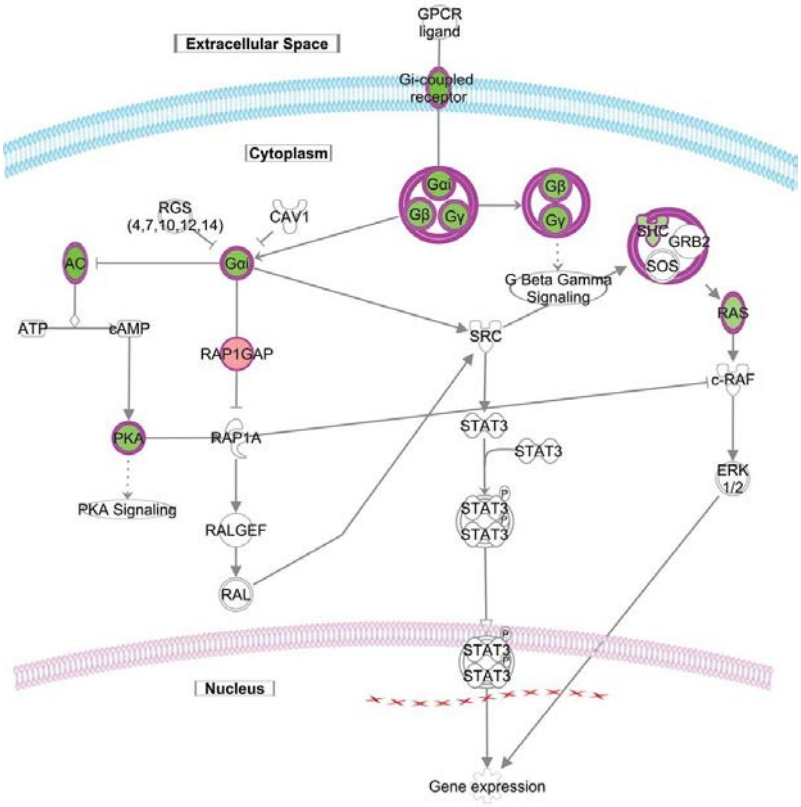

Figure 3. Gαi signaling canonical pathway was detected as involved in poorly differentiated thyroid/anaplastic carcinoma by IPA software. By comparing ATC/PDTC with NT, hypomethylation in many members of this pathway could be noticed, except for *RAP1GAP* (hypermethylated). The activation of the pathway was predicted by IPA software after conversion of hypomethylated and hypermethylated genes into putative overexpressed and underexpressed genes, respectively. **Legend.** Green - hypomethylation and red - hypermethylation in ATC/PDTC compared to non-neoplastic thyroid tissues.

Clinical relevance of DNA methylation

Altered DNA methylation pattern in specific locus can be useful as biomarkers for the identification of aggressive thyroid cancer subtypes. Based on this premise, the comparison between poor *versus* favorable outcome groups was performed revealing 197 differentially methylated probes (Supplementary Table 2). Three genes, *CENPJ* (cg13237068), *SCFD2* (cg04473654) and *RPL23* (cg27500148), and two CpG regions with no known genes (cg17765025 and cg06042504) and with AUC>0.8 (Figure 4A) were selected to construct a prognostic classifier. The combination of these five probes showed the best performance in discriminating poor from favorable outcome patients (Figure 4B), presenting a sensitivity of 77.3% and specificity of 89.6% (positive

predictive value: 77.3% and negative predictive value: 89.6%) using the cross validation analysis.

The derived values of the predictive prognostic model (DLDA) were stratified into low (above the first quartile), intermediate (interquartile range) and high (below the third quartile). The DLDA stratification was able to identify 0%, 12.9% and 86.4% of the patients presenting poor prognosis in low, intermediate and high risk groups, respectively (Figure 4C). Notably, the Kaplan-Meier curves showed that patients with well-differentiated carcinomas classified as having high risk (lower cut off on DLDA analysis) presented shorter disease-free survival compared with intermediate and low risk patients ($P=3.54E^{-10}$). These findings confirmed the prognostic value of the classifier (Figure 4D).

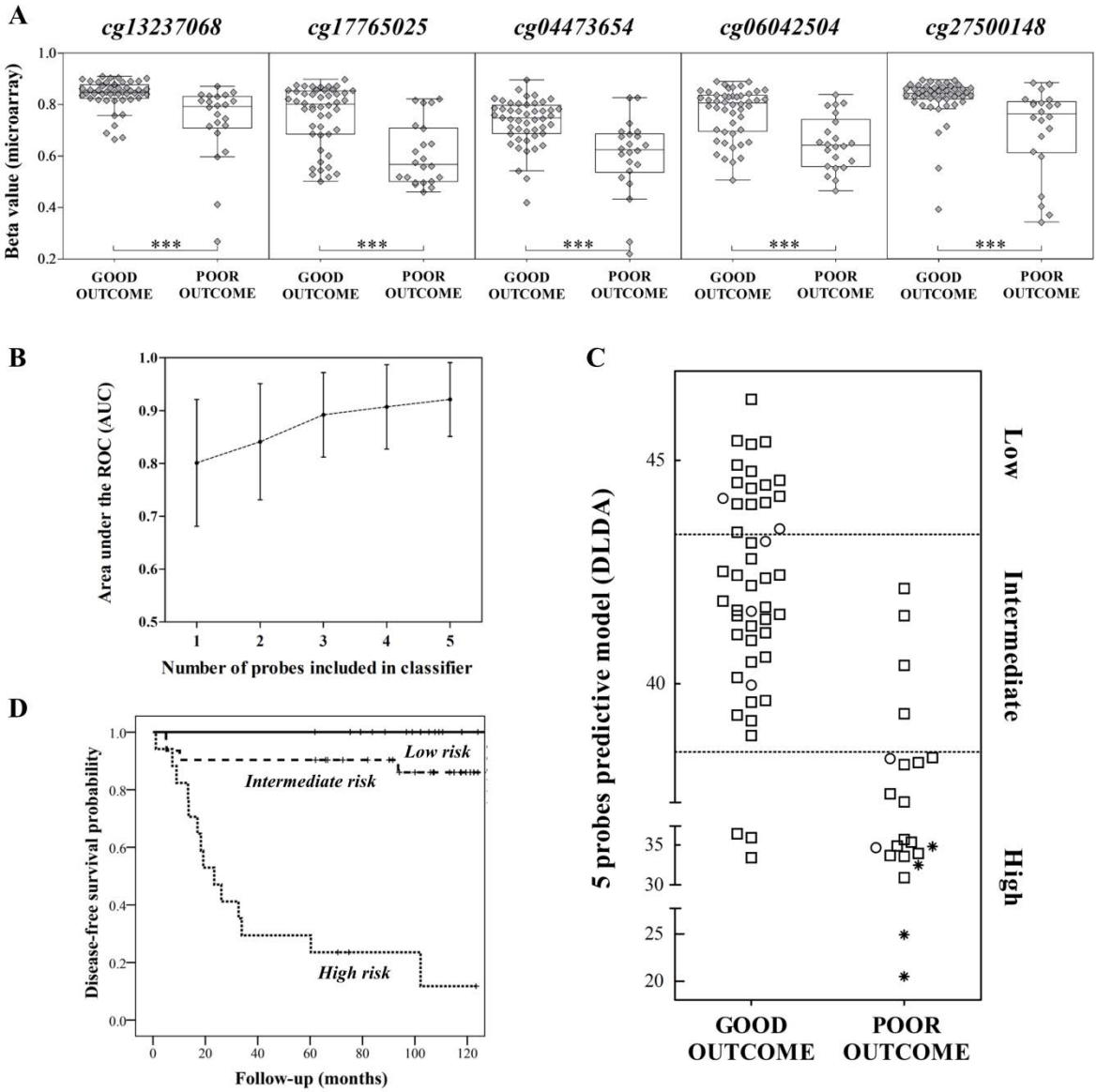

Figure 4. A. Comparison of the beta values of five probes (AUC> 0.8) according to outcome (poor and favorable). Boxplots show mean beta values and interquartile ranges. **B.** Area under the receiver operating characteristics (AUC) and confidence interval (95%) achieved according to the number of probes included in the classifier (Diagonal Linear Discriminant Analysis method). **C.** Predictive model values based on five probes in relation to good and poor outcome cases when stratified in three categories, low, intermediate and high risk. **D.** Disease-free survival curves in well-differentiated carcinomas patients stratified into low, intermediate and high risk according to the classifier.

Legend: DLDA: Diagonal Linear Discriminant Analysis; ROC: receiver operating characteristics; AUC: Area under the receiver operating characteristics curve. Square: papillary thyroid carcinoma; Circle: follicular thyroid carcinoma/Hurthle Cell Carcinoma; Star: poorly differentiate/anaplastic thyroid carcinoma.

Discussion

The novelty of this study included a comprehensive analysis of differential methylation profiling performed in a large cohort of thyroid samples, including benign lesions and distinct subtypes of thyroid cancer derived from follicular cells. Using this approach, a classifier with meaningful prognostic value was described.

Aberrant DNA methylation was confirmed as a common event in thyroid carcinogenesis across the genome. The CpG sites hypermethylation was more frequently observed in benign lesions and follicular carcinomas and hypomethylation was detected in papillary and poorly differentiated/anaplastic carcinoma subtypes. These data suggest distinct mechanisms related to gene methylation control in different thyroid lesions. Accordingly, changes in the methylation pattern in benign lesions have been also reported in several tissues (van Hoesel et al., 2013; Kim et al., 2011; Abouzeid et al., 2011) suggesting the relevance of this process at early stages of tumorigenesis.

In our analysis, follicular adenomas (8 cases) were significantly represented in the group of benign lesions. Progressive number of differentially methylated CpGs with methylation gain was detected from BTL to FTC when compared with non-neoplastic tissues. In agreement with Mancikova et al. (2014), similar methylation profile in FTC and FA was observed analyzing only the promoter regions of genes. In addition, we found altered methylation in gene body in both lesions (BTL and FTC). Together, these data suggest that besides morphological and genetic similarities (Arora et al., 2008; Caria and Vanni, 2010), both lesions share epigenetic similarities.

Papillary thyroid cancer displayed fewer aberrantly methylated genes compared with other carcinoma subtypes. In accordance with previous studies using methylation arrays, loss of methylation was more frequently observed than hypermethylated CpGs in PTC samples (Ellis et al., 2014; Mancikova et al., 2014). The mechanisms involving the hypermethylation in promoter regions of tumor suppressor genes in cancer are well established, however the contribution of hypomethylation in the carcinogenesis process is poorly unenlightened (Ehrlich and Lacey, 2013). In the present study, hypomethylation in PCT was found in promoter regions and in gene body. In acute myeloid leukemia (Qian et al., 2015) and breast cancer (Barrio-Real et al., 2014), hypomethylation of promotor CpG islands was reported as associated with tumor progression. Accordingly, we found high number of loss of methylation in more

aggressive undifferentiated thyroid carcinomas. However, the mechanism by which global DNA hypomethylation is associated with poor prognosis in thyroid cancer should be further investigated.

As expected, elevated number of aberrant CpG methylation probes was found in undifferentiated carcinomas compared to non-neoplastic tissues. These data will be meaningful in the better understanding the process of dedifferentiation involved in progression of these carcinomas.

In this study, hypermethylation was more frequently detected in CpG islands in all lesions compared to loss of methylation. The higher frequency of hypermethylated probes in CpG islands and hypomethylation in CpGs outside of these regions was also observed in reports of global analyzes in thyroid cancer (Rodriguez-Rodero et al., 2013; Mancikova et al., 2013). The hypermethylation of CpG islands located within the promoter regions of genes is associated with repression of gene transcription (Sproul and Meehan, 2013), and is mainly found in promoters of tumor suppressor genes (Feinberg e Tycko, 2004).

In all comparisons performed in this study, a large number of CpGs with aberrant methylation was found in the gene body. Methylation in gene body has been attracted the attention in the last years. Kulis et al. (2012) proposed a scenario where the differential methylation in the body regions could have a functional role in the development of leukemia. The authors found a large number of hypomethylated CpGs in the gene body that were significantly correlated with gene expression. These findings give additional evidences of new biomarkers regulated by differential methylation in the body of genes and a novel data in benign thyroid lesions as well as in carcinomas, which to our knowledge have not been reported.

A number of tumor-related genes found with aberrant methylation in our study were previously reported with altered expression in thyroid cancer. For instance, *PATZ1*, *TFF3* and *CBX7* were reported as underexpressed in non-differentiated, papillary carcinomas and adenomas, respectively (Chiappetta et al., 2015; Espinal-Enríquez et al., 2015; Monaco et al., 2014). In contrast, *CHI3L1* and *MMP1* genes were found to be overexpressed in PTC and ATC (Espinal-Enríquez et al., 2015), respectively. Differential methylation in the expected direction for these five genes was found in our study, suggesting that methylation can be one of the multiple layers of epigenetic modifications involved in the control and modulation of gene expression.

In silico pathway analysis using probes mapped in the promoter region indicated the activation of G-Protein alpha-i pathway in poorly-differentiated and anaplastic carcinomas. The G-alpha protein-i directly stimulates the kinase activity of cSRC protein (Ma et al., 2000), a member of SRC-family, involved in a variety of cell functions, as proliferation, survival and cell migration (Thomas and Brugge, 1997). Once stimulated, cSRC leads to RAS/MAPK activation, via phosphorylation of adaptor protein SHC transforming protein 1 (SHC) and recruitment of the adaptor protein growth factor receptor-bound protein 2 (GRB2) and protein Son of sevenless (SOS) (reviewed by Natarajan and Berk, 2006). Activation of RAS leads to the activation of RAF and consequently ERK (Sever and Brugge, 2015) mediating the growth effect of activated G-Protein alpha-i. Activation of *STAT3* is also observed through G-protein-coupled receptors (Yu et al., 2014) leading to cancer progression. In our study, genes involved in the activation of this pathway that codify for proteins G coupled receptor, *Gαi*, *SHC*, *RAS* were hypomethylated. Given the importance of the *SRC* gene in the carcinogenesis process, several studies aimed to determine the role of *SRC* in the growth and invasion of PTC and ATC and inhibit its signaling (Chan et al., 2012; Schweppe et al., 2009; Vanden Borre et al., 2014).

In addition to hypomethylation, the hypermethylation of *RAP1GAP*, a negative regulator of G-Protein alpha-i pathway, was detected. Downregulation of this gene was associated with migratory and invasive properties in thyroid cell lines (Tsygankova et al., 2007), enhancing the SRC-dependent signals (Dong et al., 2012). In addition, our study corroborates the Zuo et al., (2010) study that showed the promoter hypermethylation and downregulation of *RAP1GAP* in the most aggressive forms of thyroid cancer. Our data suggest that altered methylation of these upstream regulators of SRC could play a role in the regulation of this pathway during the thyroid tumorigenesis.

Interestingly, the methylation profiles of thyroid carcinomas were able to predict the outcome of the patients. Changes in DNA methylation have been associated with prognosis in several types of cancers (Deckers et al., 2015; Hoque et al., 2008; Vasiljević et al., 2014), including thyroid carcinomas. *RUNX3* hypermethylation (Wang et al., 2014) and *TSHR* hypomethylation (Smith et al., 2007) were related to PTC recurrence. In addition, using genome-wide approach and analyzing only PTC samples, Mancikova et al. (2014) described two genes (*EI24* and *WT1*) associated with increased risk of recurrence of this subtype of thyroid cancer. Nevertheless, there are limited data

addressing the investigation of molecular prognostic markers in thyroid carcinoma subtypes. Montero-Conde et al. (2008) using expression microarray analysis found differentially expressed genes functionally related to dedifferentiation and aggressiveness of 24 PTC, 7 FTC, 6 PDTC and 7 ATC. The authors found altered expression of 23 genes and 3 ESTs that were able to correctly classify 95.45% of tumors with poor prognosis in a cross validation study.

Using a cohort of patients with a standardized follow-up we described, at first time, alteration of the methylation pattern in five probes capable to distinguish PDTC/ATC and recurrent-PTC/FTC from good prognosis WDTC patients. In our study, these five probes associated with poor outcome showed loss of methylation. Other studies demonstrated that several gene showing hypomethylation were associated with poor prognosis in different tumor types (Harada et al., 2015; Li et al., 2014, Haller et al., 2015). Additionally, the *RPL23* overexpression was associated with poor prognosis in myelodysplastic syndrome (Wu et al., 2012) and multidrug resistance in gastric cells (Shi et al., 2004), suggesting that methylation could regulate expression of this gene, a direct target of MYC (Wanzel et al., 2008), involved in the cell-cycle progression. Our findings are in accordance with studies described in hepatocellular carcinomas (Villanueva et al., 2015), breast cancer (Fang et al., 2011) and neuroblastoma (Decock et al., 2012), in which methylation profile was able to predict patient outcome.

In conclusion, this exploratory study of genome wide methylation profiles of thyroid carcinoma subtypes demonstrated that despite of thyroid carcinoma subtypes present the same cellular origin, different molecular changes in DNA methylation is involved in the thyroid carcinogenesis. In addition, we reported a prognostic classifier based on the methylation changes in a small number of loci which could correctly classify the patients with poor outcome, indicating that this classifier could be used a meaningful prognostic tool in thyroid cancer.

Acknowlegments

The authors thank the A.C. Camargo Cancer Center Biobank for providing and processing the samples.

This study was supported by grants from the National Institute of Science and Technology in Oncogenomics (Fundação de Amparo à Pesquisa do Estado de São Paulo

–FAPESP Grant 2008/57887–9 and Conselho Nacional de Desenvolvimento Científico e Tecnoló ́ ico Grant CNPq 573589/08–9.

Disclosure Summary: The authors have nothing to disclose.

References

Abouzeid HE, Kassem AM, Abdel Wahab AH, El-mezayen HA, Sharad H, Abdel Rahman S. Promoter hypermethylation of RASSF1A, MGMT, and HIC-1 genes in benign and malignant colorectal tumors. Tumour Biol. 2011; 32(5):845-52.

Arora N, Scognamiglio T, Zhu B, Fahey TJ. Do benign thyroid nodules have malignant potential? An evidence-based review. World J Surg. 2008; 32(7):1237-46.

Aschebrook-Kilfoy B, Grogan RH, Ward MH, Kaplan E, Devesa SS. Follicular thyroid cancer incidence patterns in the United States, 1980-2009. Thyroid. 2013; 23(8):1015-21.

Barrio-Real L, Benedetti LG, Engel N, Tu Y, Cho S, Sukumar S, et al. Subtype-specific overexpression of the Rac-GEF P-REX1 in breast cancer is associated with promoter hypomethylation. Breast Cancer Res. 2014; 16(5):441.

Baylin SB, Jones PA. A decade of exploring the cancer epigenome - biological and translational implications. Nat Rev Cancer. 2011; 11(10):726-34.

Bhaijee F, Nikiforov YE. Molecular analysis of thyroid tumors. Endocr Pathol. 2011; 22(3):126-33.

Cancer Genome Atlas Research Network. Integrated genomic characterization of papillary thyroid carcinoma. Cell. 2014; 159(3): 676-690.

Caria P, Vanni R. Cytogenetic and molecular events in adenoma and well-differentiated thyroid follicular-cell neoplasia. Cancer Genet Cytogenet. 2010; 203(1):21-9.

Chan CM, Jing X, Pike LA, Zhou Q, Lim DJ, Sams SB, et al. Targeted inhibition of Src kinase with dasatinib blocks thyroid cancer growth and metastasis. Clin Cancer Res. 2012; 18(13):3580-91.

Chen YA, Lemire M, Choufani S, Butcher DT, Grafodatskaya D, Zanke BW, Gallinger S, Hudson TJ, Weksberg R. Discovery of cross-reactive probes and polymorphic CpGs in the Illumina Infinium HumanMethylation450 microarray. Epigenetics. 2013; 8(2):203-9.

Chiappetta G, Valentino T, Vitiello M, Pasquinelli R, Monaco M, Palma G, et al. PATZ1 acts as a tumor suppressor in thyroid cancer via targeting p53-dependent genes involved in EMT and cell migration. Oncotarget. 2015; 6(7):5310-23.

Deckers IA, Schouten LJ, Van Neste L, van Vlodrop I, Soetekouw PM, Baldewijns M, et al. Promoter methylation of CDO1 identifies clear-cell renal cell cancer patients with poor survival outcome. Clin Cancer Res. [Epub ahead of print]

Decock A, Ongenaert M, Hoebeeck J, De Preter K, Van Peer G, Van Criekinge W, et al. Genome-wide promoter methylation analysis in neuroblastoma identifies prognostic methylation biomarkers. Genome Biol. 2012; 13(10):R95.

Dong X, Tang W, Stopenski S, Brose MS, Korch C, Meinkoth JL. RAP1GAP inhibits cytoskeletal remodeling and motility in thyroid cancer cells. Endocr Relat Cancer. 2012; 19(4):575-88.

Ehrlich M, Lacey M. DNA hypomethylation and hemimethylation in cancer. Adv Exp Med Biol, v.754, p.31-56, 2013.

Elisei R, Pinchera A. Advances in the follow-up of differentiated or medullary thyroid cancer. Nat Rev Endocrinol. 2012; 8(8):466-75.

Ellis RJ, Wang Y, Stevenson HS, Boufraqech M, Patel D, Nilubol N, et al. Genome-wide methylation patterns in papillary thyroid cancer are distinct based on histological subtype and tumor genotype. J Clin Endocrinol Metab, v.99, n.2, p.329-337, 2014.

Espinal-Enríquez J, Muñoz-Montero S, Imaz-Rosshandler I, Huerta-Verde A, Mejía C, Hernández-Lemus E. Genome-wide expression analysis suggests a crucial role of dysregulation of matrix metalloproteinases pathway in undifferentiated thyroid carcinoma. BMC Genomics. 2015;16:207.

Esteller M. The necessity of a human epigenome project. Carcinogenesis. 2006; 27(6):1121-5.

Fang F, Turcan S, Rimner A, Kaufman A, Giri D, Morris LG, et al. Breast cancer methylomes establish an epigenomic foundation for metastasis. Sci Transl Med. 2011; 3: 75ra25.

Feinberg AP. The epigenetics of cancer etiology. Semin Cancer Biol. 2004; 14(6):427-32.

Feinberg AP, Tycko B. The history of cancer epigenetics. Nat Rev Cancer. 2004;4(2):143-153.

Graff JR, Greenberg VE, Herman JG, Westra WH, Boghaert ER, Ain KB, et al. Distinct patterns of E-cadherin CpG island methylation in papillary, follicular, Hurthle's cell, and poorly differentiated human thyroid carcinoma. Cancer Res. 1998; 58(10):2063-6.

Guan H, Ji M, Hou P, Liu Z, Wang C, Shan Z, et al. Hypermethylation of the DNA mismatch repair gene hMLH1 and its association with lymph node metastasis and T1799A BRAF mutation in patients with papillary thyroid cancer. Cancer. 2008; 113(2):247-55.

Haller F, Zhang JD, Moskalev EA, Braun A, Otto C, Geddert H, et al. Combined DNA methylation and gene expression profiling in gastrointestinal stromal tumors reveals

hypomethylation of SPP1 as an independent prognostic factor. Int J Cancer. 2015; 136(5):1013-23.

Harada K, Baba Y, Ishimoto T, Chikamoto A, Kosumi K, Hayashi H, et al. LINE-1 methylation level and patient prognosis in a database of 208 hepatocellular carcinomas. Ann Surg Oncol. 2015; 22(4):1280-7.

Hay ID, Thompson GB, Grant CS, Bergstralh EJ, Dvorak CE, Gorman CA, et al. Papillary thyroid carcinoma managed at the Mayo Clinic during six decades (1940-1999): temporal trends in initial therapy and long-term outcome in 2444 consecutively treated patients. World J Surg. 2002; 26(8):879-85.

Hoque MO, Begum S, Brait M, Jeronimo C, Zahurak M, Ostrow KL, Rosenbaum E, Trock B, Westra WH, Schoenberg M, Goodman SN, Sidransky D. Tissue inhibitor of metalloproteinases-3 promoter methylation is an independent prognostic factor for bladder cancer. J Urol. 2008; 179(2):743-7.

Hu S, Liu D, Tufano RP, Carson KA, Rosenbaum E, Cohen Y, Holt EH, et al. Association of aberrant methylation of tumor suppressor genes with tumor aggressiveness and BRAF mutation in papillary thyroid cancer. Int J Cancer. 2006; 119(10):2322-9.

Jones PA, Baylin SB. The fundamental role of epigenetic events in cancer. Nat Rev Genet. 2002; 3(6):415-28.

Kim JH, Dhanasekaran SM, Prensner JR, Cao X, Robinson D, Kalyana-Sundaram S, et al. Deep sequencing reveals distinct patterns of DNA methylation in prostate cancer. Genome Res. 2011; 21(7):1028-41.

Kulis M, Heath S, Bibikova M, Queirós AC, Navarro A, Clot G, et al. Epigenomic analysis detects widespread gene-body DNA hypomethylation in chronic lymphocytic leukemia. Nat Genet. 2012; 44 (11):1236-42.

Li C, Cai S, Wang X, Jiang Z. Hypomethylation-associated up-regulation of TCF3 expression and recurrence in stage II and III colorectal cancer. PLoS One. 2014; 9(11):e112005.

Ma YC, Huang J, Ali S, Lowry W, Huang XY. Src tyrosine kinase is a novel direct effector of G proteins. Cell. 2000; 102(5):635-46.

Mancikova V, Buj R, Castelblanco E, Inglada-Pérez L, Diez A, de Cubas AA, et al. DNA methylation profiling of well-differentiated thyroid cancer uncovers markers of recurrence free survival. Int J Cancer, v.135, n.3, p.598-610, 2014.

Monaco M, Chiappetta G, Aiello C, Federico A, Sepe R, Russo D, et al. CBX7 Expression in Oncocytic Thyroid Neoplastic Lesions (Hürthle Cell Adenomas and Carcinomas). Eur Thyroid J. 2014; 3(4):211-6.

Montero-Conde C, Martín-Campos JM, Lerma E, Gimenez G, Martínez-Guitarte JL, Combalía N, et al. Molecular profiling related to poor prognosis in thyroid carcinoma. Combining gene expression data and biological information. Oncogene. 2008; 27(11):1554-61.

Natarajan K, Berk BC. Crosstalk coregulation mechanisms of G protein-coupled receptors and receptor tyrosine kinases. Methods Mol Biol. 2006; 332:51-77.

Qian J, Chen Q, Yao DM, Yang L, Yang J, Wen XM, e al. MOK overexpression is associated with promoter hypomethylation in patients with acute myeloid leukemia. Int J Clin Exp Pathol. 2015; 8(1):127-36.

Rodríguez-Rodero S, Delgado-Álvarez E, Fernández AF, Fernández-Morera JL, Menéndez-Torre E, Fraga MF. Epigenetic alterations in endocrine-related cancer. Endocr Relat Cancer. 2014; 21(4):R319-30.

Rodríguez-Rodero S, Fernández AF, Fernández-Morera JL, Castro-Santos P, Bayon GF, Ferrero C, et al. DNA methylation signatures identify biologically distinct thyroid cancer subtypes. Clin Endocrinol Metab. 2013; 98(7):2811-21.

Schweppe RE, Kerege AA, French JD, Sharma V, Grzywa RL, Haugen BR Inhibition of Src with AZD0530 reveals the Src-Focal Adhesion kinase complex as a novel therapeutic target in papillary and anaplastic thyroid cancer. J Clin Endocrinol Metab. 2009; 94(6):2199-203.

Sever R, Brugge JS. Signal Transduction in Cancer. Cold Spring Harb Perspect Med. 2015; 5(4) pii: a006098.

Shi Y, Zhai H, Wang X, Han Z, Liu C, Lan M, et al. Ribosomal proteins S13 and L23 promote multidrug resistance in gastric cancer cells by suppressing drug-induced apoptosis. Exp Cell Res. 2004; 296(2):337-46.

Siegel RL, Miller KD, Jemal A. Cancer statistics, 2015. CA Cancer J Clin. 2015; 65(1):5-29.

Siironen P, Hagström J, Mäenpää HO, Louhimo J, Heikkilä A, Heiskanen I, et al. Anaplastic and poorly differentiated thyroid carcinoma: therapeutic strategies and treatment outcome of 52 consecutive patients. Oncology. 2010; 79(5-6):400-8.

Smith JA, Fan CY, Zou C, Bodenner D, Kokoska MS. Methylation status of genes in papillary thyroid carcinoma. Arch Otolaryngol Head Neck Surg. 2007; 133(10):1006-11.

Sproul D, Meehan RR. Genomic insights into cancer-associated aberrant CpG island hypermethylation. Brief Funct Genomics. 2013;12(3):174-190.

Teschendorff AE, Marabita F, Lechner M, Bartlett T, Tegner J, Gomez-Cabrero D, Beck S. A beta-mixture quantile normalization method for correcting probe design bias in Illumina Infinium 450 k DNA methylation data. Bioinformatics. 2013; 29(2):189-96.

Thomas SM, Brugge JS. Cellular functions regulated by Src family kinases. Annu Rev Cell Dev Biol. 1997; 13:513-609.

Tsygankova OM, Prendergast GV, Puttaswamy K, Wang Y, Feldman MD, Wang H, et al. Downregulation of Rap1GAP contributes to Ras transformation. Mol Cell Biol. 2007; 27(19):6647-58.

Vanden Borre P, Gunda V, McFadden DG, Sadow PM, Varmeh S, Bernasconi M, et al. Combined BRAF(V600E)- and SRC-inhibition induces apoptosis, evokes an immune response and reduces tumor growth in an immunocompetent orthotopic mouse model of anaplastic thyroid cancer. Oncotarget. 2014; 5(12):3996-4010.

van Hoesel AQ, Sato Y, Elashoff DA, Turner RR, Giuliano AE, Shamonki JM, et al. Assessment of DNA methylation status in early stages of breast cancer development. Br J Cancer. 2013;108(10):2033-8.

Vasiljević N, Ahmad AS, Thorat MA, Fisher G, Berney DM, Møller H, et al. DNA methylation gene-based models indicating independent poor outcome in prostate cancer. BMC Cancer. 2014; 14:655.

Villanueva A, Portela A, Sayols S, Battiston C, Hoshida Y, Méndez-González J, et al. DNA methylation-based prognosis and epidrivers in hepatocellular carcinoma. Hepatology. 2015. [Epub ahead of print]

Wang D, Cui W, Wu X, Qu Y, Wang N, Shi B, et al. RUNX3 site-specific hypermethylation predicts papillary thyroid cancer recurrence. Am J Cancer Res. 2014; 4(6):725-37.

Wanzel M, Russ AC, Kleine-Kohlbrecher D, Colombo E, Pelicci PG, Eilers M. A ribosomal protein L23-nucleophosmin circuit coordinates Mizl function with cell growth. Nat Cell Biol. 2008 Sep;10(9):1051-61.

Wu L, Li X, Xu F, Chang C, He Q, Zhang Z, et al. Over-expression of RPL23 in myelodysplastic syndromes is associated with apoptosis resistance of CD34+ cells and predicts poor prognosis and distinct response to CHG chemotherapy or decitabine. Ann Hematol. 2012; 91(10):1547-54.

Yu H, Lee H, Herrmann A, Buettner R, Jove R. Revisiting STAT3 signalling in cancer: new and unexpected biological functions. Nat Rev Cancer. 2014; 14(11):736-46.

Xing M. Gene methylation in thyroid tumorigenesis. Endocrinology. 2007; 148(3):948-53.

Xing M. Molecular pathogenesis and mechanisms of thyroid cancer. Nat Rev Cancer. 2013; 13(3):184-99.

Zane M, Agostini M, Enzo MV, Casal Ide E, Del Bianco P, Torresan F, et al. Circulating cell-free DNA, SLC5A8 and SLC26A4 hypermethylation, BRAF(V600E): A non-invasive tool panel for early detection of thyroid cancer. Biomed Pharmacother. 2013; 67(8):723-30.

Zuo H, Gandhi M, Edreira MM, Hochbaum D, Nimgaonkar VL, Zhang P, et al. Downregulation of Rap1GAP through epigenetic silencing and loss of heterozygosity promotes invasion and progression of thyroid tumors. Cancer Res. 2010; 70(4):1389-97.

Supplementary Material

Sample decision

Patient samples were included in this retrospective study according to the availability of A.C. Camargo Cancer Center BioBank. We included 50 surrounding normal tissues, 8 follicular adenomas (FA), 6 nodular goiter (NG), 3 lymphocytic thyroiditis (LT), 60 papillary carcinomas (PTC), 10 follicular/Hurthle cell carcinomas (FTC/HCC) and 4 poorly differentiated/anaplastic carcinoma (PDTC/ATC). The PTC and FTC samples were obtained from patients treated with total thyroidectomy. The cases selected presented a minimum follow-up of five years, except for cases that presented recurrence. Two FTC and one PTC sample were excluded from comparisons with clinical data for loss of follow-up. Thyroid samples collection and clinical information were processed after approval of the Institutional Ethics Committee (Protocol 475.385). The written informed consent was obtained from all individuals.

Supplementary Table 1. Clinicopathologic characteristics of the patients with PTC, FTC, HCC, PDTC and ATC enrolled in the study.

Characteristics	CPT		Other Subtypes	
	N	%	N	%
Age				
<45 years	37	61,67	4	28,57
≥45 years	23	38,33	10	71,43
Gender				
Female	44	73,33	10	71,43
Male	16	26,67	4	28,57
Histology (excluded PTC)				
FTC	-	-	8	57,14
HCC	-	-	2	14,29
PDTC	-	-	1	7,14
ATC	-	-	3	21,43
Predominant variant (PTC only)				
Classical	47	78,33	-	-
Follicular	10	16,67	-	-
Other	3	5,00	-	-
Tumor dimension (cm)				
Median (interval)	1,3 (0,5-5,5)	-	2,3 (0,9-13)	-
mCPT(≤1cm)	25	41,67	-	-
CPT (>1cm)	35	58,33	-	-
Extrathyroidal extension				

No	30	52,63	7	53,85
Yes	27	47,37	6	46,15
Ni	3	-	1	-
Vascular invasion				
Blood invasion	2	3,39	5	38,46
Lymphatic	3	5,08	1	7,69
Both	1	1,69	2	15,38
No	53	89,83	5	38,46
Ni	1	-	1	-
Perineural invasion				
No	42	93,33	10	23,08
Yes	3	6,67	3	76,92
Ni	15		1	-
Lymph node metastasis				
No (cN0, pN0)	32	53,33	9	69,23
Yes (pN1)	28	46,67	4	30,77
Ni	-	-	1	-
Clinical evolution				
Free of disease	43	73,33	5	71,43
Recurrence	16	26,67	2	28,57
Ni*	1	-	7	-
Death				
No	59	98,33	10	71,43
Yes	1	1,67	4	28,57
Follow-up(months)#	83,8 (1,1-142,9)	-	63,3[o] (4,0-139,4)	-

Abbreviation. Ni: not informed; cN: no clinical evidence of cancer in the regional lymph nodes; pN0: no pathologically evidence of cancer in regional lymph nodes; pN1: pathological confirmation of cancer in regional lymph nodes.* 1 FTC with loss of follow-up, 1 PTC and 2 FTC without 5 years of follow-up and 4 non- differentiated carcinomas with aggressive disease and death before the recurrence diagnosis. # data up to August, 2014. [o] only for FTC samples.

Supplementary Table 2. Probes differentially methylated identified in four comparisons using $|\Delta\beta| = 0.2$ and $P<0.05$. (File in excel format)

Supplementary Table 3. Canonical pathways ($P<0.05$) identified in the four comparisons of the study by IPA software.

Analysis	Pathway (IPA)	P (Fisher)	P (BH
BTL vs NT	Reelin Signaling in Neurons	0.002	0.438
	eNOS Signaling	0.003	0.438
	Leukocyte Extravasation Signaling	0.006	0.443
	IL-4 Signaling	0.009	0.443
	CCR3 Signaling in Eosinophils	0.014	0.443
	FAK Signaling	0.015	0.443
	L-dopachrome Biosynthesis	0.017	0.443
	RhoA Signaling	0.017	0.443

	Amyotrophic Lateral Sclerosis Signaling	0.025	0.443
	IL-12 Signaling and Production in Macrophages	0.026	0.443
	Growth Hormone Signaling	0.028	0.443
	Rac Signaling	0.031	0.443
	Sulfate Activation for Sulfonation	0.033	0.443
	iCOS-iCOSL Signaling in T Helper Cells	0.035	0.443
	phagosome formation	0.039	0.443
	MSP-RON Signaling Pathway	0.042	0.443
	Thrombin Signaling	0.042	0.443
	Breast Cancer Regulation by Stathmin1	0.042	0.443
	CXCR4 Signaling	0.043	0.443
	Signaling by Rho Family GTPases	0.044	0.443
	nNOS Signaling in Neurons	0.044	0.443
	Ceramide Signaling	0.046	0.443
	Ephrin A Signaling	0.046	0.443
	Gα12/13 Signaling	0.047	0.443
	CD28 Signaling in T Helper Cells	0.048	0.443
	Methionine Salvage II (Mammalian)	0.049	0.443
FTC vs NT	Inhibition of Matrix Metalloproteases	0.014	0.946
	Leukocyte Extravasation Signaling	0.015	0.946
	eNOS Signaling	0.016	0.946
	Tec Kinase Signaling	0.017	0.946
	HGF Signaling	0.020	0.946
	Reelin Signaling in Neurons	0.021	0.946
	FAK Signaling	0.036	0.946
	Fatty Acid α-oxidation	0.047	0.946
	VDR/RXR Activation	0.049	0.946
	Factors Promoting Cardiogenesis in Vertebrates	0.049	0.946
PTC vs NT	TREM1 Signaling	0.000	0.044
	IL-10 Signaling	0.000	0.079
	RhoGDI Signaling	0.003	0.192
	Signaling by Rho Family GTPases	0.003	0.192
	The Visual Cycle	0.003	0.192
	LXR/RXR Activation	0.003	0.192
	VDR/RXR Activation	0.005	0.232
	LPS/IL-1 Mediated Inhibition of RXR Function	0.005	0.232
	Integrin Signaling	0.008	0.301
	Role of JAK1 and JAK3 in γc Cytokine Signaling	0.009	0.301
	Gα12/13 Signaling	0.010	0.301
	Granulocyte Adhesion and Diapedesis	0.010	0.301
	Glycolysis I	0.014	0.366
	Agranulocyte Adhesion and Diapedesis	0.015	0.379
	Toll-like Receptor Signaling	0.017	0.379
	Heparan Sulfate Biosynthesis (Late Stages)	0.019	0.391
	Hepatic Fibrosis / Hepatic Stellate Cell Activation	0.020	0.391
	UDP-N-acetyl-D-galactosamine Biosynthesis I	0.020	0.391
	Heparan Sulfate Biosynthesis	0.029	0.486
	Retinoate Biosynthesis I	0.029	0.486
	Oncostatin M Signaling	0.032	0.486

	p38 MAPK Signaling	0.032	0.486
	Altered T Cell and B Cell Signaling in Rheumatoid Arthritis	0.034	0.486
	Role of JAK2 in Hormone-like Cytokine Signaling	0.034	0.486
	Regulation of Actin-based Motility by Rho	0.038	0.508
	Alanine Degradation III	0.040	0.508
	Alanine Biosynthesis II	0.040	0.508
	Atherosclerosis Signaling	0.041	0.508
ATC vs NT	Agranulocyte Adhesion and Diapedesis	0.000	0.001
	Atherosclerosis Signaling	0.000	0.002
	LXR/RXR Activation	0.000	0.004
	Transcriptional Regulatory Network in Embryonic Stem Cells	0.000	0.004
	FXR/RXR Activation	0.000	0.009
	Granulocyte Adhesion and Diapedesis	0.000	0.009
	GABA Receptor Signaling	0.000	0.031
	Estrogen Biosynthesis	0.001	0.033
	Gαi Signaling	0.001	0.033
	Gαs Signaling	0.001	0.045
	Cellular Effects of Sildenafil (Viagra)	0.001	0.056
	Serotonin Receptor Signaling	0.001	0.066
	Hepatic Cholestasis	0.002	0.093
	Graft-versus-Host Disease Signaling	0.004	0.150
	G-Protein Coupled Receptor Signaling	0.004	0.150
	Altered T Cell and B Cell Signaling in Rheumatoid Arthritis	0.005	0.158
	Bupropion Degradation	0.005	0.162
	Complement System	0.006	0.167
	Acetone Degradation I (to Methylglyoxal)	0.007	0.200
	LPS/IL-1 Mediated Inhibition of RXR Function	0.009	0.236
	Differential Regulation of Cytokine Production in Intestinal Epithelial Cells by IL-17A and IL-17F	0.009	0.236
	cAMP-mediated signaling	0.014	0.333
	Eicosanoid Signaling	0.017	0.333
	Catecholamine Biosynthesis	0.017	0.333
	α-tocopherol Degradation	0.017	0.333
	Glycolysis I	0.017	0.333
	Gluconeogenesis I	0.017	0.333
	CCR3 Signaling in Eosinophils	0.019	0.353
	Phospholipase C Signaling	0.020	0.366
	Differential Regulation of Cytokine Production in Macrophages and T Helper Cells by IL-17A and IL-17F	0.022	0.389
	Glutamate Receptor Signaling	0.024	0.406
	Phototransduction Pathway	0.026	0.407
	Role of NFAT in Regulation of the Immune Response	0.028	0.407
	Phospholipases	0.028	0.407
	Asparagine Degradation I	0.028	0.407
	Glutamate Dependent Acid Resistance	0.028	0.407
	The Visual Cycle	0.029	0.407
	α-Adrenergic Signaling	0.030	0.407
	Endothelin-1 Signaling	0.030	0.407
	Role of Hypercytokinemia/hyperchemokinemia in the Pathogenesis of Influenza	0.032	0.416

Dopamine Receptor Signaling	0.032	0.420
TREM1 Signaling	0.036	0.437
Citrulline-Nitric Oxide Cycle	0.037	0.437
Glutamate Degradation III (via 4-aminobutyrate)	0.037	0.437
PAK Signaling	0.038	0.437
Triacylglycerol Degradation	0.038	0.437
G Protein Signaling Mediated by Tubby	0.041	0.449
Retinol Biosynthesis	0.041	0.449
Role of Cytokines in Mediating Communication between Immune Cells	0.042	0.449
Gustation Pathway	0.047	0.491
CXCR4 Signaling	0.048	0.491
Synaptic Long Term Depression	0.049	0.491
Oncostatin M Signaling	0.049	0.491

Supplementary Table 4. Canonical pathways (P<0.01) identified in four comparisons of the study by KOBAS 2.0 software.

Analysis	Pathway (KOBAS 2.0)	Database	Genes found / database	P (Fisher exact test)	P (BH correction)
BTL vs NT	TCR signaling	Reactome	6/64	0.001	0.840
	Generation of second messenger molecules	Reactome	4/32	0.003	0.840
FTC vs NT	GPCR downstream signaling	Reactome	106/914	0.000	0.000
	Signaling by GPCR	Reactome	114/1029	0.000	0.000
	Olfactory Signaling Pathway	Reactome	58/375	0.000	0.000
	Olfactory transduction	KEGG PATHWAY	60/408	0.000	0.000
	Signal Transduction	Reactome	158/2029	0.000	0.000
	Neuroactive ligand-receptor interaction	KEGG PATHWAY	34/275	0.000	0.001
	Metabolic disorders of biological oxidation enzymes	Reactome	55/610	0.000	0.008
	Defective ACTH causes Obesity and Pro-opiomelanocortinin deficiency (POMCD)	Reactome	43/438	0.000	0.008
	GPCR ligand binding	Reactome	43/438	0.000	0.008
	Neuronal System	Reactome	31/278	0.000	0.010
	Class B/2 (Secretin family receptors)	Reactome	15/87	0.000	0.011
	Extracellular matrix organization	Reactome	29/267	0.000	0.020
	Collagen degradation	Reactome	11/62	0.001	0.067
	Voltage gated Potassium channels	Reactome	9/43	0.001	0.070
	Degradation of the extracellular matrix	Reactome	15/116	0.001	0.128
	Gastrin-CREB signalling pathway via PKC and MAPK	Reactome	22/211	0.001	0.144
	G alpha (q) signalling events	Reactome	20/185	0.002	0.147
	Developmental Biology	Reactome	42/518	0.002	0.170
	Potassium Channels	Reactome	13/99	0.002	0.184
	G alpha (s) signalling events	Reactome	15/125	0.002	0.186
	Class A/1 (Rhodopsin-like receptors)	Reactome	28/313	0.003	0.223
	Transmission across Chemical Synapses	Reactome	20/199	0.003	0.245
	Adipocytokine signaling pathway	KEGG PATHWAY	10/70	0.004	0.308
	Glucagon-type ligand receptors	Reactome	6/30	0.006	0.395
	Beta3 integrin cell surface interactions	PID	8/43	0.006	0.397
	Axon guidance	Reactome	28/340	0.008	0.495
	Beta1 integrin cell surface interactions	PID	10/66	0.008	0.495

	Striated Muscle Contraction	Reactome	6/33	0.009	0.503
PTC vs NT	Signaling by Interleukins	Reactome	10/111	0.000	0.103
	G alpha (q) signalling events	Reactome	13/185	0.000	0.103
	Gastrin-CREB signalling pathway via PKC and MAPK	Reactome	14/211	0.000	0.103
	Cell-Cell communication	Reactome	10/132	0.001	0.218
	Assembly of collagen fibrils and other multimeric structures	Reactome	6/54	0.001	0.332
	The canonical retinoid cycle in rods (twilight vision)	Reactome	4/22	0.002	0.332
	Interleukin-7 signaling	Reactome	3/11	0.003	0.332
	Collagen degradation	Reactome	6/62	0.003	0.332
	Collagen formation	Reactome	7/85	0.003	0.332
	Cell junction organization	Reactome	7/87	0.003	0.332
	Toll-Like Receptors Cascades	Reactome	9/142	0.004	0.332
	Degradation of the extracellular matrix	Reactome	8/116	0.004	0.332
	MyD88:Mal cascade initiated on plasma membrane	Reactome	7/93	0.005	0.332
	Toll Like Receptor TLR6:TLR2 Cascade	Reactome	7/93	0.005	0.332
	Retinoid cycle disease events	Reactome	3/14	0.005	0.332
	TAK1 activates NFkB by phosphorylation and activation of IKKs complex	Reactome	4/30	0.005	0.332
	p73 transcription factor network	PID	8/79	0.005	0.332
	Toll Like Receptor TLR1:TLR2 Cascade	Reactome	7/96	0.006	0.332
	Toll Like Receptor 2 (TLR2) Cascade	Reactome	7/96	0.006	0.332
	Extracellular matrix organization	Reactome	13/267	0.006	0.333
	Nucleotide-like (purinergic) receptors	Reactome	3/16	0.007	0.356
	il-7 signal transduction	BioCarta	3/15	0.007	0.382
	Muscarinic acetylcholine receptors	Reactome	2/5	0.008	0.401
	Class A/1 (Rhodopsin-like receptors)	Reactome	14/313	0.009	0.401
	Glycosaminoglycan biosynthesis - keratan sulfate	KEGG PATHWAY	3/15	0.009	0.401
	gluconeogenesis	BioCyc	4/24	0.009	0.401
ATC vs NT	Olfactory Signaling Pathway	Reactome	227/375	0.000	0.000
	GPCR downstream signaling	Reactome	374/914	0.000	0.000
	Signaling by GPCR	Reactome	394/1029	0.000	0.000
	Olfactory transduction	KEGG PATHWAY	234/408	0.000	0.000
	Signal Transduction	Reactome	520/2029	0.000	0.000
	Metabolic disorders of biological oxidation enzymes	Reactome	168/610	0.000	0.000
	Defective ACTH causes Obesity and Pro-opiomelanocortinin deficiency (POMCD)	Reactome	128/438	0.000	0.000
	GPCR ligand binding	Reactome	128/438	0.000	0.000
	Neuronal System	Reactome	90/278	0.000	0.000
	Potassium Channels	Reactome	42/99	0.000	0.000
	Class A/1 (Rhodopsin-like receptors)	Reactome	91/313	0.000	0.000
	G alpha (i) signalling events	Reactome	69/234	0.000	0.002
	Peptide ligand-binding receptors	Reactome	59/190	0.000	0.002
	Transmembrane transport of small molecules	Reactome	144/613	0.000	0.003
	G alpha (q) signalling events	Reactome	54/185	0.000	0.015
	Transmission across Chemical Synapses	Reactome	55/199	0.000	0.034
	G alpha (s) signalling events	Reactome	39/125	0.000	0.034
	Gastrin-CREB signalling pathway via PKC and MAPK	Reactome	57/211	0.000	0.034
	Voltage gated Potassium channels	Reactome	19/43	0.000	0.034
	Neuroactive ligand-receptor interaction	KEGG PATHWAY	79/275	0.000	0.034
	Creation of C4 and C2 activators	Reactome	9/11	0.001	0.034
	Ion channel transport	Reactome	47/169	0.001	0.034
	Defective CYP27A1 causes	Reactome	27/78	0.001	0.034

Cerebrotendinous xanthomatosis (CTX)				
Defective CYP11B1 causes Adrenal hyperplasia 4 (AH4)	Reactome	27/78	0.001	0.034
Defective CYP17A1 causes Adrenal hyperplasia 5 (AH5)	Reactome	27/78	0.001	0.034
Defective FMO3 causes Trimethylaminuria (TMAU)	Reactome	27/78	0.001	0.034
Defective MAOA causes Brunner syndrome (BRUNS)	Reactome	27/78	0.001	0.034
Defective TBXAS1 causes Ghosal hematodiaphyseal dysplasia (GHDD)	Reactome	27/78	0.001	0.034
Defective CYP21A2 causes Adrenal hyperplasia 3 (AH3)	Reactome	27/78	0.001	0.034
Defective CYP11A1 causes Adrenal insufficiency, congenital, with 46,XY sex reversal (AICSR)	Reactome	27/78	0.001	0.034
Defective CYP7B1 causes Spastic paraplegia 5A, autosomal recessive (SPG5A) and Congenital bile acid synthesis defect 3 (CBAS3)	Reactome	27/78	0.001	0.034
Defective CYP27B1 causes Rickets vitamin D-dependent 1A (VDDR1A)	Reactome	27/78	0.001	0.034
Defective CYP11B2 causes Corticosterone methyloxidase 1 deficiency (CMO-1 deficiency)	Reactome	27/78	0.001	0.034
Defective CYP4F22 causes Ichthyosis, congenital, autosomal recessive 5 (ARCI5)	Reactome	27/78	0.001	0.034
Defective CYP2U1 causes Spastic paraplegia 56, autosomal recessive (SPG56)	Reactome	27/78	0.001	0.034
Defective CYP26C1 causes Focal facial dermal dysplasia 4 (FFDD4)	Reactome	27/78	0.001	0.034
Defective CYP26B1 causes Radiohumeral fusions with other skeletal and craniofacial anomalies (RHFCA)	Reactome	27/78	0.001	0.034
Defective CYP2R1 causes Rickets vitamin D-dependent 1B (VDDR1B)	Reactome	27/78	0.001	0.034
Phase 1 - Functionalization of compounds	Reactome	27/78	0.001	0.034
Defective CYP1B1 causes Glaucoma	Reactome	27/78	0.001	0.034
Defective CYP19A1 causes Aromatase excess syndrome (AEXS)	Reactome	27/78	0.001	0.034
Defective CYP24A1 causes Hypercalcemia, infantile (HCAI)	Reactome	27/78	0.001	0.034
Inflammation mediated by chemokine and cytokine signaling pathway	PANTHER	54/194	0.001	0.034
Cell junction organization	Reactome	29/87	0.001	0.035
Defensins	Reactome	20/50	0.001	0.037
Phenylalanine metabolism	KEGG PATHWAY	12/18	0.001	0.048
Cell-Cell communication	Reactome	38/132	0.001	0.055
Innate Immune System	Reactome	122/566	0.001	0.055
Cytochrome P450 - arranged by substrate type	Reactome	22/61	0.001	0.057
Class B/2 (Secretin family receptors)	Reactome	28/87	0.001	0.057
Neurotransmitter Release Cycle	Reactome	17/41	0.001	0.058
gluconeogenesis	BioCyc	13/24	0.001	0.058
SLC-mediated transmembrane transport	Reactome	62/253	0.002	0.066
Arachidonic acid metabolism	Reactome	19/50	0.002	0.067
Staphylococcus aureus infection	KEGG PATHWAY	23/57	0.002	0.071
GABA receptor activation	Reactome	20/55	0.002	0.075
Stimuli-sensing channels	Reactome	30/99	0.002	0.075
Synthesis of Leukotrienes (LT) and Eoxins (EX)	Reactome	11/21	0.002	0.087

Transport of glucose and other sugars, bile salts and organic acids, metal ions and amine compounds	Reactome	29/96	0.002	0.089
Beta defensins	Reactome	16/40	0.003	0.090
Complement cascade	Reactome	15/38	0.004	0.131
amb2 Integrin signaling	PID	15/40	0.004	0.135
Disease	Reactome	347/1887	0.004	0.138
GABA B receptor activation	Reactome	15/39	0.005	0.149
Activation of GABAB receptors	Reactome	15/39	0.005	0.149
Initial triggering of complement	Reactome	10/20	0.005	0.154
Amine ligand-binding receptors	Reactome	15/41	0.007	0.209
Type I hemidesmosome assembly	Reactome	7/11	0.007	0.214
activation of csk by camp-dependent protein kinase inhibits signaling through the t cell receptor	BioCarta	13/39	0.007	0.214
Fatty acids	Reactome	8/15	0.008	0.257
glycolysis	BioCyc	11/24	0.009	0.257
the co-stimulatory signal during t-cell activation	BioCarta	8/18	0.009	0.262
Eicosanoids	Reactome	7/12	0.010	0.282

5. CONCLUSÃO

Neste estudo foi identificado um perfil diferencial de metilação em lesões benignas de tireoide, carcinomas papíliferos, carcinomas foliculares e carcinomas não diferenciados em relação ao tecido não neoplásico. Foi encontrado um maior número de CpGs hipermetiladas em lesões benignas e carcinomas foliculares e maior número de CpGs hipometiladas em carcinomas papilíferos e não diferenciados de tireoide. Estes achados confirmam, em parte, dados prévios da literatura obtidos com análises menos abrangentes e geram novos dados que contribuem para o avanço do conhecimento dos mecanismos envolvidos nos processos de carcinogenese de células foliculares de tireoide.

O algoritmo baseado em padrões alterados de metilação de nove locos (*SLC22A18*/*SLC22A18AS, SCNN1A, DCUN1D3, ELOVL5, ELK3, EHF, SOX10, LTK* e um CpG não mapeado em um gene) permitiu a correta classificação com alta sensibilidade (91.9%) e especificidade (76.5%)de tecidos normais, lesões benignas e carcinomas de tireoide. Embora ainda não validado, a análise dessas alterações tem potencial para contribuir para a prática clínica. Os menores escores gerados para o classificador diagnóstico em PTC foram associados com o maior risco de acometimento linfonodal.

A análise *in silico* destacou as principais vias alteradas nas lesões benignas e malignas de tireoide, entre elas a *Gαi signaling* predita como ativada, mostrando alterações de metilação do DNA como uma possível aternativa para a ativação da via MAPK em carcinomas pouco diferenciados.

A análise do perfil de metilação de DNA permitiu a identificação de cinco locos/genes hipometilados (*CENPJ*, *SCFD2, RPL23* e 2 não mapeados em genes conhecidos), os quais revelaram ser potenciais marcadores prognósticos e capazes de classificar as amostras tumorais de pacientes com pior prognóstico.

6. REFERÊNCIAS BIBLIOGRÁFICAS

ALEXANDER, E.K.; KENNEDY, G.C.; BALOCH, Z.W. et al. Preoperative diagnosis of benign thyroid nodules with indeterminate cytology. **N Engl J Med**, v.367, n.8, p.705-715, 2012.

ALVAREZ-NUÑEZ, F.; BUSSAGLIA, E.; MAURICIO, D. et al. PTEN promoter methylation in sporadic thyroid carcinomas. **Thyroid,**v.16, n.1, p.17-23, 2006.

ASIOLI, S.; ERICKSON, L.A.; RIGHI, A. et al. Poorly differentiated carcinoma of the thyroid: validation of the Turin proposal and analysis of IMP3 expression. **Mod Pathol**, v.23, n.9, p.1269-1278, 2010.

BALOCH, Z.W.; LIVOLSI, V.A. Follicular-patterned afflictions of the thyroid gland: reappraisal of the most discussed entity in endocrine pathology. **Endocr Pathol**, v.25, n.1, p.12-20, 2014.

BERDASCO, M.; ESTELLER, M. Aberrant epigenetic landscape in cancer: how cellular identity goes awry. **Dev Cell**, v.19, n.5, p.698-711, 2010.

BERNSTEIN, B.E.; MEISSNER, A.; LANDER, E.S.The mammalian epigenome.**Cell**, v.128, n.4, p.669-681, 2007.

BHAIJEE, F.; NIKIFOROV, Y.E. Molecular analysis of thyroid tumors.**Endocr Pathol**, v. 22, n.3, p.126-133, 2011.

BIBIKOVA, M.; BARNES, B.; TSAN, C. et al. High density DNA methylation array with single CpG site resolution.**Genomics**, v.98, p.288-295, 2011.

BOSE, S.; WALTS, AE. Thyroid fine needle aspirate: a post-Bethesda update. **Adv Anat Pathol**, v.19, n.3, p.160-169, 2012.

BRAIT, M.; LOYO, M.; ROSENBAUM, E. et al. Correlation between BRAF mutation and promoter methylation of TIMP3, RARβ2 and RASSF1A in thyroid cancer. **Epigenetics**, v.7, p.710-719, 2012.

BRZEZIANSKA, E.; PASTUSZAK-LEWANDOSKA, D. A minireview: the role of MAPK/ERK and PI3K/Akt pathways in thyroid follicular cell-derived neoplasm. **Front Biosci (Landmark Ed),** v.16, p.422-439, 2011.

CAMARGO BARROS-FILHO, M.; ALBUQUERQUE, F. M.; PINTO, C.A. et al. High diagnostic accuracy based on CLDN10, HMGA2 and LAMB3 transcripts in papillary thyroid carcinoma. **J Clin Endocrinol Metab**. 2015 Apr 13:jc20144053. [Epub ahead of print]

CANTARA, S.; PILLI, T.; SEBASTIANI, G. et al. Circulating miRNA95 and miRNA190 are sensitive markers for the differential diagnosis of thyroid nodules in a Caucasian population. **J Clin Endocrinol Metab**, v.99, n.11, p. 4190-4198, 2014.

CANTWELL-DORRIS, E.R.; O'LEARY, J.J; SHEILS, OM. BRAFV600E: implications for carcinogenesis and molecular therapy. **Mol Cancer Ther**, v.10, p.385-394, 2011.

CARONIA, L.M.; PHAY, J.E.; SHAH, M.H. Role of BRAF in thyroid oncogenesis. **Clin Cancer Res,** v.17, p.7511-7, 2011.

CHEN, Y.A.; LEMIRE, M.; CHOUFANI, S. *et al*. Discovery of cross-reactive probes and polymorphic CpGs in the Illumina Infinium HumanMethylation450 microarray.**Epigenetics**,v.8, n.2, p.203-9, 2013.

CHENG, X.; BLUMENTHAL, R.M. Mammalian DNA methyltransferases: a structural perspective. **Structure**, v.16, n.3, p.341-350, 2008.

CHIASERA, J.M. Back to the basics: thyroid gland structure, function and pathology. **Clin Lab Sci**, v.26, n.2, p.112-117, 2013.

CIAMPI, R.; KNAUF, J.A.; KERLER, R. et al. Oncogenic AKAP9-BRAF fusion is a novel mechanism of MAPK pathway activation in thyroid cancer. **J Clin Invest**, v.115, p.94-101, 2005.

CIBAS, E.S.; ALI, S.Z.The Bethesda System for Reporting Thyroid Cytopathology.**Thyroid,** v.19, n.11, p.1159-1165, 2009.

COOPER, D.S.; DOHERTY, G.M; HAUGEN, B.R. et al. Revised American Thyroid Association management guidelines for patients with thyroid nodules and differentiated thyroid cancer. **Thyroid**, v.19, p.1167-214, 2009.

COSTELLO, J.F.; PLASS, C. Methylation matters.**J Med Genet**, v.38, n.5, p.285-303, 2001.

CZARNECKA, K.; PASTUSZAK-LEWANDOSKA, D.; MIGDALSKA-SEK, M. et al. 2011, Aberrant methylation as a main mechanism of TSGs silencing in PTC. **Front Biosci (Elite Ed),** v.3, p.137-157, 2011.

DALIRI, M.; ABBASZADEGAN, M.R.; MEHRABI BAHAR, M. et al. The role of BRAF V600E mutation as a potential marker for prognostic stratification of papillary thyroid carcinoma: a long-term follow-up study. **Endocr Res**, Mar. 2014. In press.

DAVIES, H.; BIGNELL, G.R.; COX, C. et al. Mutations of the BRAF gene in human cancer. **Nature**, v.417, p.949-954, 2002.

MUKHERJEE, D.; KUNDU, S.; KOUSIK PRAMANICK, K. et al (2011). Calcitonin Functions Both as a Hypocalcemic Hormone and Stimulator of Steroid Production and Oocyte Maturation in Ovarian Follicles of Common Carp, Cyprinus carpio, Update on Mechanisms of Hormone Action - Focus on Metabolism, Growth and Reproduction, **Prof. Gianluca Aimaretti** (Ed.), ISBN: 978-953-307-341-5, 2011.

DOI, A.; PARK, I.H.; WEN, B. *et al*. Differential methylation of tissue- and cancer-specific CpG island shores distinguishes human induced pluripotent stem cells, embryonic stem cells and fibroblasts. **Nat Genet**. 2009;41:1350–3

DOWNWARD, J. Signal transduction.New exchange, new target.**Nature**, v. 396, p.416-417, 1998.

DU, P.; ZHANG, X.; HUANG, C.C. et al. Comparison of Beta-value and M-value methods for quantifying methylation levels by microarray analysis.**BMC Bioinformatics,** v.30, p.11:587, 2010.

DURANTE, C.; PUXEDDU, E.; FERRETTI, E. et al. BRAF mutations in papillary thyroid carcinomas inhibit genes involved in iodine metabolism. **J Clin Endocrinol Metab**, v.92, p.2840-2843, 2008.

ELISEI, R.; PINCHERA, A. Advances in the follow-up of differentiated or medullary thyroid cancer. **Nat Rev Endocrinol**, v.8, p.466-475,2012.

ELLIS, R.J.; WANG, Y.; STEVENSON, H.S. et al. Genome-wide methylation patterns in papillary thyroid cancer are distinct based on histological subtype and tumor genotype. **J Clin Endocrinol Metab**, v.99, n.2, p.329-337, 2014.

ESPADA, J.; ESTELLER, M. DNA methylation and the functional organization of the nuclear compartment. **Semin Cell Dev Biol**, v.21, n.2, p.238-246, 2010.

ESTELLER, M. Cancer epigenomics: DNA methylomes and histone-modification maps. **Nat Rev Genet**, v.8, n.4, p.286-298, 2007.

ESTELLER, M. Epigenetics in cancer. **N Engl J Med**, v.358, n.11, p.1148-1159, 2008.

ESTELLER, M.; HERMAN, J.G. Cancer as an epigenetic disease: DNA methylation and chromatin alterations in human tumours. **J Pathol**, v.196, n.1, p.1-7, 2002.

EZZAT, S.; SARTI, D.A.; CAIN, D.R. et al. Thyroid incidentalomas.Prevalence by palpation and ultrasonography. **Arch Intern Med**, v.154, n.16, p.1838-1840, 1994.

FAGIN, J.A.; MITSIADES, N. Molecular pathology of thyroid cancer: diagnostic and clinical implications. **Best Pract Res Clin Endocrinol Metab**, v.22, n.6, p.955-969, 2008.

FEINBERG, A.P. Phenotypic plasticity and the epigenetics of human disease. **Nature**, v.447, p.433-440, 2007.

FEINBERG, A.P.; TYCKO, B.The history of cancer epigenetics. **Nat Rev Cancer,** v.4, p.143-153, 2004.

FERRAZ, C.; ESZLINGER, M.; PASCHKE, R. Current state and future perspective of molecular diagnosis of fine-needle aspiration biopsy of thyroid nodules. **J Clin Endocrinol Metab**, v.96, n.7, p.2016-2026, 2011.

FRATES, M.C.; BENSON, C.B.; CHARBONEAU, J.W. et al. Society of Radiologists in Ultrasound. Management of thyroid nodules detected at US: Society of Radiologists in Ultrasound consensus conference statement. **Radiology**, v.237, n.3, p.794-800, 2005.

GARDNER, R.E.; TUTTLE, R.M.; BURMAN, K.D. et al. Prognostic importance of vascular invasion in papillary thyroid carcinoma. **Arch Otolaryngol Head Neck Surg**, v.126, p.309-312, 2000.

GÓMEZ SÁEZ, J.M. Diagnostic and prognostic markers in differentiated thyroid cancer. **Curr Genomics**, v.12, p. 597-608, 2011.

GONZALEZ-GONZALEZ, R.; BOLOGNA-MOLINA, R.; CARREON-BURCIAGA, R.G. *et al*. Papillary thyroid carcinoma: differential diagnosis and prognostic values of its different variants: review of the literature. **ISRN Oncol**, v.2011, p.915925, 2011.

GOODMAN, J.I.; WATSON, R.E. Altered DNA methylation: a secondary mechanism involved in carcinogenesis. **Annu Rev Pharmacol Toxicol**, v.42, p. 501-525, 2002.

GROS, C.; FAHY, J.; HALBY, L. et al. DNA methylation inhibitors in cancer: recent and future approaches. **Biochimie**, v.94, n.11, p.2280-2296, 2012.

GUAN, H.; JI, M.; HOU, P. *et al*. Hypermethylation of the DNA mismatch repair gene hMLH1 and its association with lymph node metastasis and T1799A BRAF mutation in patients with papillary thyroid cancer. **Cancer**, v.113, p.247-255, 2008.

GUERRA, A.; FUGAZZOLA, L.; MAROTTA, V. *et al*. A high percentage of BRAFV600E alleles in papillary thyroid carcinoma predicts a poorer outcome. **J Clin Endocrinol Metab**, v.97, p.2333-2340, 2012.

GUIL, S.; ESTELLER, M. DNA methylomes, histone codes and miRNAs: tying it all together. **Int J Biochem Cell Biol**, v.41, n.1, p.87-95, 2009.

GUTH, S.; THEUNE, U.; ABERLE, J. *et al*. Very high prevalence of thyroid nodules detected by high frequency (13 MHz) ultrasound examination. **Eur J Clin Invest**,

v.39, n.8, p.699-706, 2009.

GUYTON, A.C; HALL, J.E. **Textbook of Medical Physiology** (eleventh edition), Elsevier Sanders, 0-7216-0240-1, Philadelphia. 2006

HAN, L.; ZHAO, Z. CpG islands or CpG clusters: how to identify functional GC-rich regions in a genome? **BMC Bioinformatics**, 10:65, 2009.

HANEL, W.; MOLL, U.M. Links between mutant p53 and genomic instability. **J Cell Biochem**, v.113, n.2, p.433-439, 2012.

HERMANN, A.; SCHMITT, S.; JELTSCH, A. The human Dnmt2 has residual DNA-(cytosine-C5) methyltransferase activity. **J Biol Chem**, v.278, n.34, p.31717–31721, 2003.

HILTZIK, D.; CARLSON, D.L.; TUTTLE, R.M. et al. Poorly differentiated thyroid carcinomas defined on the basis of mitosis and necrosis: a clinicopathologic study of 58 patients. **Cancer**, v.106, n.6, p.1286–1295, 2006.

HOQUE, M.O.; ROSENBAUM, E.; WESTRA, W.H. *et al*. Quantitative assessment of promoter methylation profiles in thyroid neoplasms. **J Clin Endocrinol Metab**, v. 90, p. 4011-4018, 2005.

HOU, P.; JI, M.; XING, M. Association of PTEN gene methylation with genetic alterations in the phosphatidylinositol 3-kinase/AKT signaling pathway in thyroid tumors. **Cancer**, v.113, n.9, p.2440-2447, 2008.

HOU, P.; LIU, D.; XING, M. Genome-wide alterations in gene methylation by the BRAF V600E mutation in papillary thyroid cancer cells. **Endocr Relat Cancer**, v.18, p.687-697, 2011.

HOWELL, G.M.; HODAK, S.P.; YIP, L. RAS mutations in thyroid cancer. **Oncologist**, v.18, n.8, p.926-932, 2013.

HU, S.; EWERTZ, M.; TUFANO, R.P. et al. Detection of serum deoxyribonucleic acid methylation markers: a novel diagnostic tool for thyroid cancer. **J Clin Endocrinol Metab**, v.91, n.1, p.98-104, 2006a.

HU, S.; LIU, D.; TUFANO, R.P. et al. Association of aberrant methylation of tumor suppressor genes with tumor aggressiveness and BRAF mutation in papillary thyroid cancer. **Int J Cancer,** v.119, p.2322-2329, 2006b.

IACOBUZIO-DONAHUE, C.A. Epigenetic changes in cancer. **Annu Rev Pathol**, v.4, p.229-249, 2009.

INCA, Estimativa 2014- Incidência de câncer no Brasil: Rio de Janeiro, p.118, 2011.

IRIZARRY, R.A.; LADD-ACOSTA, C.; WEN, B. et al. The human colon cancer methylome shows similar hypo- and hypermethylation at conserved tissue-specific CpG island shores. **Nat Genet,** v.41, n.2, p.178-186, 2009.

ITO, Y.; MIYAUCHI, A. Prognostic factors and therapeutic strategies for differentiated carcinomas of the thyroid. **Endocr J**, v.56, p.177-192, 2009.

IYER, N.G.; SHAHA, A.R. Central compartment dissection for well differentiated thyroid cancer … and the band plays on. **Curr Opin Otolaryngol Head Neck Surg**, v.19, n.2, p.106-112, 2011.

JARZAB, B.; HANDKIEWICZ-JUNAK, D. Differentiated thyroid cancer in children and adults: same or distinct disease?. **Hormones (Athens),** v.6, p.200-209, 2007.

JIN, J.; PHITAYAKORN, R.; WILHELM, S.M.; MCHENRY, C.R. Advances in management of thyroid cancer. **Curr Probl Surg,** v.50, p.241-289, 2013.

JONES, P.A. Functions of DNA methylation: islands, start sites, gene bodies and beyond. **Nat Rev Genet**, v.13, n.7, p.484-492, 2012.

JOSEPH, B.; JI, M.; LIU, D. *et al*. Lack of mutations in the thyroid hormone receptor (TR) alpha and beta genes but frequent hypermethylation of the TRbeta gene in differentiated thyroid tumors**. J Clin Endocrinol Metab**, v.92, p.4766-4770, 2007.

JUNG, T.S.; KIM, T.Y.; KIM, K.W. et al. Clinical features and prognostic factors for survival in patients with poorly differentiated thyroid carcinoma and comparison to the patients with the aggressive variants of papillary thyroid carcinoma. **Endocr J**, v.54, n.2, p.265-274, 2007.

KABAKER, A.S.; TUBLIN, M.E.; NIKIFOROV, Y.E. et al. Suspicious Ultrasound Characteristics Predict BRAF V600E-Positive Papillary Thyroid Carcinoma. **Thyroid**, v.22, n.6, p.585-589, 2012.

KANWAL, R.; GUPTA, S. Epigenetic modifications in cancer. **Clin Genet**, v.81, p.303-311, 2012.

KARGER, S.; KRAUSE, K.; GUTKNECHT, M. et al. ADM3, TFF3 and LGALS3 are discriminative molecular markers in fine-needle aspiration biopsies of benign and malignant thyroid tumours. **Br J Cancer**, v.106, n.3, p.562-568, 2012.

KELLER, S.; ANGRISANO, T.; FLORIO, E. et al. DNA methylation state of the galectin-3 gene represents a potential new marker of thyroid malignancy. **Oncol Lett**, v.6, n.1, p.86-90, 2013.

KHANAFSHAR, E.; LLOYD, R.V. The spectrum of papillary thyroid carcinoma variants. **Adv Anat Pathol**, v. 18, p. 90-97, 2011.

KIKUCHI, Y.; TSUJI, E.; YAGI, K.; et al. Aberrantly methylated genes in human papillary thyroid cancer and their association with BRAF/RAS mutation. **Front Genet**, v.5, n.4, p.271, 2013.

KIM, S.Y.; HAHN, W.C. Cancer genomics: integrating form and function. **Carcinogenesis**, v. 28, p. 1387-1392, 2007.

KIM, T.H.; PARK, Y.J.; LIM, J.A. et al. The association of the BRAF(V600E) mutation with prognostic factors and poor clinical outcome in papillary thyroid cancer: A Meta-Analysis. **Cancer**, v.118, n.7, p.1764-1773, 2012.

KIM, T.Y.; KIM, K.W.; JUNG, T.S. et al. Prognostic factors for Korean patients with anaplastic thyroid carcinoma. **Head Neck**, v.29, n.8, p.765-772, 2007.

KIM, T.Y.; KIM, W.G.; KIM, W.B. et al. Current status and future perspectives in differentiated thyroid cancer. **Endocrinol Metab (Seoul)**, v.29, n.3, p.217-225, 2014.

KISELJAK-VASSILIADES, K.; XING, M. Association of Cigarette Smoking with Aberrant Methylation of the Tumor Suppressor Gene RARβ2 in Papillary Thyroid Cancer. **Front Endocrinol (Lausanne),** v.2, p.99, 2011.

KO, H.J.; KIM, B.Y.; JUNG, C.H. *et al*. DNA methylation of RUNX3 in papillary thyroid cancer. **Korean J Intern Med**, v.27, p.407-410, 2012.

KONDO, T.; ASA, S.L.; EZZAT, S. Epigenetic dysregulation in thyroid neoplasia. **Endocrinol Metab Clin North Am**, v.37, p.389-400, 2008.

LAIRD, P.W. Cancer epigenetics. **Hum Mol Genet**, v.14, n. 1, p.R65-76, 2005.

LAIRD, P.W.The power and the promise of DNA methylation markers.**Nat Rev Cancer**, v.3, n.4, p.253-266, 2003.

LAL, G.; PADMANABHA, L.; SMITH, B.J. *et al*. RIZ1 is epigenetically inactivated by promoter hypermethylation in thyroid carcinoma. **Cancer**, v.107, p.2752-2759, 2006.

LEEK, J.T.; JOHNSON, W.E.; PARKER, H.S. et al.The sva package for removing batch effects and other unwanted variation in high-throughput experiments. **Bioinformatics**, v.28, n.6, p.882-883, 2012.

LI, X.; ABDEL-MAGEED, A.B.; KANDIL, E. BRAF mutation in papillary thyroid carcinoma. **Int J Clin Exp Med**, v.5, n.4, p.310-315, 2012.

LIN, J.D.; CHAO, T.C.; HSUEH, C. Clinical characteristics of poorly differentiated thyroid carcinomas compared with those of classical papillary thyroid carcinomas. **Clin Endocrinol (Oxf)**, v.66, n.2, p.224-228, 2007.

LIVOLSI, V.A. Papillary thyroid carcinoma: an update. **Mod Pathol**, v. 24, n.2, p.S1-9, 2011.

LOPEZ, J.; PERCHARDE, M.; COLEY, H.M. et al. The context and potential of epigenetics in oncology. **Br J Cancer,** v.100, p.571-577, 2009.

LUPI, C.; GIANNINI, R.; UGOLINI, C.; et al. Association of BRAF V600E mutation with poor clinicopathological outcomes in 500 consecutive cases of papillary thyroid carcinoma. **J Clin Endocrinol Metab**, v.92, p.4085-4090, 2007.

MACCORKLE, R.A.; TAN, T.H. Mitogen-activated protein kinases in cell-cycle control. **Cell Biochem Biophys**, v.43, p.451-461, 2005.

MACIEL, R.M.; KIMURA, E.T.; CERUTTI, J.M. Pathogenesis of differentiated thyroid cancer (papillary and follicular). **Arq Bras Endocrinol Metabol**, v.49, p.691-700, 2005.

MANCIKOVA, V.; BUJ, R.; CASTELBLANCO, E. et al. DNA methylation profiling of well-differentiated thyroid cancer uncovers markers of recurrence free survival. **Int J Cancer,** v.135, n.3, p.598-610, 2014.

MAZZAFERRI, E.L.; JHIANG, S.M. Long-term impact of initial surgical and medical therapy on papillary and follicular thyroid cancer. **Am J Med**, v.97, n.5, p.418-428, 1994.

MICCOLI, P. Application of molecular diagnostics to the evaluation of the surgical approach to thyroid cancer. **Curr Genomics**, v.15, n.3, p.184-189, 2014.

MOELLER, L.C.; FÜHRER, D. Thyroid hormone, thyroid hormone receptors, and cancer: a clinical perspective. **Endocr Relat Cancer**, v.20, n.2, p.R19-29, 2013.

MONTERO-CONDE, C.; MARTÍN-CAMPOS, J.M.; LERMA, E, Molecular profiling related to poor prognosis in thyroid carcinoma. Combining gene expression data and biological information. **Oncogene**, v.27, n.11, p.1554-1561, 2008.

MOTOI, N.; SAKAMOTO, A.; YAMOCHI, T. et al. Role of ras mutation in the progression of thyroid carcinoma of follicular epithelial origin.**Pathol Res Pract**, v.196, n.1, p.1-7, 2000.

NAKAMURA, N.; CARNEY, J.A.; JIN, L. et al. RASSF1A and NORE1A methylation and BRAFV600E mutations in thyroid tumors. **Lab Invest,** v.85, p. 1065-1075, 2005.

NIEDZIELA, M. Thyroid nodules. **Best Pract Res Clin Endocrinol Metab**, v.28, n.2, p.245-277, 2014.

NIKIFOROVA, M.N.; WALD, A.I.; ROY, S. et al.Targeted next-generation sequencing panel (ThyroSeq) for detection of mutations in thyroid cancer. **J Clin Endocrinol Metab**, v.98, n.11, p.E1852-60, 2013.

NIKIFOROV, Y.E. Molecular analysis of thyroid tumors. **Mod Pathol,** v.24, n.2, p.S34-43, 2011.

NIKIFOROV, Y.E.; NIKIFOROVA, M.N. Molecular genetics and diagnosis of thyroid cancer. **Nat Rev Endocrinol**, v.7, p. 569-580, 2011.

NIKIFOROV, Y.E.; OHORI, N.P.; HODAK, S.P. et al. Impact of mutational testing on the diagnosis and management of patients with cytologically indeterminate thyroid nodules: a prospective analysis of 1056 FNA samples. **J Clin Endocrinol Metab**, v.96, n.11, p.3390-3397, 2011.

NIKIFOROV, Y.E.; STEWARD, D.L.; ROBINSON-SMITH, T.M. et al. Molecular testing for mutations in improving the fine-needle aspiration diagnosis of thyroid nodules. **J Clin Endocrinol Metab**, v.94, n.6, p.2092-2098, 2009.

NIKIFOROVA, M.N.; KIMURA, E.T.; GANDHI, M. et al. BRAF mutations in thyroid tumors are restricted to papillary carcinomas and anaplastic or poorly differentiated carcinomas arising from papillary carcinomas. **J Clin Endocrinol Metab,** v.88, p.5399-404, 2003a.

NIKIFOROVA, M.N.; LYNCH, R.A.; BIDDINGER, P.W. et al. RAS point mutations and PAX8-PPAR gamma rearrangement in thyroid tumors: evidence for distinct molecular pathways in thyroid follicular carcinoma. **J Clin Endocrinol Metab**, v.88, n.5, p.2318-2326, 2003b.

OGOSHI, K.l.; HASHIMOTO, S.; NAKATANI, Y. et al. Genome-wide profiling of DNA methylation in human cancer cells. **Genomics**, v.98, n.4, p.280-7, 2011.

O'NEILL, J.P.; POWER, D.; CONDRON, C. et al. Anaplastic thyroid cancer, tumorigenesis and therapy. **Ir J Med Sci**, v.179, n.1, p.9-15, 2010.

O'NEILL, J.P.; SHAHA, A.R. Anaplastic thyroid cancer. **Oral Oncol**, v.49, n.7, p.702-706, 2013.

PARK, Y.J.; CLAUS, R.; WEICHENHAN, D. et al. Genome-wide epigenetic modifications in cancer.**Prog Drug Res**, v.67, p.25-49, 2011.

PATEL, K.N.; SHAHA, A.R. Poorly differentiated thyroid cancer. **Curr Opin Otolaryngol Head Neck Surg**, v.22, n.2, p.121-126, 2014.

PFEIFER, G.P.; DAMMANN, R. Methylation of the tumor suppressor gene RASSF1A in human tumors. **Biochemistry (Mosc),** v.70, n.5, p.576-583, 2005.

PIANA, S.; FRASOLDATI, A.; FERRARI, M. et al. Is a five-category reporting scheme for thyroid fine needle aspiration cytology accurate? Experience of over 18,000 FNAs reported at the same institution during 1998-2007. **Cytopathology**, v.22, n.3, p.164-173, 2011

R CORE TEAM. R: A language and environment for statistical computing. R Foundation for Statistical Computing, Vienna, Austria.URL http://www.R-project.org/. 2013.

RAHBARI, R.; ZHANG, L.; KEBEBEW, E. Thyroid cancer gender disparity. **Future Oncol,** v.6, p.1771-1779, 2010.

REN, Q.; GUO, Z.; WANG, X. Review on thyroid carcinoma of molecular pathology. **Life Science Journal,** v.4, p.4, 2007.

RIESCO-EIZAGUIRRE, G.; SANTISTEBAN, P. Molecular biology of thyroid cancer initiation. **Clin Transl Oncol,** v.9, p.686-693, 2007.

RÍOS, A.; RODRÍGUEZ, J.M.; FERRI, B. et al. Are prognostic scoring systems of value in patients with follicular thyroid carcinoma? **Eur J Endocrinol**, v.169, n.6, p. 821–827, 2013.

RITCHIE, M.E.; PHIPSON, B.; WU, D. et al. limma powers differential expression analyses for RNA-sequencing and microarray studies. **Nucleic Acids Res**. pii: gkv007. [Epub ahead of print], 2015.

ROBERTSON, K.D. DNA methylation and human disease. **Nat Rev Genet**, v.6, n.8, p.597-610, 2005.

ROCHA, A.S.; SOARES, P.; SERUCA, R. *et al*. Abnormalities of the E-cadherin/catenin adhesion complex in classical papillary thyroid carcinoma and in its diffuse sclerosing variant. **J Pathol**, v.194, n.3, p.358-366, 2001.

RODRÍGUEZ-PAREDES, M.; ESTELLER, M. Cancer epigenetics reaches mainstream oncology. **Nat Med**, v.17, n.3, p.330-339, 2011.

RODRÍGUEZ-RODERO, S.; FERNÁNDEZ, A.F.; FERNÁNDEZ-MORERA, J.L. et al. DNA methylation signatures identify biologically distinct thyroid cancer subtypes. **J Clin Endocrinol Metab,** v. 98, p. 2811-2821, 2013.

ROSEN, J.; HE, M.; UMBRICHT, C.; ALEXANDER, H.R. et al.A six-gene model for differentiating benign from malignant thyroid tumors on the basis of gene expression. **Surgery,** v.138, n.6, p.1050-1056, 2005.

ROSSI, M.; BURATTO, M.; BRUNI, S. et al. Role of ultrasonographic/clinical profile, cytology, and BRAF V600E mutation evaluation in thyroid nodule screening for

malignancy: a prospective study. **J Clin Endocrinol Metab**, v. 97, p.2354-61, 2012.

RUSSO, D.; DAMANTE, G.; PUXEDDU, E. et al. Epigenetics of thyroid cancer and novel therapeutic targets. **J Mol Endocrinol**, v.46, n.3, p.R73-81, 2011.

SANTORO, M.; MELILLO, R.M.; FUSCO, A. RET/PTC activation in papillary thyroid carcinoma: European Journal of Endocrinology Prize Lecture. **Eur J Endocrinol**, v.155, n.5, p.645-653, 2006.

SANTOS, J.C.; BASTOS, A.U.; CERUTTI, J.M.; RIBEIRO, M. L. Correlation of MLH1 and MGMT expression and promoter methylation with genomic instability in patients with thyroid carcinoma. **BMC Cancer**, v.13, p.79, 2013.

SASSA, M.; HAYASHI, Y.; WATANABE, R. *et al*. Aberrant promoter methylation in overexpression of CITED1 in papillary thyroid cancer. **Thyroid**, v.21, p.511-517, 2011.

SAWAN, C.; VAISSIÈRE, T.; MURR, R. et al. Epigenetic drivers and genetic passengers on the road to cancer. **Mutat Res**, v.642, n.1-2, p.1-13, 2008.

SCARPINO, S.; DI NAPOLI, A. *et al*. Papillary carcinoma of the thyroid: methylation is not involved in the regulation of MET expression. **Br J Cancer,** v.91, p.703-706, 2004.

SCHAGDARSURENGIN, U.; GIMM, O.; DRALLE, H.; C. HOANG-VU, C.; DAMMANN, R. CpG island methylation of tumor-related promoters occurs preferentially in undifferentiated carcinoma. **Thyroid**, v.16, p.633-642, 2006.

SCHAGDARSURENGIN, U.; RICHTER, A.M.; HORNUNG, J. *et al*. Frequent epigenetic inactivation of RASSF2 in thyroid cancer and functional consequences. **Mol Cancer**, v.9, p.264, 2010.

SCHALKWYK L.C.; PIDSLEY, R.; WONG, C.C. *et al*. WateRmelon: Illumina 450 methylation array normalization and metrics. R package version 1.4.0, 2013.

SCHNEIDER, D.F.; CHEN, H. New developments in the diagnosis and treatment of thyroid cancer. **CA Cancer J Clin**, v.63, n.6, p.374-394, 2013.

SCHÜBELER, D.; ELGIN, S.C. Defining epigenetic states through chromatin and RNA. **Nat Genet**, v.37, n.9, p.917-918, 2005.

SCLABAS, G.M.; STAERKEL, G.A.; SHAPIRO, S.E. et al. Fine-needle aspiration of the thyroid and correlation with histopathology in a contemporary series of 240 patients. **Am J Surg**,v.186, p.702-709, 2003.

SHARMA, S.; KELLY, T.K.; JONES, P.A. Epigenetics in cancer. **Carcinogenesis**, v.31, p.27-36, 2010.

SHERMAN, S.I. Thyroid carcinoma. **Lancet**, v.361, p.501-511, 2003.

SIEGMUND, K.D.; LAIRD, P.W. Analysis of complex methylation data. **Methods**, v.27, p.170-178, 2002.

SIRAJ, A.K.; HUSSAIN, A.R.; AL-RASHEED, M. *et al*. Demethylation of TMS1 gene sensitizes thyroid cancer cells to TRAIL-induced apoptosis. **J Clin Endocrinol Metab,** v.96, p.E215-24, 2011.

SMITH, N.; NUCERA, C. Personalized therapy in patients with anaplastic thyroid cancer: targeting genetic and epigenetic alterations. **J Clin Endocrinol Metab**. 2014 Oct 27:jc20142803. [Epub ahead of print]

SOBRINHO-SIMÕES, M.; ELOY, C.; MAGALHÃES, J. et al. Follicular thyroid carcinoma. **Mod Pathol**, v.24, n.2, p.S10-18, 2011.

STEPHEN, J.K.; CHITALE, D.; NARRA, V. *et al*. DNA methylation in thyroid tumorigenesis. **Cancers (Basel),** v.3, n.2, p.1732-1743, 2011.

STIRZAKER, C.; TABERLAY, P.C.; STATHAM, A.L. et al. Mining cancer methylomes: prospects and challenges. **Trends Genet**, v.30, n.2, p.75-84, 2014.

STRATTON, M.R.; CAMPBELL, P.J.; FUTREAL, P.A. The cancer genome. **Nature**, v.9, n.458(7239), p.719-724, 2009.

SUBRAMANIAM, D.; THOMBRE, R.; DHAR, A. et al. DNA methyltransferases: a novel target for prevention and therapy. **Front Oncol**, v.4, p.80, 2014.

SYRENICZ, A.; KOZIOŁEK, M.; CIECHANOWICZ, A. et al.New insights into the diagnosis of nodular goiter. **Thyroid Res**, v. 17, 7:6. 2014

TABY, R.; ISSA, J.P. Cancer epigenetics. **CA Cancer J Clin**, v.60, n.6, p.376-392, 2010.

TAKAI, D.; JONES, P. A. Comprehensive analysis of CpG islands in human chromosomes 21 and 22. **Proc Natl Acad Sci. USA**, v. 99, n.6, p.3740–3745, 2002.

TALLINI, G. Poorly differentiated thyroid carcinoma. Are we there yet? **Endocr Pathol**, v.22, n.4, p.190-194, 2011.

TANG, K.T.; LEE, C.H. BRAF mutation in papillary thyroid carcinoma: pathogenic role and clinical implications. **J Chin Med Assoc**, v.73, p.113-128, 2010.

TESCHENDORFF, A.E.; MARABITA, F.; LECHNER, M. et al.A beta-mixture quantile normalization method for correcting probe design bias in Illumina Infinium 450 k DNA methylation data. **Bioinformatics**, v.29, n.2, p.189-196, 2013.

The Cancer Genome Atlas Research Network. Integrated genomic characterization of papillary thyroid carcinoma. **Cell**, v.159, n.3, p.676-690, 2014.

TIMP, W.; BRAVO, H.C.; MCDONALD, O.G. et al. Large hypomethylated blocks as a universal defining epigenetic alteration in human solid tumors. **Genome Med**, v. 6, n.8, p.61, 2014.

VIGLIETTO, G.; DE MARCO, C. Molecular Biology of Thyroid Cancer, *in* E. Diamanti-Kandarakis, ed., Contemporary Aspects of Endocrinology: Croatia, InTech, p.189-234, 2011.

VOLANTE, M.; RAPA, I.; PAPOTTI, M. Poorly differentiated thyroid carcinoma: diagnostic features and controversial issues. **Endocr Pathol**, v.19, n.3, p.150-155, 2008.

VU-PHAN, D.; KOENIG, R.J. Genetics and epigenetics of sporadic thyroid cancer. **Mol Cell Endocrinol,** v.386, n.1-2, p.55-66, 2014.

WANG, C.C.; FRIEDMAN, L.; KENNEDY, G.C, et al.A large multicenter correlation study of thyroid nodule cytopathology and histopathology. **Thyroid**, v.21, n.3, p.243-251, 2011.

WEI, W.J.; SHEN, C.T.; SONG, H.J.et al. MicroRNAs as a potential tool in the differential diagnosis of thyroid cancer: a systematic review and meta-analysis. **Clin Endocrinol (Oxf)**.doi: 10.1111/cen.12696. [Epub ahead of print], 2014.

WISEMAN, S.M.; HADDAD, Z.; WALKER, B. et al. Whole-transcriptome profiling of thyroid nodules identifies expression-based signatures for accurate thyroid cancer diagnosis. **J Clin Endocrinol Metab**, v.98, n.10, p.4072-4079, 2013.

WITT, R. L.; FERRIS, R. L.; PRIBITKIN, E. A. et al. Diagnosis and management of differentiated thyroid cancer using molecular biology: **Laryngoscope**, v. 123, p. 1059-64, 2013.

World Health Organization Classification of Tumours. Pathology and Genetics of Tumours of Endocrine Organs (eds DeLellis, R. A., Lloyd R. V., Heitz, P. U. & Eng, C.) **(IARC Press**, Lyon, 2004).

WREESMANN, V.B.; SIECZKA, E.M.; SOCCI, N.D. et al. Genome-wide profiling of papillary thyroid cancer identifies MUC1 as an independent prognostic marker. **Cancer Res**, v.64, n.11, p.3780-3789, 2004.

XING, M. BRAF mutation in papillary thyroid cancer: pathogenic role, molecular bases, and clinical implications. **Endocr Rev**, v.28, p.742-762, 2007a.

XING, M. Gene methylation in thyroid tumorigenesis. **Endocrinology**, v.148, n.3, p.948-953, 2007b.

XING, M. Molecular pathogenesis and mechanisms of thyroid cancer. **Nat Rev Cancer,** v.13, p.184-199, 2013.

XING, M.; CLARK, D.; GUAN, H. BRAF mutation testing of thyroid fine-needle aspiration biopsy specimens for preoperative risk stratification in papillary thyroid cancer. **J Clin Oncol**, v.27, p.2977-2982, 2009.

XING, M.; COHEN, Y.; MAMBO, E. et al. Early occurrence of RASSF1A hypermethylation and its mutual exclusion with BRAF mutation in thyroid tumorigenesis. **Cancer Res**, v.64, p.1664-1668, 2004.

XING, M.; LIU, R.; LIU, X. et al. BRAF V600E and TERT Promoter Mutations Cooperatively Identify the Most Aggressive Papillary Thyroid Cancer With Highest Recurrence. **J Clin Oncol**, pii: JCO.2014.55.5094, 2014.

XING, M.; TOKUMARU, Y.; WU, G. et al. Hypermethylation of the Pendred syndrome gene SLC26A4 is an early event in thyroid tumorigenesis. **Cancer Res**, v.63, p.2312-2315, 2003b.

XING, M.; USADEL, H.; COHEN, Y. et al. Methylation of the thyroid-stimulating hormone receptor gene in epithelial thyroid tumors: a marker of malignancy and a cause of gene silencing. **Cancer Res,** v.63, p.2316-2321, 2003a.

YANG, J.; SCHNADIG, V.; LOGRONO, R.; WASSERMAN, P.G. Fine-needle aspiration of thyroid nodules: a study of 4703 patients with histologic and clinical correlations. **Cancer**; v.111, p.306-315, 2007.

YLAGAN, L.R.; FARKAS, T.; DEHNER, L.P. Fine needle aspiration of the thyroid: a cytohistologic correlation and study of discrepant cases. **Thyroid**, v.14, n.1, p.35-41, 2004.

ZHANG, B.; LIU, S.; ZHANG, Z.; WEI, J. *et al*. Analysis of BRAF(V600E) mutation and DNA methylation improves the diagnostics of thyroid fine needle aspiration biopsies. **Diagn Pathol**, v. 9, p.45, 2014.

ANEXOS

Anexo 1. Parecer do Comitê de Ética em Pesquisa com Seres Humanos do A.C. Camargo Cancer Center

A.C.Camargo Cancer Center

FUNDAÇÃO ANTÔNIO PRUDENTE-HOSPITAL DO CÂNCER A C CAMARGO

Plataforma Brasil

PARECER CONSUBSTANCIADO DO CEP

DADOS DO PROJETO DE PESQUISA

Título da Pesquisa: Análise do metiloma em carcinomas de tireoide
Pesquisador: Silvia Regina Rogatto
Área Temática: Genética Humana:
(Trata-se de pesquisa envolvendo Genética Humana que não necessita de análise ética por parte da CONEP;);
Versão: 1
CAAE: 22454813.5.0000.5432
Instituição Proponente: Fundação Antônio Prudente-Hospital do Câncer-A C Camargo
Patrocinador Principal: Financiamento Próprio

DADOS DO PARECER

Número do Parecer: 475.385
Data da Relatoria: 05/11/2013

Apresentação do Projeto:
O projeto visa a análise do padrão de metilação de genes importantes na carcinogênese e de alterações genômicas no desenvolvimento do carcinoma papilífero de tireoide em comparação ao tecido normal da tireoide. A partir da análise realizada com a plataforma de microarray Infinium® Human Methylation450 BeadChip (Illumina), os dados obtidos serão comparados com parâmetros histopatológicos, a fim de se investigar a associação de alterações epigenéticas a fatores prognósticos para o carcinoma papilífero de tireoide.

Objetivo da Pesquisa:
Identificar o perfil de metilação em carcinomas papilíferos da tireoide segundo a mutação em BRAF para identificar marcadores moleculares regulados por metilação cuja expressão do transcrito esteja alterada.

Avaliação dos Riscos e Benefícios:
O presente estudo não apresenta riscos ao paciente e o benefício é a melhor caracterização dos tumores papilíferos de tireoide.

Endereço: Rua Professor Antônio Prudente, 211
Bairro: Liberdade **CEP:** 01.509-900
UF: SP **Município:** SAO PAULO
Telefone: (11)2189-5020 **Fax:** (11)2189-5020 **E-mail:** cep_hcancer@accamargo.org.br

APÊNDICES

Apêndice 1. Representação gráfica da localização das sondas diferencialmente metiladas escolhidas para a construção dos classificadores diagnósticos

SLC22A18AS/SLC22A18- cg18419977

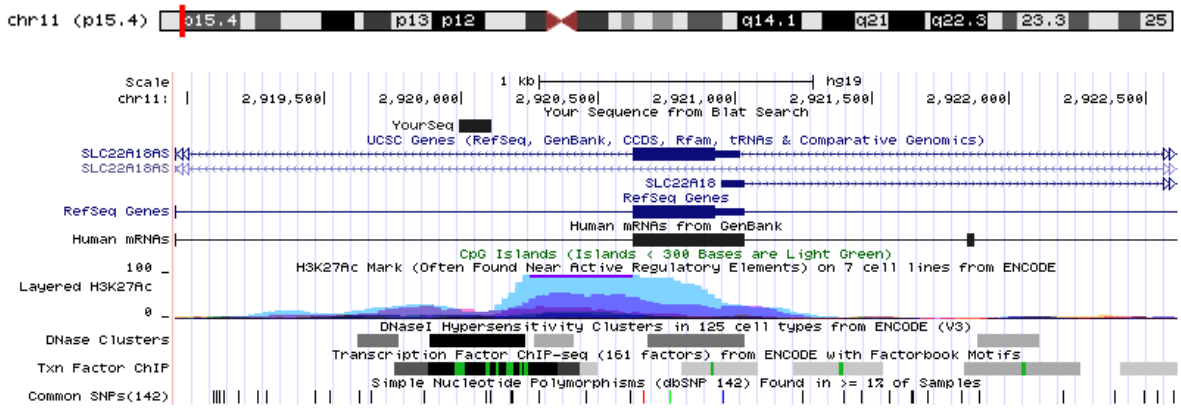

SCNN1A - cg26244013

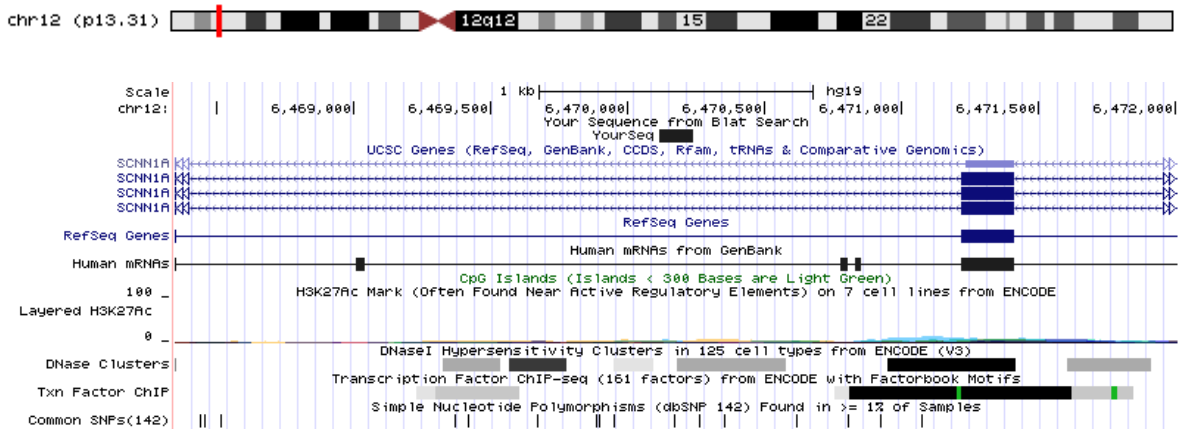

DCUN1D3- cg06533895

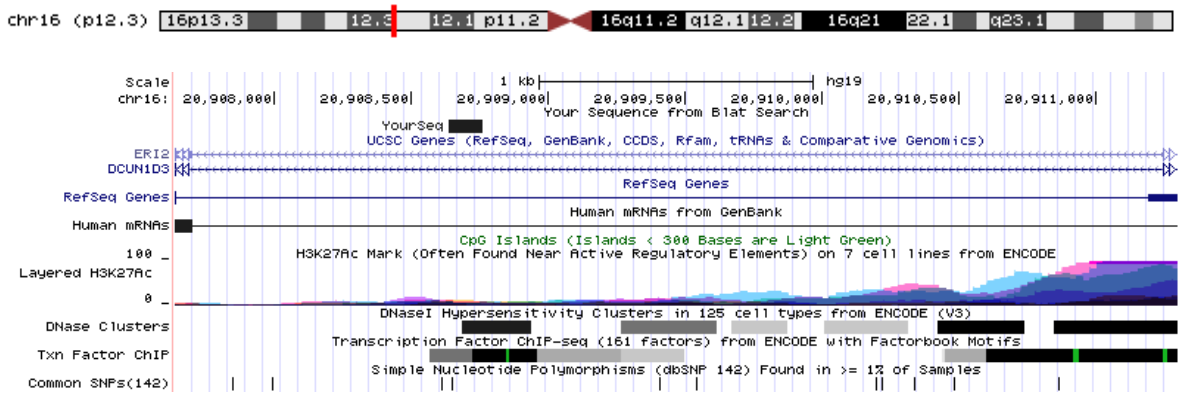

ELOVL5- cg08597067

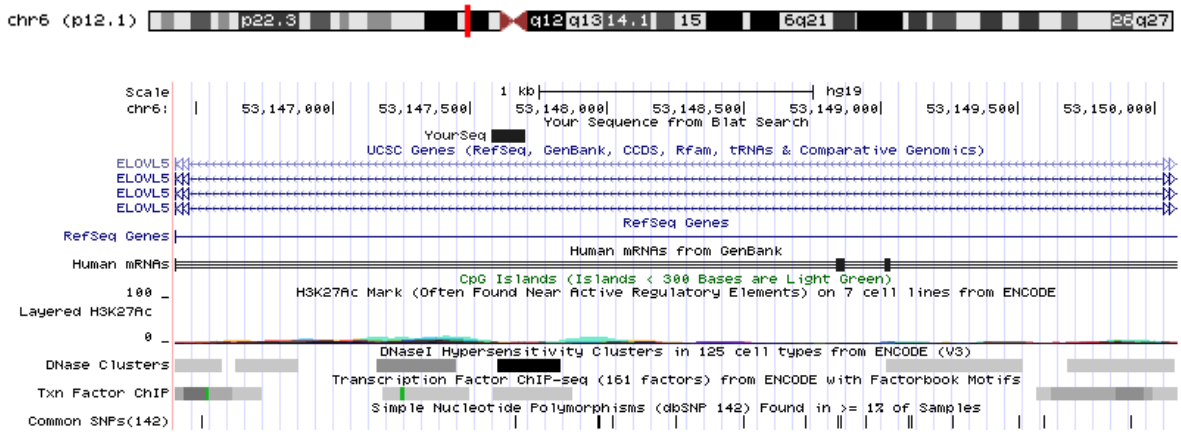

ELK3- cg01291854

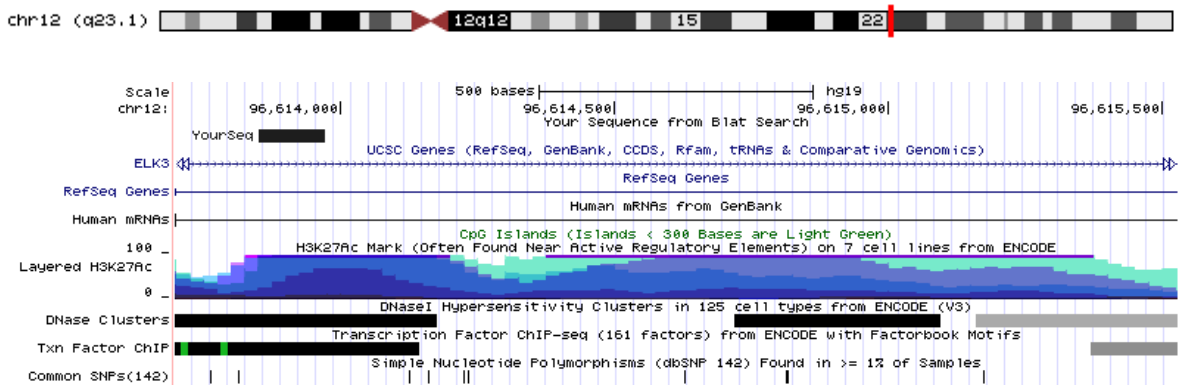

EHF- cg05503887

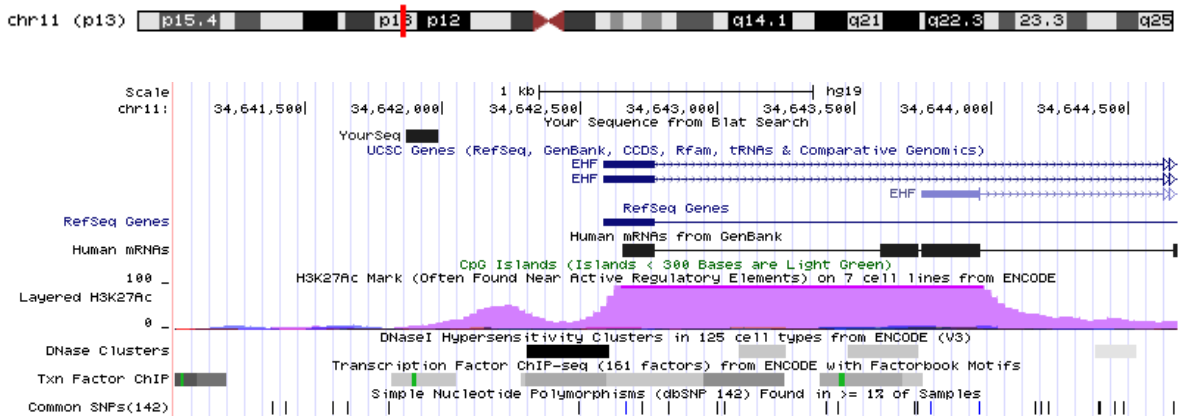

SOX10 - cg23109891

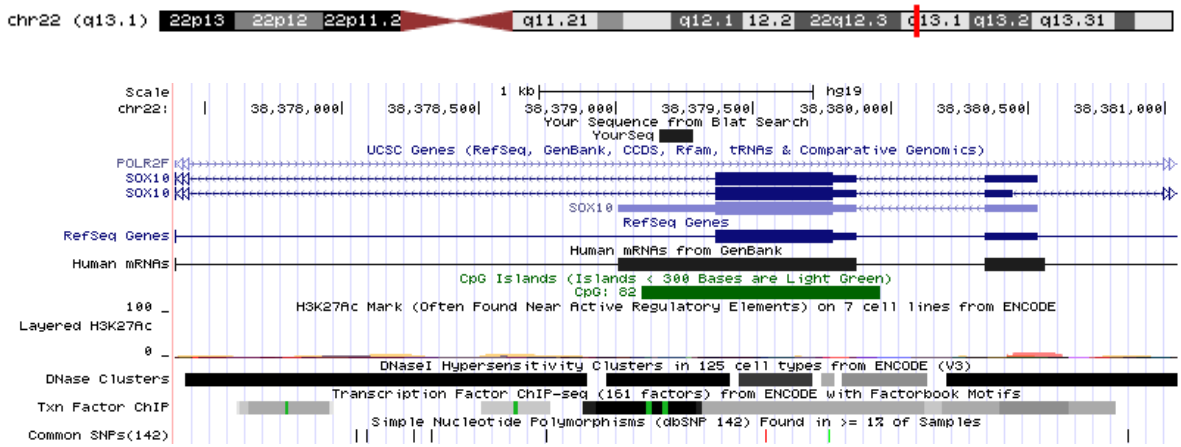

Não mapeada - cg27141871

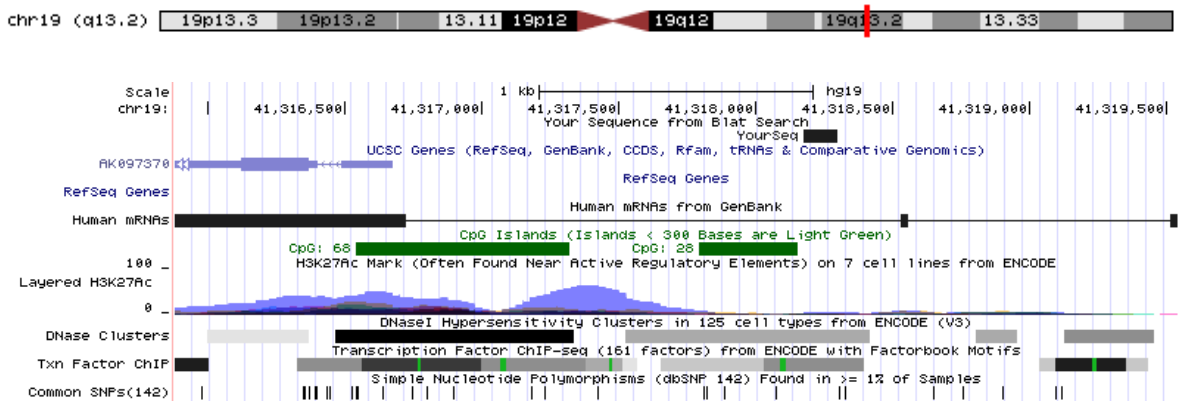

LTK - cg03321553

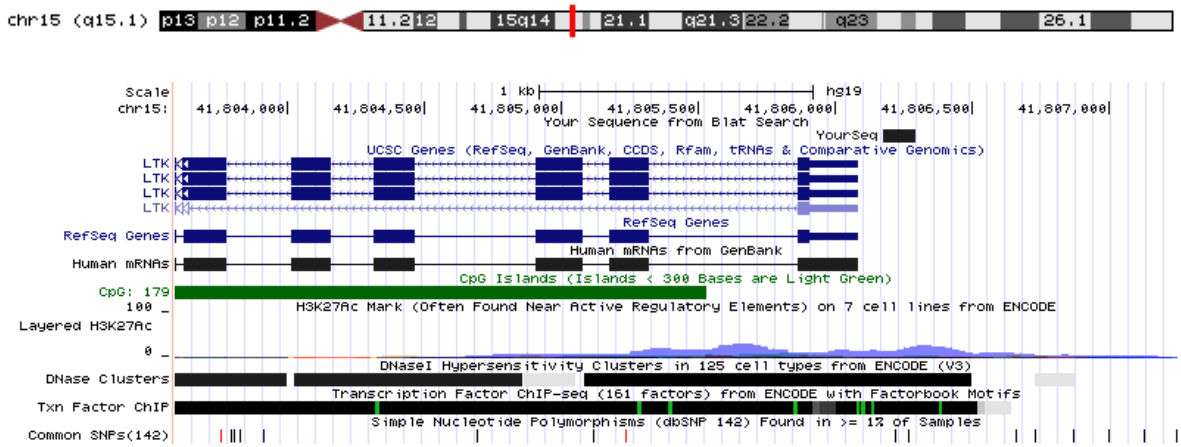

Apêndice 2. Controles de qualidade utilizados nas análises de microarray

Antes de iniciar a análise dos dados de metilação diferencial entre as amostras de LT e normais djacentes, foi realizada uma análise de controle de qualidade do experimento na Plataforma Infinium® Human Methylation450 BeadChip. De acordo com os parâmetros estabelecidos, uma amostra apresentando 1% das sondas com valor de P>0,05 foi removida. Foram removidas 502 sondas com *beadcount*< 3 em 5% das amostras e 2.811 sondas que apresentaram p > 0,05 em 1% das amostras. Após a remoção de sondas com SNPs (7.683), sondas que co-hibridizam (11.229) e as mapeadas nos cromossomos X e Y (11.184), as análises prosseguiram com 452.162 sondas.

Apêndice 3. Número de sondas diferencialmente hiper e hipometilados em relação a localização genômica, contexto e localização cromossômica entre as comparações incluindo as lesões benignas, carcinoma papilífero, folicular e não diferenciadosda tireoide.

	Sondas Hipermetiladas LBT	Sondas Hipometiladas LBT	Sondas Hipermetiladas PTC	Sondas Hipometiladas PTC	Sondas Hipermetiladas FTC/CCH	Sondas Hipometiladas FTC/CHH	Sondas Hipermetiladas PDTC/ATC	Sondas Hipometiladas PDTC/ATC
Distribuição Genômica								
Promotor	374	64	38	599	1148	379	2164	5740
Corpo do Gene	714	56	152	1135	1600	392	2646	9468
3'UTR	60	6	10	97	137	52	229	846
Região Intergênica	383	96	42	942	1215	652	1876	12198
Conteúdo de CpG e Contexto								
Ilha	437	6	26	33	1234	38	3269	1601
Shore	441	27	32	474	1288	267	1802	4695
Shelf	88	48	15	338	238	203	304	3874
Outros/*Open Sea*	565	141	169	1928	1340	967	1540	18082
Cromossomo								
1	157	15	31	348	442	138	676	2753
2	120	13	23	226	359	104	565	1943
3	6	12	17	178	189	72	338	1178
4	56	11	13	114	133	63	326	927
5	101	19	19	158	268	105	534	1642
6	110	15	18	193	282	72	571	1667
7	64	19	9	152	206	116	468	2945
8	62	11	6	130	152	84	268	1984
9	32	4	7	43	92	19	135	329
10	86	10	11	154	210	80	323	1963
11	101	18	30	215	267	116	396	1876
12	85	23	8	126	190	114	301	1645
13	40	7	4	77	101	35	166	600
14	49	5	4	76	124	52	266	1276
15	35	8	6	111	133	53	214	1009
16	79	3	7	94	201	40	198	985
17	95	11	12	164	273	57	416	1004
18	19	4	1	20	47	15	82	364
19	101	8	8	99	260	76	402	894
20	30	2	2	27	78	35	133	597
21	13	0	2	21	19	8	57	267
22	28	4	4	47	74	21	80	404

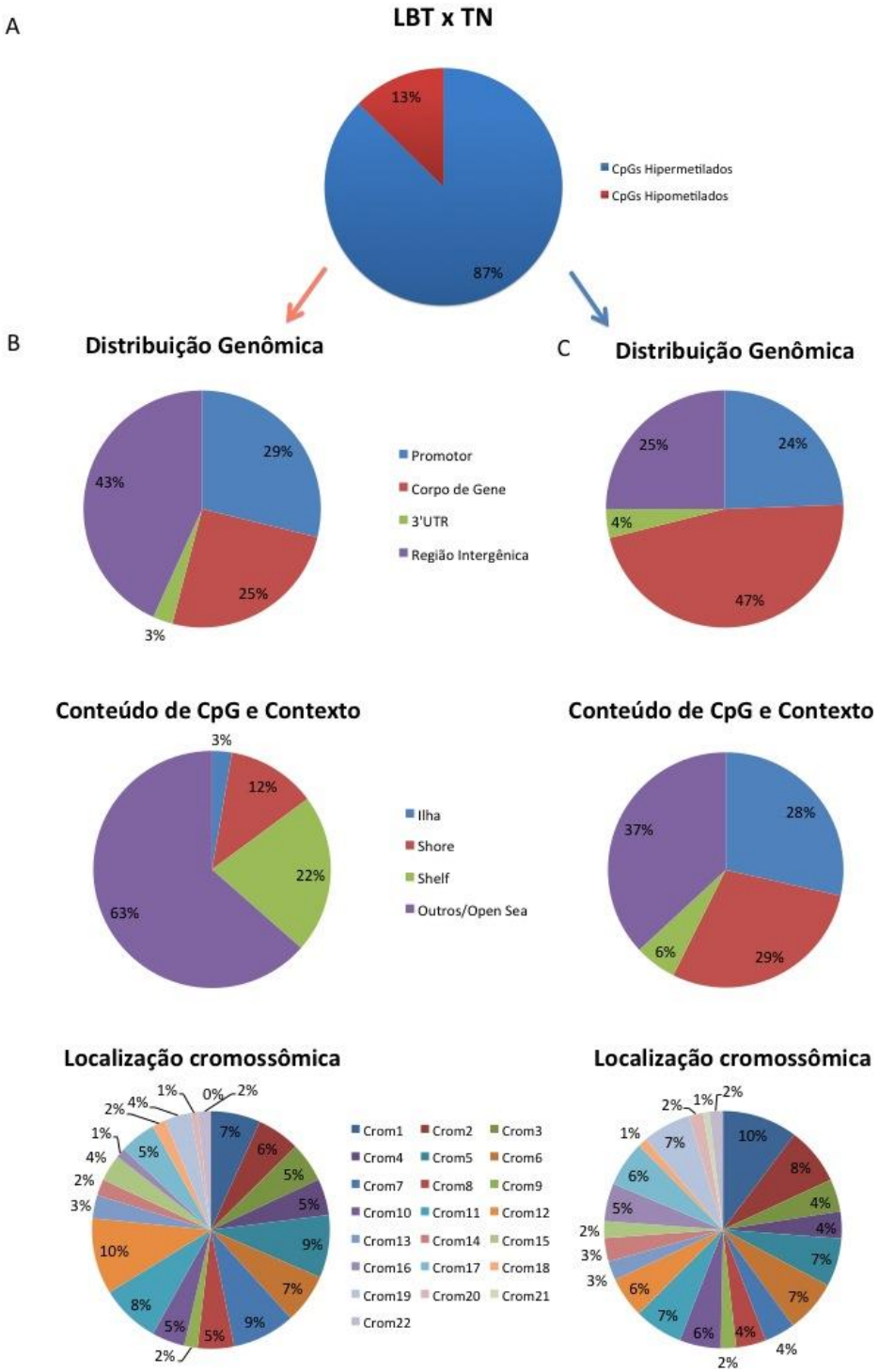

Figura 1: Caracterização das sondas diferencialmente metiladas encontradas na análise comparativa entre LBT e tecido não neoplásico. (A) Porcentagem de sondas hiper e hipometiladas nas lesões. (B) Distribuição de CpGs hipometilados no tecido tumoral de acordo com sua distribuição genômica, conteúdo de CpG na região e seu contexto e localização cromossômica. (C) Distribuição de CpGs hipermetilados no tecido tumoral de acordo com sua distribuição genômica, conteúdo de CpG na região e seu contexto e localização cromossômica.

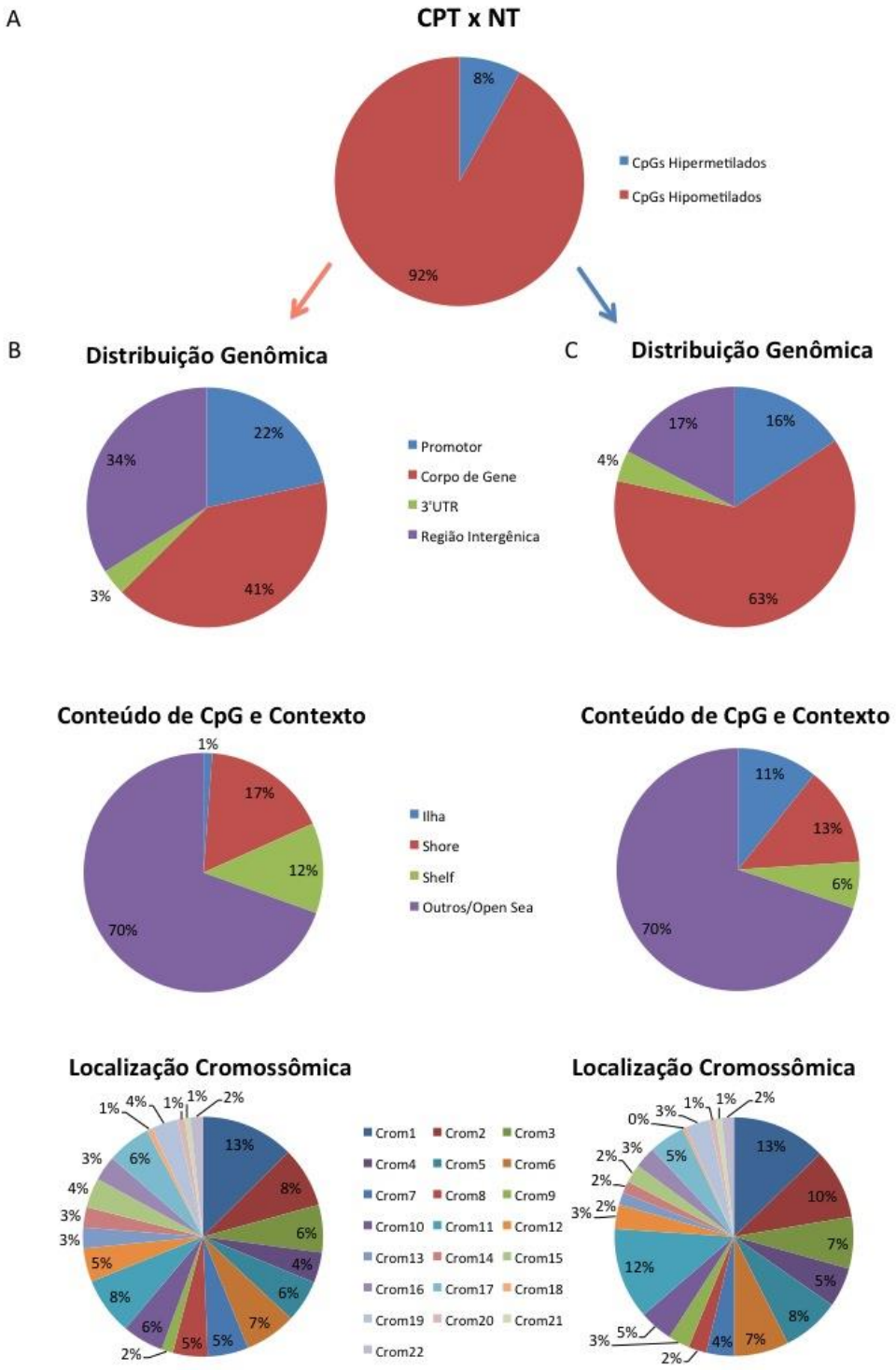

Figura 2: Caracterização das sondas diferencialmente metiladas encontradas na análise comparativa entre CPT e tecido não neoplásico. (A) Porcentagem de sondas hiper e hipometiladas no tecido tumoral. (B) Distribuição de CpGs hipometilados no tecido tumoral de acordo com sua distribuição genômica, conteúdo de CpG na região e seu contexto e localização cromossômica. (C) Distribuição de CpGs hipermetilados no tecido tumoral de acordo com sua distribuição genômica, conteúdo de CpG na região e seu contexto e localização cromossômica.

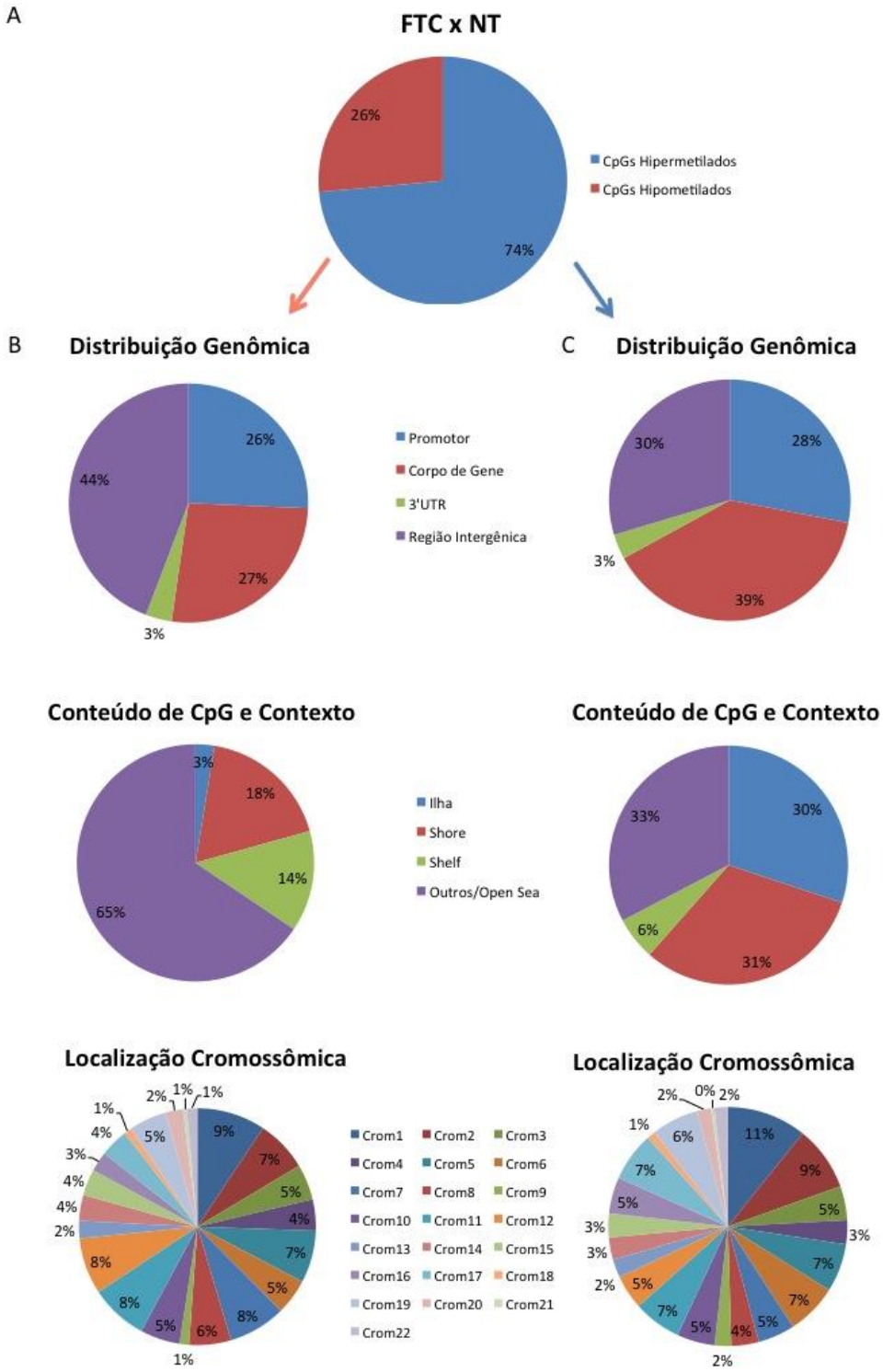

Figura 3: Caracterização das sondas diferencialmente metiladas encontradas na análise comparativa entre CFT/CCH e não neoplásico. (A) Porcentagem de sondas hiper e hipometiladas no tecido tumoral. (B) Distribuição de CpGs hipometilados no tecido tumoral de acordo com sua distribuição genômica, conteúdo de CpG na região e seu contexto e localização cromossômica. (C) Distribuição de CpGs hipermetilados no tecido tumoral de acordo com sua distribuição genômica, conteúdo de CpG na região e seu contexto e localização cromossômica.

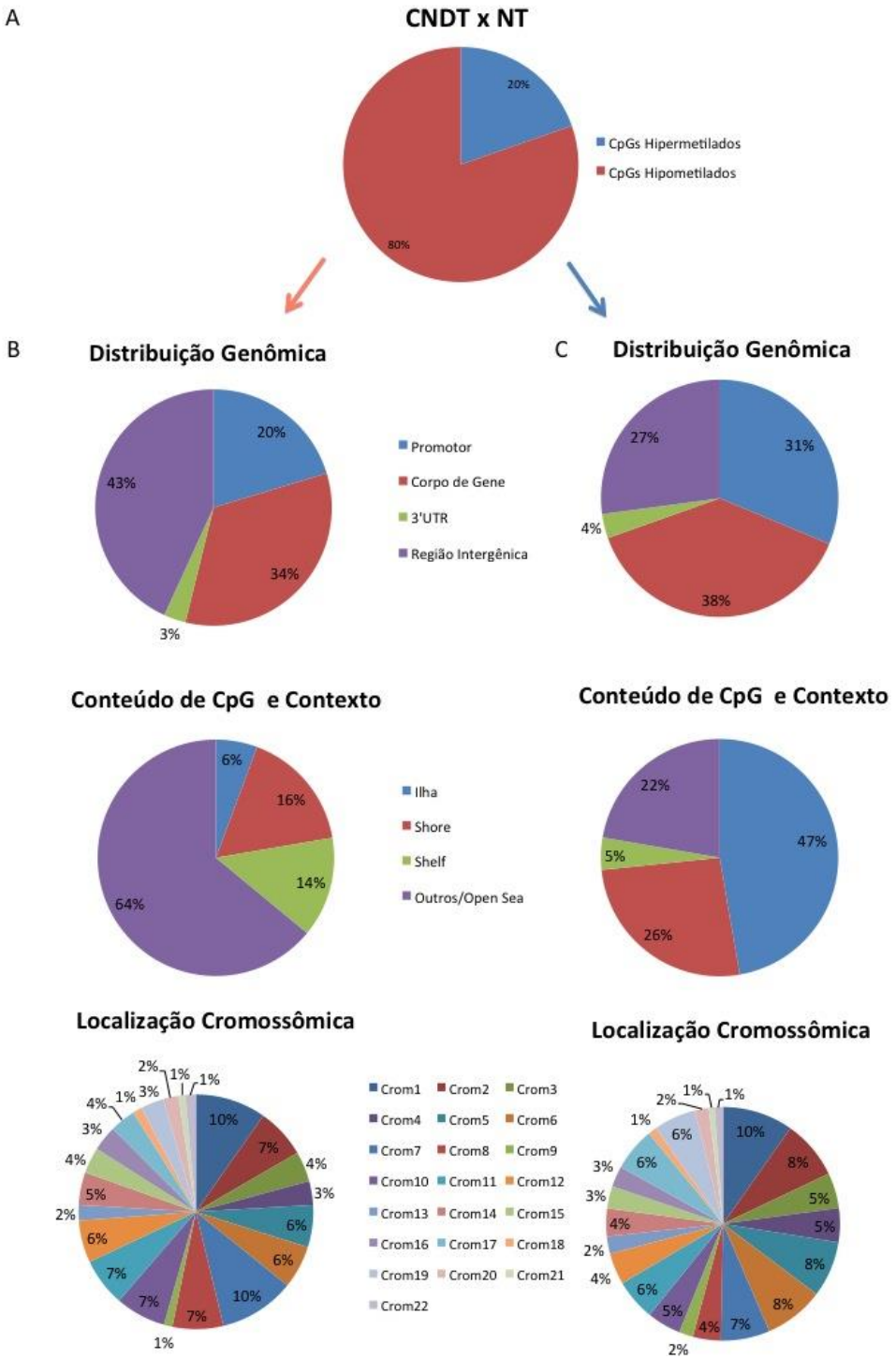

Figura 4: Caracterização das sondas diferencialmente metiladas encontradas na análise comparando carcinomas não diferenciados (CPDT e CAT) e não neoplásico. (A) Porcentagem de sondas hiper e hipometiladas no tecido tumoral. (B) Distribuição de CpGs hipometilados no tecido tumoral de acordo com sua distribuição genômica, conteúdo de CpG na região e seu contexto e localização cromossômica. (C) Distribuição de CpGs hipermetilados no tecido tumoral de acordo com sua distribuição genômica, conteúdo de CpG na região e seu contexto e localização cromossômica.

Apêndice 4. Lista das sondas diferencialmente metiladas obtidas no presente estudo

Tabela 1: As principais 20 sondas hipermetiladas e hipometiladas nos carcinomas em relação a lesões benignas de tireoide

Gene	Nome	Sonda	Localização	Δβ	P ajustado
ACOX3	acyl-CoA oxidase 3, pristanoyl	cg17781866	Corpo do gene	0.37	3.636E-07
RIC3	RIC3 acetylcholine receptor chaperone	cg16484162	Corpo do gene	0.37	4.526E-13
FHL2	four and a half LIM domains 2	cg08239282	5'UTR	0.34	4.025E-07
TPO	thyroid peroxidase	cg15977002	Corpo do gene	0.32	1.519E-07
FBXO32	F-box protein 32	cg01955203	3'UTR	0.32	5.612E-06
TTC23	tetratricopeptide repeat domain 23	cg10765992	Corpo do gene	0.32	1.678E-07
METTL7A	methyltransferase like 7A	cg16424082	Corpo do gene	0.31	4.84E-12
TENM2	teneurin transmembrane protein 2	cg06793849	Corpo do gene	0.31	3.381E-07
NEK11	NIMA-related kinase 11	cg06239593	Corpo do gene	0.31	1.364E-08
TPO	thyroid peroxidase	cg23136645	TSS200	0.30	3.094E-05
LRIG1	leucine-rich repeats and immunoglobulin-like domains 1	cg06096184	Corpo do gene	0.30	2.971E-05
PDE8B	phosphodiesterase 8B	cg11062417	Corpo do gene	0.29	3.155E-06
JMJD1C	jumonji domain containing 1C	cg24409808	Corpo do gene	0.29	2.108E-09
TULP4	tubby like protein 4	cg23816737	1stExon	0.28	6.121E-06
VPS13D	vacuolar protein sorting 13 homolog D (S. cerevisiae)	cg10039523	Corpo do gene	0.28	4.587E-09
PRDM16	PR domain containing 16	cg08110058	Corpo do gene	0.27	1.174E-07
CASZ1	castor zinc finger 1	cg18236877	Corpo do gene	0.27	7.274E-07
TULP4	tubby like protein 4	cg18978680	1stExon	0.27	1.613E-07
ZNF474	zinc finger protein 474	cg01024618	5'UTR	0.27	2.892E-06
TNC	tenascin C	cg21236655	5'UTR	0.27	7.285E-07
MAML2	mastermind-like 2 (Drosophila)	cg08141395	Corpo do gene	-0.45	5.125E-07
ITGA2	integrin, alpha 2 (CD49B, alpha 2 subunit of VLA-2 receptor)	cg08446038	Corpo do gene	-0.43	7.832E-09
ERC1	ELKS/RAB6-interacting/CAST family member 1	cg14971574	Corpo do gene	-0.42	3.184E-07
ETV6	ets variant 6	cg00610577	Corpo do gene	-0.42	5.081E-07
ECM1	extracellular matrix protein 1	cg01076495	1stExon	-0.41	2.008E-10
EIF2B3	eukaryotic translation initiation factor 2B, subunit 3 gamma, 58kDa	cg17298989	Corpo do gene	-0.41	4.852E-06
SF3B3	splicing factor 3b, subunit 3, 130kDa	cg00864954	Corpo do gene	-0.41	9.019E-11
TBC1D14	TBC1 domain family, member 14	cg20834178	Corpo do gene	-0.40	1.441E-05
BTF3P11	basic transcription factor 3 pseudogene 11	cg01665118	Corpo do gene	-0.40	4.115E-07
ACSL5	acyl-CoA synthetase long-chain family member 5	cg25780389	TSS1500	-0.39	1.344E-14
CPVL	carboxypeptidase, vitellogenic-like	cg00233633	Corpo do gene	-0.39	1.009E-05
FAM53B	family with sequence similarity 53, member B	cg04370247	3'UTR	-0.39	3.014E-10
ANXA1	annexin A1	cg13591783	5'UTR	-0.39	7.763E-06
SORL1	sortilin-related receptor, L(DLR class) A repeats containing	cg13606889	Corpo do gene	-0.39	3.559E-08
C17orf62	chromosome 17 open reading frame 62	cg12882189	Corpo do gene	-0.39	1.45E-08
KIAA1598	KIAA1598	cg08908131	Corpo do gene	-0.39	1.058E-06
XKR6	XK, Kell blood group complex subunit-related family, member 6	cg23007325	Corpo do gene	-0.39	7.722E-06
SUFU	suppressor of fused homolog (Drosophila)	cg18661379	3'UTR	-0.38	3.091E-06
CDCP1	CUB domain containing protein 1	cg09220326	Corpo do gene	-0.38	2.329E-05
GSE1	Gse1 coiled-coil protein	cg04120520	3'UTR	-0.38	0.0015381

Tabela 2: As principais 20 sondas hipermetiladas e hipometiladas nas amostras de lesões benignas de tireoide em relação o tecido não neoplásico

Gene	Nome	Sonda	Localização	Δβ	P ajustado
SSBP4	single stranded DNA binding protein 4	cg13331354	Body	0.39	3.7476E-18
SSBP4	single stranded DNA binding protein 4	cg10790698	Body	0.39	2.1458E-20
LPCAT1	lysophosphatidylcholine acyltransferase 1	cg23483886	Body	0.39	5.7894E-17
LMF1	lipase maturation factor 1	cg05578056	Body	0.38	1.5679E-19
SSBP4	single stranded DNA binding protein 4	cg18547371	Body	0.38	1.1911E-18
DOCK6	dedicator of cytokinesis 6	cg12019614	Body	0.38	2.2854E-17
AKT1	v-akt murine thymoma viral oncogene homolog 1	cg07160992	Body	0.36	4.1214E-11
SSBP4	single stranded DNA binding protein 4	cg07561894	Body	0.36	1.9927E-15
SOX10	SRY (sex determining region Y)-box 10	cg23109891	Body	0.36	9.4759E-20
WDR90	WD repeat domain 90	cg01252526	Body	0.36	3.4364E-09
PTDSS1	phosphatidylserine synthase 1	cg14914552	Body	0.35	7.6271E-15
DOC2A	double C2-like domains, alpha	cg03890691	TSS1500	0.35	2.4552E-16
ATXN7L1	ataxin 7-like 1	cg13007207	Body	0.34	8.1639E-17
LPCAT1	lysophosphatidylcholine acyltransferase 1	cg01900358	Body	0.34	6.9349E-20
KIAA1217	KIAA1217	cg16442712	Body	0.34	2.0332E-14
MIR346	microRNA 346	cg02632490	Body	0.34	5.613E-12
PROSER2	proline and serine rich 2	cg08584759	Body	0.33	2.9648E-19
LIMCH1	LIM and calponin homology domains 1	cg06663149	Body	0.33	1.9309E-16
PTDSS1	phosphatidylserine synthase 1	cg09267188	Body	0.33	3.8273E-18
CCDC102A	coiled-coil domain containing 102A	cg00348900	Body	0.33	2.0389E-16
PIK3CD	phosphatidylinositol-4,5-bisphosphate 3-kinase, catalytic subunit delta	cg20994801	TSS1500	-0.310	5.34E-12
DCC	DCC netrin 1 receptor	cg21263710	TSS1500	-0.309	6.187E-13
S100A7L2	S100 calcium binding protein A7-like 2	cg13356175	TSS1500	-0.294	1.5883E-10
BTNL2	butyrophilin-like 2	cg14096229	Corpo do gene	-0.291	3.3802E-10
GRM8	glutamate receptor, metabotropic 8	cg04386614	Corpo do gene	-0.283	3.5103E-12
TOMM5	translocase of outer mitochondrial membrane 5 homolog (yeast)	cg13987885	Corpo do gene	-0.275	2.0869E-07
HIST3H2BB	histone cluster 3, H2bb	cg00146645	TSS1500	-0.272	1.3402E-10
EFNA2	ephrin-A2	cg23658462	Corpo do gene	-0.267	2.2833E-11
LHX3	LIM homeobox 3	cg25952247	Corpo do gene	-0.266	5.5627E-09
CNTN1	contactin 1	cg06730161	TSS1500	-0.266	1.5283E-10
ASCL4	achaete-scute family bHLH transcription factor 4	cg20318358	TSS1500	-0.265	2.3579E-08
PTPRN2	protein tyrosine phosphatase, receptor type, N polypeptide 2	cg04336561	Corpo do gene	-0.263	1.3129E-11
PIK3R6	phosphoinositide-3-kinase, regulatory subunit 6	cg06613765	TSS200	-0.261	5.9326E-10
OR8D2	olfactory receptor, family 8, subfamily D, member 2 (gene/pseudogene)	cg25528806	1°Éxon	-0.260	2.0157E-13
GRP	gastrin-releasing peptide	cg00980625	Corpo do gene	-0.260	7.3186E-07
HBD	hemoglobin, delta	cg09751515	TSS200	-0.258	1.4126E-07
KCNK10	potassium channel, two pore domain subfamily K, member 10	cg12866656	Corpo do gene	-0.255	4.0849E-08
CACNG5	calcium channel, voltage-dependent, gamma subunit 5	cg06226384	TSS200	-0.251	1.2491E-09
SLITRK3	SLIT and NTRK-like family, member 3	cg01882260	5'UTR	-0.243	5.9292E-09
TMEM132D	transmembrane protein 132D	cg07067993	Corpo do gene	-0.243	4.3238E-09

Legenda: Δβ – delta beta: valores positivos indicam sondas hipermetiladas e valores negativos, sondas hipometiladas

Tabela 3: As principais 20 sondas hipermetiladas e hipometiladas nas amostras de carcinoma papilífero de tireoide relação o tecido não neoplásico

Gene	Nome	Sonda	Localização	Δβ	P ajustado
ACOX3	acyl-CoA oxidase 3, pristanoyl	cg17781866	Corpo de gene	0.376	1.0176E-29
ELOVL5	ELOVL fatty acid elongase 5	cg08597067	Corpo de gene	0.372	1.582E-29
LRP8	low density lipoprotein receptor-related protein 8, apolipoprotein e receptor	cg04483460	Corpo de gene	0.357	1.318E-25
R3HCC1L	R3H domain and coiled-coil containing 1-like	cg12715136	3'UTR	0.348	2.8702E-24
TPO	thyroid peroxidase	cg23136645	TSS200	0.339	4.5659E-23
TULP4	tubby like protein 4	cg23816737	1°Éxon	0.333	5.1284E-23
SORBS2	sorbin and SH3 domain containing 2	cg15923139	5'UTR	0.331	8.6063E-28
TPO	thyroid peroxidase	cg15977002	Corpo de gene	0.330	8.7253E-26
TNC	tenascin C	cg21236655	5'UTR	0.324	1.8668E-24
CASZ1	castor zinc finger 1	cg18236877	Corpo de gene	0.323	4.4201E-21
LRIG1	leucine-rich repeats and immunoglobulin-like domains 1	cg06096184	Corpo de gene	0.320	8.1829E-20
TSGA10IP	testis specific, 10 interacting protein	cg05151496	TSS1500	0.316	9.1096E-26
VPS13D	vacuolar protein sorting 13 homolog D (S. cerevisiae)	cg10039523	Corpo de gene	0.310	2.8668E-25
ICAM5	intercellular adhesion molecule 5, telencephalin	cg04295144	Corpo de gene	0.307	4.83E-20
FBXO32	F-box protein 32	cg01955203	3'UTR;	0.306	3.6772E-21
TULP4	tubby like protein 4	cg18978680	1°Éxon	0.301	1.0673E-24
DLEU7	deleted in lymphocytic leukemia, 7	cg01257309	TSS1500	0.299	3.2111E-20
RNF216	ring finger protein 216	cg07899076	Corpo de gene	0.297	2.5415E-20
ALK	anaplastic lymphoma receptor tyrosine kinase	cg11374596	Corpo de gene	0.297	8.0338E-23
GPR107	G protein-coupled receptor 107	cg13393408	Corpo de gene	0.292	1.0957E-11
TBC1D14	TBC1 domain family, member 14	cg20834178	Corpo de gene	-0.482	2.8134E-31
ATXN1	ataxin 1	cg11228682	Corpo de gene	-0.467	4.6465E-29
SORL1	sortilin-related receptor, L(DLR class) A repeats containing	cg13606889	Corpo de gene	-0.465	4.3354E-29
GABRR2	gamma-aminobutyric acid (GABA) A receptor, rho 2	cg03301058	Corpo de gene	-0.460	7.3855E-29
ANXA1	annexin A1	cg13591783	5'UTR	-0.450	3.1401E-25
SERPINA1	serpin peptidase inhibitor, clade A (alpha-1 antiproteinase, antitrypsin), member 1	cg09968361	5'UTR	-0.444	7.0971E-29
SLC22A18AS	solute carrier family 22 (organic cation transporter), member 18 antisense	cg18458509	Corpo de gene	-0.439	7.0494E-30
MCTP1	multiple C2 domains, transmembrane 1	cg06778183	Corpo de gene	-0.431	6.1482E-29
KIAA1598	KIAA1598	cg08908131	Corpo de gene	-0.430	2.0752E-24
GIGYF1	GRB10 interacting GYF protein 1	cg21638357	Corpo de gene	-0.430	1.8678E-26
SH3RF3	SH3 domain containing ring finger 3	cg03063658	Corpo de gene	-0.429	1.5002E-28
ELK3	ELK3, ETS-domain protein (SRF accessory protein 2)	cg01291854	5'UTR	-0.426	4.5265E-28
MAP3K5	mitogen-activated protein kinase kinase kinase 5	cg07474842	Corpo de gene	-0.425	2.9414E-25
TSPAN18	tetraspanin 18	cg20968743	5'UTR	-0.424	1.8412E-26
SMIM3	small integral membrane protein 3	cg09501687	Corpo de gene	-0.424	1.1307E-28
MCC	mutated in colorectal cancers	cg13531667	TSS1500	-0.422	5.9243E-25
LUZP1	leucine zipper protein 1	cg26530485	TSS1500	-0.421	2.7023E-29
SMG9	SMG9 nonsense mediated mRNA decay factor	cg03214420	5'UTR	-0.421	3.0867E-27
NAA25	N(alpha)-acetyltransferase 25, NatB	cg18700744	Corpo de gene	-0.420	3.1127E-27

	auxiliary subunit				
EGFR	epidermal growth factor receptor	cg02166842	Corpo de gene	-0.420	3.1607E-27

Legenda: Δβ – delta beta: valores positivos indicam sondas hipermetiladas e valores negativos, sondas hipometiladas

Tabela 4: As principais 20 sondas hipermetiladas e hipometiladas nas amostras de carcinoma folicular de tireoide (CFT e CCH) em relação o tecido não neoplásico

Gene	Nome	Sonda	Localização	Δβ	P ajustado
SOX10	SRY (sex determining region Y)-box 10	cg23109891	Corpo de gene	0.479	2.204E-23
AKT1	v-akt murine thymoma viral oncogene homolog 1	cg07160992	Corpo de gene	0.477	2.403E-13
ZZEF1	zinc finger, ZZ-type with EF-hand domain 1	cg21851534	3'UTR	0.434	1.238E-16
DCTD	dCMP deaminase	cg09557149	Corpo de gene	0.428	5.741E-13
LPCAT1	lysophosphatidylcholine acyltransferase 1	cg23483886	Corpo de gene	0.417	3.972E-13
HSPG2	heparan sulfate proteoglycan 2	cg25138553	Corpo de gene	0.414	1.45E-13
WDR90	WD repeat domain 90	cg01252526	Corpo de gene	0.410	4.533E-08
H2AFY	H2A histone family, member Y	cg24628744	TSS1500	0.410	1.225E-23
TEX26	testis expressed 26	cg08379987	Corpo de gene	0.400	8.469E-20
AMT	aminomethyltransferase	cg20191453	Corpo de gene	0.398	8.301E-23
ALDOC	aldolase C, fructose-bisphosphate	cg14668747	TSS200	0.398	7.126E-21
PTGDR2	prostaglandin D2 receptor 2	cg12528056	3'UTR	0.397	1.009E-12
SND1	staphylococcal nuclease and tudor domain containing 1	cg19414711	Corpo de gene	0.397	2.351E-17
RERE	arginine-glutamic acid dipeptide (RE) repeats	cg27561786	Corpo de gene	0.396	5.353E-15
RIMBP2	RIMS binding protein 2	cg09744452	5'UTR	0.386	4.593E-10
PARD3B	par-3 family cell polarity regulator beta	cg03025473	Corpo de gene	0.385	3.664E-14
DOCK6	dedicator of cytokinesis 6	cg12019614	Corpo de gene	0.385	4.934E-12
EHBP1L1	EH domain binding protein 1-like 1	cg18757468	Corpo de gene	0.385	4.339E-12
SLC11A1	solute carrier family 11 (proton-coupled divalent metal ion transporter), member 1	cg03291396	Corpo de gene	0.384	2.132E-19
ATXN7L1	ataxin 7-like 1	cg13007207	Corpo de gene	0.383	2.694E-15
TPM4	tropomyosin 4	cg07810884	TSS1500	-0.393	5.411E-18
NRXN1	neurexin 1	cg09271709	Corpo de gene	-0.371	2.366E-14
GPRC5A	G protein-coupled receptor, class C, group 5, member A	cg03534847	5'UTR	-0.370	3.053E-12
ADAM29	ADAM metallopeptidase domain 29	cg10327756	5'UTR	-0.370	2.639E-13
CD1C	CD1c molecule	cg00173005	TSS1500	-0.369	4.909E-14
CDKN1B	cyclin-dependent kinase inhibitor 1B (p27, Kip1)	cg13289884	3'UTR	-0.362	1.441E-07
TPM4	tropomyosin 4	cg17744295	TSS1500	-0.357	2.181E-13
TARM1	T cell-interacting, activating receptor on myeloid cells 1	cg21966754	TSS200	-0.356	5.953E-05
C1orf21	chromosome 1 open reading frame 21	cg21118367	Corpo de gene	-0.354	1.991E-05
CST9	cystatin 9 (testatin)	cg24168221	TSS1500	-0.353	1.478E-12
PIK3R6	phosphoinositide-3-kinase, regulatory subunit 6	cg06613765	TSS200	-0.351	8.383E-11
CACNA1C	calcium channel, voltage-dependent, L type, alpha 1C subunit	cg12496211	Corpo de gene	-0.350	1.803E-14
CATSPER1	cation channel, sperm associated 1	cg14894216	TSS1500	-0.345	4.601E-12
TMOD3	tropomodulin 3 (ubiquitous)	cg19686152	TSS1500	-0.342	7.778E-17
NRXN1	neurexin 1	cg23851515	Body;Body	-0.342	2.738E-11
PPP1R17	protein phosphatase 1, regulatory subunit 17	cg23950788	5'UTR;5'UTR	-0.342	5.411E-12
THSD7B	thrombospondin, type I, domain containing 7B	cg08231096	TSS200	-0.341	8.197E-16
OLFM2	olfactomedin 2	cg13455326	Corpo de gene	-0.341	4.65E-15
CLCN1	chloride channel, voltage-sensitive 1	cg27497928	3'UTR	-0.341	1.307E-20
CD1B	CD1b molecule	cg15952487	Corpo de gene	-0.340	2.908E-15

Legenda: Δβ – delta beta: valores positivos indicam sondas hipermetiladas e valores negativos, sondas hipometiladas

Tabela 5: As principais 20 sondas hipermetiladas e hipometiladas nas amostras de carcinomas não diferenciados de tireoide (CPDT e ATC) em relação o tecido não neoplásico.

Gene	Nome	Sonda	Localização	Δβ	P ajustado
CIPC	CLOCK-interacting pacemaker	cg16209517	Corpo de gene	0.646	2.71E-15
SMG6	SMG6 nonsense mediated mRNA decay factor	cg17648080	Corpo de gene	0.595	2.09E-18
CELSR1	cadherin, EGF LAG seven-pass G-type receptor 1	cg22969397	Corpo de gene	0.587	2.71E-14
CAPN2	calpain 2, (m/II) large subunit	cg14178043	Corpo de gene	0.583	3.1E-13
MTHFD1L	methylenetetrahydrofolate dehydrogenase (NADP+ dependent) 1-like	cg18920088	Corpo de gene	0.576	1.2E-14
CMIP	c-Maf inducing protein	cg01494399	Corpo de gene	0.571	7.12E-13
RNF39	ring finger protein 39	cg15877520	Corpo de gene	0.570	2.17E-16
TNFAIP3	tumor necrosis factor, alpha-induced protein 3	cg01981433	Corpo de gene	0.564	9.14E-12
MSI2	musashi RNA-binding protein 2	cg07159758	Corpo de gene	0.558	1.62E-10
SOX10	SRY (sex determining region Y)-box 10	cg23109891	Corpo de gene	0.556	4.1E-18
UVRAG	UV radiation resistance associated	cg00223767	Corpo de gene	0.556	1.34E-11
ATXN7L1	ataxin 7-like 1	cg20821442	Corpo de gene	0.556	4.49E-12
TRIM67	tripartite motif containing 67	cg04096525	3'UTR	0.552	4.35E-13
EHBP1L1	EH domain binding protein 1-like 1	cg18757468	Corpo de gene	0.549	1.42E-12
TULP4	tubby like protein 4	cg07165851	1°Éxon	0.546	2.49E-14
CHD7	chromodomain helicase DNA binding protein 7	cg07050692	Corpo de gene	0.546	2.61E-08
CFTR	cystic fibrosis transmembrane conductance regulator (ATP-binding cassette sub-family C, member 7)	cg09181792	TSS1500	0.545	2.32E-26
DCTD	dCMP deaminase	cg00612828	Corpo de gene	0.543	9.99E-11
FOXK2	forkhead box K2	cg20173014	Corpo de gene	0.543	1.08E-11
MBP	myelin basic protein	cg11598403	Corpo de gene	0.538	2.82E-11
RUNX1	runt-related transcription factor 1	cg04915566	5'UTR	-0.639	2.46E-13
PRKAG2	protein kinase, AMP-activated, gamma 2 non-catalytic subunit	cg01058360	Corpo de gene	-0.625	1.46E-17
TIMP2	TIMP metallopeptidase inhibitor 2	cg27549186	Corpo de gene	-0.609	9.25E-19
PARP4	poly (ADP-ribose) polymerase family, member 4	cg17117459	5'UTR	-0.603	2.21E-14
GATAD2B	GATA zinc finger domain containing 2B	cg08202226	TSS1500	-0.601	2.28E-21
PTPRN2	protein tyrosine phosphatase, receptor type, N polypeptide 2	cg26554834	Corpo de gene	-0.593	1.64E-33
PTPRN2	protein tyrosine phosphatase, receptor type, N polypeptide 2	cg05328339	Corpo de gene	-0.580	3.74E-42
PRKAG2	protein kinase, AMP-activated, gamma 2 non-catalytic subunit	cg06436185	Corpo de gene	-0.579	1.82E-12
ANXA1	annexin A1	cg13591783	5'UTR	-0.575	2.01E-09
PTPN22	protein tyrosine phosphatase, non-receptor type 22 (lymphoid)	cg00916635	5'UTR	-0.574	1.24E-12
PTPRN2	protein tyrosine phosphatase, receptor type, N polypeptide 2	cg20519944	Corpo de gene	-0.571	1.53E-29
RUNX1	runt-related transcription factor 1	cg13030790	5'UTR	-0.570	6.01E-10
SORL1	sortilin-related receptor, L(DLR class) A repeats containing	cg13606889	Corpo de gene	-0.569	1.76E-08
SPTA1	spectrin, alpha, erythrocytic 1	cg22730004	TSS1500	-0.569	4.9E-18
KCNQ2	potassium channel, voltage gated KQT-like subfamily Q, member 2	cg13782274	Corpo de gene	-0.567	1.24E-31
NLRP8	NLR family, pyrin domain containing 8	cg14571622	3'UTR	-0.567	5.57E-23

TRPM2	transient receptor potential cation channel, subfamily M, member 2	cg08191854	TSS200	-0.566	7.55E-16
PTPN22	protein tyrosine phosphatase, non-receptor type 22 (lymphoid)	cg00041401	TSS200	-0.566	1.13E-08
LILRB4	leukocyte immunoglobulin-like receptor, subfamily B (with TM and ITIM domains), member 4	cg02421734	TSS1500	-0.565	1.49E-16
RUNX1	runt-related transcription factor 1	cg01519261	5'UTR	-0.565	1.96E-14

Legenda: Δβ – delta beta: valores positivos indicam sondas hipermetiladas e valores negativos, sondas hipometiladas